Fermilab

TM-1196

BEAM ABORT DUMP SAFETY ANALYSIS

C.T.Murphy, F.Turkot, and A.VanGinneken

June 1983

ABSTRACT

Radiation and environmental safety aspects of the beam abort dump which is common to the Main Ring and Energy Saver are discussed. Design aspects of the dump relevant to the maintenance of its integrity are presented, and a program for monitoring its integrity is suggested. The results of calculations about the following radiation hazards are presented: ground water activation, above-ground muon flux, residual dose in the tunnel, instantaneous energy deposition in superconducting magnets, vacuum pipe monitoring, and handling methods if the core ever has to be dug up and replaced. It is concluded that the dump is adequate to handle 3×10^{13} protons per pulse at 1 TeV, subject to a monitoring program. Before exceeding that limit, beam sweeping during the spill should be implemented, and the actual performance data of the dump should be carefully reviewed.

TABLE OF CONTENTS

I. Introduction

The beam abort dump is a device buried in the earth at C13 for the purpose of absorbing the entire Main Ring or Energy Saver beam in one-turn extraction (21 μsec) in case of an urgent need to dump the beam quickly. The beam is automatically triggered to deflect to this dump if exceptionally high losses are detected or if wild excurisions in the beam orbit are detected in the position detectors.

The dump and its instrumentation package were documented shortly after its installation in August 1980 (see Refs. 1 and 2, also included as Appendix I and II of this report). The beam lines leading up to the dump are described in Refs. 3 and 4. In this report we amplify and bring up to date the radiation hazards results discussed in Ref. 1; all the calculations have been repeated with the exact as-built geometry and some improvements in the model used by the computer program. We discuss in more detail possible failure modes for the core of the dump and the surrounding shielding mass and present a suggested program for monitoring the integrity of the system.

The core of this beam dump is a special grade of graphite selected for its ability to withstand the thermal shock of an intense proton beam without cracking or melting. The graphite is encased in a water-cooled aluminum box to remove the heat. The aluminum box is surrounded by a large steel shield to absorb hadrons in order to prevent ground-water activation problems (see Fig. 1). The

entire mass is also encased in a waterproofed, poured concrete box in order to prevent removal of radionuclides such as tritium from the steel shielding via the ground water. The entire mass is buried under 20 feet of earth.

II. Dump Core Integrity - Single Pulse Limit

The proper functioning of the Tevatron aborted-beam dump depends totally on maintaining the integrity of the material which makes up the first five hadronic absorption lengths (λ_a) of the central core. It has been amply demonstrated, both at Fermilab and CERN, that a primary proton beam of 400 GeV in energy and 10^{13} protons per pulse (21 μs duration) can drastically alter the shape and form of solids such as iron, copper, and aluminum as a result of the high energy density (ε) created in the material. A beam of 3×10^{13} protons of kinetic energy 1 TeV has an energy of 4.8 MJ. Calculations[5] indicate that ε rises by a factor $\sim$5 in going from the Main Ring at 0.4 TeV to the Tevatron at 1 TeV.

Substantial effort[6] has been devoted to examining available materials with regard to their ability to remain intact under the severe conditions created during beam absorption. Calculations show that graphite has the lowest ε among a number of possible solid materials. This feature, together with its high softening point (2600°C) and low thermal expansion coefficient (3×10^{-6}/°C) made it the prime candidate for the core material.

The transverse size of the incident 1 TeV proton beam[1] at the dump is ~2 mm (σ_x = 1.2 mm, σ_y = 0.68 mm). The spatial distribution of ε in the graphite was calculated[5] with the Monte Carlo nuclear cascade program MAXIM. The specific heat, C_p, is then used to find the temperature distribution that exists in the graphite immediately following the absorption of the beam pulse. A maximum ε of 3.6 kJ/cm^3 (for 3×10^{13} protons) occurs along the line of the beam at a depth of z = 1.2m into the graphite (z is the distance into the graphite from the front face); the corresponding temperature is 1365°C (see Appendix IV) well below the softening point of graphite. When integrated over transverse space, the maximum energy deposition occurs at a depth of 2.2m and amounts to 24 kJ per graphite block (a temperature rise of 30°C if spread uniformly over the 6"×6"×1" block).

On a scale of centimeters, the temperature distribution is like a "spike" at r = 0 (r being the transverse distance from the line of the beam); this gives rise to a mechanical stress in the graphite. In a static stress calculation the most important stress is compressional, occurs at r = 0, and is given by

$$S = \alpha E(1-\nu)\Delta T \qquad (1)$$

where α = linear expansion coefficient, E = Young's modulus, and ν = Poisson's ratio. For the type of graphite used (see Appendix III for table of properties) and ΔT = 1365°C, the compressional stress is 3880 psi, to be compared to a compressive

strength of 6500 psi for the material. The calculated beam intensity that would just reach the comparessive strength is 5.9×10^{13} protons. This should not be taken literally for two reasons: (1) the calculation of ε_{max} is uncertain to ±30%, and (2) the quasi-static stress analysis is only a reasonable approximation to the real situation.

It is encouraging to note that a similar graphite has been successfully used[7] in a rotating target at the LAMPF accelerator since 1976. The target (3 cm thick) has operated successfully for a few hours at average beam currents as high as 1.2 ma, corresponding to peak temperatures of 1700°C and a calculated stress about 60% of the material strength. One target has operated for two years at an average current of 0.5 ma; for a given point on the target this corresponds to $\sim10^7$ beam pulses (each 500 μs long) at an intensity of 2.6×10^{13} ppp, a total flux of 2×10^{20} protons in a spot size of 3.5 mm.

Given the uncertainties it would seem prudent not to use the dump at beam intensities above 3×10^{13} protons at 1 TeV; the addition of a pulsed magnet in the abort line to sweep the beam over a larger area of the graphite would permit use at higher intensities.

The temperature rise in a thin window upstream of the dump as a result of ionization energy loss by the beam has also been calculated.

At the dump, a 3×10^{13} pulse at 1 TeV will yield a $\Delta T = 365°C$ in titanium. At a point 50 m downstream of CØ (a convenient location for a vacuum window), where the beam spot is smaller, a $\Delta T = 665°C$ is indicated. The melting point of titanium is 1670°C. Taken literally, this calculation says that the window will melt at a beam intensity of 7.5×10^{13}. Thus sweeping the beam during the 21 μsec spill is also necessary to protect this window.

III. Dump Core Integrity Under High Power Operation

A. Heat Transfer and Temperature Build-up

The maximum repetition rate of the Tevatron at 1 TeV is expected to be 1 cycle per 23s; at a beam of 3×10^{13} ppp, the average beam power is 209 kW. If the graphite were thermally isolated, and 0.5 of the beam energy is deposited in the total mass of the graphite, then it would take 7 beam pulses to raise its temperature from 35°C to 100°C.

The graphite is contained in a close-fitting aluminum box,[1] as shown in Fig. 2, with 3" thick walls; there are two independent cooling water circuits, one for the inner channels and another for the outer channels. Each circuit admits a measured flow of 72 gpm at a pressure drop of 110 psi. Static pressure tests were performed at 250 psi. At this flow rate, a power input of 209 kW will yield a temperature rise of 5.4°C. If necessary the dump box could be operated with flow in only one circuit, but at a reduced power level.

An estimate has been made of the maximum temperature build-up in the graphite under continuous beam aborts at a 23s cycle and 3×10^{13} ppp. An effective heat transfer coefficient at the graphite-aluminum interface of 0.11 w/cm^2-°C was assumed (consistent with test measurements on a single block). Taking a cooling water temperature of 35°C and assuming no longitudinal heat flow, we estimate a central temperature of 193°C at a point on the beam line at $z = 2.2$m. A platinum-resistance transducer is inserted in the graphite block at this location, about 1/2" from the edge of the block. The unconstrained thermal expansion of the block in the transverse direction is estimated to be 0.06 mm. The resulting pressure increase at the graphite-aluminum interface will enhance heat transfer, thus providing a desirable negative feedback. Hydraulic pressure from the water flow in the walls of the box gives an unconstrained inward deflection of the inner wall of $\sim$0.05 mm, which also aids in heat transfer at the interface.

B. Long Term Effects in Graphite Core

Immediately following a beam pulse, the temperature spike occupies a cylindrical volume in the graphite, about 3 mm in diameter and 2 m long. A 3×10^{13} pulse at 1 TeV results in peak temperatures in this volume of $\sim$1400°C. By thermal diffusion the temperature will halve in 30 ms.

Graphite oxidizes at elevated temperatures, losing 1% of its

weight per day at 450°C; radiation enhances the oxidation rate. Although the duty cycle at high temperature is quite small (<0.1%), it was decided to provide a dry argon atmosphere at the graphite.

A second long term concern is that of radiation damage. Under an irradiation of 1×10^{20} neutrons/cm^2 ($\sim$1 MeV) at 30°C, graphite expands 1% in linear dimension; at 200°C the expansion is a factor of 10 smaller. In our case, there will be significant radiation damage effects, but they will be confined to a few mm from the beam axis, and are unlikely to cause a 1% change in overall dimension. In this region the probability of a hadron interacting with a given carbon nucleus over the lifetime of the dump is $\sim10^{-4}$.

IV. Dump Instrumentation

The basic dump instrumentation[2] consists of temperature readouts at five locations in the dump and a strip ion chamber in front of the graphite to give the x-y position of the incident beam.

Platinum resistors are utilized for the temperature transducers. Two are located in the graphite at the point of maximum energy deposition at 1 TeV (z = 2.2 m); one is on the Main Ring side, the other on the Tevatron side (see Fig. 2). These transducers are intended to be the primary monitor of the dump temperature. At the downstream end of the graphite (z = 4.5 m) are located two 1/2" thick aluminum plates which are designed to act as thermal

calorimeters with a decay time constant of ∿30s. Each plate carries two platinum resistors. The MAXIM calculation predicts a temperature rise of 6°C for a 3×10^{13} pulse at 1 TeV. These calorimeters are intended to be the primary monitors of the integrity of the graphite. Any diminution of the absorptive capability of the graphite will reflect itself in a larger temperature rise per aborted proton in the calorimeter. The seventh platinum resistor is located in the steel shielding just outside the aluminum box (see Fig. 1) at z = 2.4m.

The beam position ion chamber, located at z = -15 cm, has six horizontal strips to measure y and 12 vertical strips to measure x. The 2 cm wide strips are spaced 2.64 cm center-to-center. Just upstream of the ion chamber there is a circular steel flange for a titanium vacuum window which has an inside diameter of 10".

V. A Dump Monitoring Program

A program has been initiated for monitoring the integrity of this dump by continuous computer-controlled alarms based on temperature sensors in the dump and by periodic sampling of water drawn from tubes which go from the tunnel to the inside of the concrete box and to the granular fill under the dump. The start-up version of this program is described in Appendix V. After necessary empirical data have been obtained and after the frequency necessary for periodic water sampling has been established, as required in Appendix V, a permanent program

will be formulated. Responsibility for the execution of this program lies with the Head of the Accelerator Division, with the Safety Section playing a "watchdog" role.

Described here are the items to be monitored and the purposes they serve. The integrity of the graphite core is monitored by two calorimeters in the steel behind the graphite (see Fig. 2). A sudden or gradual development of cracks in the graphite which allow more of the primary beam to leak directly through to the steel will lead to a sudden or gradual temperature rise in these monitors. The calorimeters are wired into the Main Control Room alarm and data-logging systems. After start-up studies have established the normal temperature rise as a function of intensity, energy, and abort frequency, alarm limits will be established and enforced. As stated in Section II above, the expected temperature rise in these calorimeters is 6°C per pulse at 1 TeV with 3×10^{13} protons incident.

The aluminum box is cooled by low-conductivity water, a parallel branch in the Main Ring LCW system. Both the inlet and outlet of this branch can be valved off as the pipes leave the tunnel and go through the earth to the dump. If both the inlet and outlet valves are accidentally left closed, and the system is leak-tight, a potential for a disaster exists. A temperature rise of a mere 6°C in the water, averaged over the whole system, will raise the pressure to 250 psi, the value at which the system was hydrostatically tested. Since the graphite at the shower maximum can rise 30°C in one pulse, it may take only a few pulses to rupture the aluminum box.

Therefore, the three valves in the outlet line will be locked open, thus allowing the thermal expansion in the water to have the entire Main Ring water system as a cushion. The key will be held by the Safety Group, who will have the responsibility of verifying that the valves are locked open again after any necessary tests or repairs. The handles from the inlet valves will be removed to discourage capricious closing.

The temperature monitors in the graphite at z = 2.2 meters (the shower maximum) serve to warn that the graphite is not being adequately cooled by the LCW during periods of frequent aborts; they are probably the best remote indicator that the inlet valves to the LCW line have been accidently left valved off. As shown in Section III above, the graphite temperature can rise hundreds of degrees in a fraction of an hour if there is no cooling. While such temperatures pose no threat to the graphite, there is a risk of damaging the aluminum box because of thermal stress.

We recommend that these two temperature sensors set an alarm. Until empirical data are obtained about what is "normal," we recommend an alarm point of 60°C.

The temperature monitor imbedded in the steel shielding at z = 2.4 m is in principle not necessary; the steel should not heat more than a few °C, even at 10^{14} protons per pulse. It was added for redundancy or to detect unforeseen causes for the steel to heat up, expanding and possibly cracking the concrete box. We recommend that this temperature monitor be set to alarm at 50°C.

A tube leading from the tunnel to the inside of the concrete box will be pumped periodically to determine whether there is any water inside the concrete box (there should be none). A perforated underdrain running the length of the beam dump underneath the concrete box which connects to the tunnel allows sampling of the radionuclides in the water in this underdrain. Should the concentration of radioactivity exceed some concentration (a value yet to be decided) because of cracks in the concrete box or because of other unidentified causes, this underdrain will be pumped out (continually if necessary), thus collecting the water-borne radioactivity from the dump for proper handling and disposal. The frequency of the above two water samplings is to be established as part of the start-up monitoring program (Appendix V).

If the underground part of the LCW circuit springs a leak, then potentially radioactive water leaks either into the abort shielding mass or into the granular fill. However, the concentration of tritium is so small because of the large dilution factor (see Sector VI) that there is no concern about adding to the ground activation problem. Furthermore, most of this water ought to end up in the Main Ring sump system, not in the uncontrolled soil. Of greater concern is the fact that if the leak is into the abort shielding mass, this water might wash long-lived activity off the surface of the steel into the earth. Therefore it seems wise periodically to valve off the dump and measure the leak rate. A

large observed leak rate would suggest a greater frequency of monitoring the water level inside the concrete box and measuring the activity in the water in the underdrain beneath the dump.

VI. Radiation Safety Calculations

A number of radiation hazards created by use of this dump have been calculated in detail using the nuclear cascade program CASIM.[8] The accuracy of CASIM's predictions of beam-on neutron rates through thick and thin shields has been documented[9] at 400 GeV, but its predictions of muon rates has not been tested at high energies.

Each hazard studied leads to an upper limit allowed for dump usage in terms of protons-per-year, protons-per-hour, or protons-per-pulse; which parameter is relevant depends on the nature of the hazard. These upper limits are summarized in Table I.

Before discussing individual hazards, let us present some conservative upper limits on the number of protons expected to be dumped per year, per hour, and per pulse, based on either well-known or reasonable operating conditions. The current upper limit on the number of protons which can be aborted per pulse is 3×10^{13}, based on Main Ring limitations which are not likely to be overcome very quickly. This also corresponds to the limit recommended in Section II above, based on the allowed thermal stressing of the graphite. Higher intensities can be permitted by implementing sweeping of the aborted beam during the 21 μsec spill.

The maximum number of protons which can be aborted per hour is given by 3×10^{13} protons per pulse at the maximum repetition rate of 23 secs, or 4.7×10^{15} protons per hour. However, we cannot imagine any reasonable situation in which this would actually occur for a whole hour. The closest approach to this limit which seems reasonably possible is dedicated machine studies at a reduced intensity of 5×10^{12} protons per pulse at a time when the Switchyard dump is not available, leading to 0.8×10^{15} protons per hour. Experience shows that the only machine studies which need the full intensity of the machine are slow extraction studies, during which the beam by definition is being extracted to Switchyard most of the time.

The upper limit on the number of protons expected to be aborted per year is based on the following expected operating conditions for the next few years: 3×10^{13} protons accelerated per minute during one-third of the year for fixed target experiments with an abort rate of 2.5%; three pulses per day aborted per day for one-third of the year during collider operation, and 5×10^{12} protons per pulse aborted deliberately during machine studies for eight hours every six weeks. The fixed-target abort rate of 2.5% stated above is twice that experienced in the Main Ring during calendar year 1979, which was a "high" year for aborts because of the 450 GeV run. Experience in the Main Ring has shown that abort rates of higher than about 3% lead to intolerable (to the experimenters) losses of operating efficiency because of the additional pulses lost after each abort and the extraction instabilities which are the most usual cause of aborts.

The above operating conditions lead to an expectation that no more than 1.9×10^{17} protons will be aborted per year. The above three expected operating maxima are also summarized in Table I.

Finally, we emphasize that the number of protons aborted per year, per hour, or per pulse is subject to administrative control via operational decisions, in a manner very similar to the way in which radiation doses to personnel are controlled. If any of the above predictions of abort rates turn out to be too low and are in violation of allowed upper limits (such as those suggested in Table I or its subsequent revisions after data are available), constraints will be applied. For instance, the dump monitoring program requires quarterly reports to the Head of the Accelerator Division giving the cumulative number of protons aborted during the calendar year. If a projection of this number to the end of the year suggests a probable violation of the limit set by ground water activation standards (see below), a deliberate reduction in either beam intensity or energy must be made, either of which will reduce the instabilities which trigger aborts.

In the remainder of this Section, we present the results of the calculations of various radiation hazards and compare them with allowed standards. For the benefit of previewing the reader, we mention that the protons-per-year limit is set by the ground water activation limit (see A below), the protons-per-hour limit is set by the on-site muon hazard (see C below), and the protons-per-pulse limit is set by the graphite thermal stress limit (see Section II above).

A. Ground Water Activation

The steel and concrete shielding mass which surrounds the core of the dump was designed to be large enough to shield uncontrolled soil adequately from irradiation. Uncontrolled soil is soil whose water content will not be drained by the Main Ring underdrain into Lake Law but may eventually reach the aquifer. We regard as "controlled" soil the granular fill which surrounds the abort dump and is above the Main Ring underdrain. Figure 3 shows a cross section of the dump and its surroundings at z = 2 meters. The circles labeled "underdrain" represent a 4" perforated plastic tube which encircles the dump and is connected to the Main Ring sump pump system, which empties into Lake Law. The trapezoidal area above these underdrains represents the region of granular fill which we regard as "controlled" soil. Figure 4 shows the same items for a cross section along the beam.

The exact geometry of Figs. 3 and 4 was coded into the program CASIM to determine the rate of star production in both controlled and uncontrolled soil. Two runs with 1 TeV protons incident were made with different random number seeds; the detailed results are shown in Table II. The averaged result is that there are 0.316 ± 0.062 stars/incident proton in the uncontrolled soil and 0.397 ± 0.039 stars/incident proton in the controlled soil. A "star" is a non-universal unit defined in CASIM to mean a nuclear interaction with an incident energy greater than 0.3 GeV. The differences between the two sets of results are consistent with the assigned errors.

Between 60 and 80% of the irradiation of uncontrolled soil is from the region below the underdrain; a glance at Fig. 3 strongly suggests that most of this irradiation is in the granular fill under the drain between the dump and the tunnel, since this region has the shortest path length to the core of the dump. The water in this region will flow through the granular fill to the "sampling underdrain" (see Fig. 3); if at some future date a decision is made to pump continuously on the "sampling underdrain," the irradiation of uncontrolled soil can be reduced to 0.10 stars/incident proton.

The Laboratory standard for the maximum allowed irradiation of uncontrolled soil is recognized to be 2.44×10^{17} stars/yr for any single dump, based on the research done by Gollon[10] on the original anti-proton target box. Jonckheere[11] has criticized some of Gollon's assumptions as overly conservative and has brought to light some possibly relevant data not discussed by Gollon. The design of this dump adheres to the Gollon limit because the steel costs were not prohibitive.

From the Gollon limit and the CASIM result for this dump (0.316 stars/incident protons in the uncontrolled soil) one derives a limit of 7.7×10^{17} protons per year at 1 TeV which may be aborted to this dump. This limit is a factor four higher than the number which are expected to be aborted (see above).

Since the dump will also be used at energies lower than 1 TeV, the energy dependence of the CASIM result was also studied. A cylindrically symmetric approximation of the dump was coded into CASIM and the program was run with 8, 150, 500, and 1000 GeV incident protons. The energy dependence of the star density, averaged over two meters along the beam at the shower maximum, is shown in Fig. 5. It is seen that the energy dependence obeys a simple $E^{3/4}$ law at all radii. This result is consistent with an empirical study by Thomas and Thomas[12] who find an $E^{0.8}$ dependence, independent of the program CASIM.

In comparing the protons aborted per year with the 1 TeV Gollon limit of 7.7×10^{17} protons, it is proper to "weight" each proton according to its energy. At each energy, the weight is given by the ratio of the star density at that energy to the star density at 1 TeV from Fig. 5 at r = 112.5 cm. This radius corresponds to the position of the uncontrolled soil which is closest to the core of the dump. These weights for a few very popular energies are:

Energy	Weight
1000 GeV	1.000
800 GeV	0.845
500 GeV	0.595
400 GeV	0.503
150 GeV	0.241
8 GeV	0.026

B. Ground Water Activation From Gas Scattering

Should the 30 meter long beam vacuum pipe leading from the tunnel to the dump be let up to an atmosphere of air, the contribution of interactions of the beam with the gas to the ground water activation is significant. The beam pipe is surrounded by controlled soil out to a radius of 54 cm. Beyond that radius the soil is regarded as uncontrolled. CASIM predicts that there will be 0.22 stars/incident proton in the uncontrolled soil as a result of interactions with the gas, a number which is comparable to the number of stars from the dump. If the pipe can be filled with an atmosphere of helium, the dose is reduced to 0.031 stars/incident proton. Alternately, one can leave the pipe full of air and reduce the number of protons allowed to be dumped per year.

C. Above-Ground Muon Dose Rate

The second problem studied in detail was that of the muon dose rate above ground following an aborted pulse. The exact geometry of the dump was coded into CASIM, and the program then calculated muon dose rates at ground level between the dump and the site boundary, following the contour of the land. The elevation of the ground with respect to the extrapolated Doubler aborted beam line and the predicted muon dose rates are shown in Fig. 6. The maximum dose rate on-site occurs at a low spot about 400 m from the dump and is 1.01×10^{-18} rem per incident 1 TeV proton.

The Fermilab Radiation Guide requires that on-site regions be posted if the dose rate could be greater than 2.5 mrem/hr. If the maximum intensity of 3×10^{13} ppp were aborted every pulse at the maximum repetition rate of 23 secs, the above CASIM result implies an hourly dose rate of 4.7 mrem/hr, so that the region would need posting. However, we have suggested that it will be operationally easy to limit hour-long periods of steady dumping at fast repetition rates to an intensity of 0.5×10^{13} ppp, which would keep the dose a factor three less than 2.5 mrem/hr.

Finally, measurements must be made before taking steps to post or fence. The predictions of CASIM are known to be accurate only to a factor of two, and for muon rates have not been compared with measurements at either 400 GeV or 1 TeV.

At the site boundary, which corresponds roughly to 100' west of the corner of Butterfield and Eola Roads, the muon rate was calculated as a function of height above the ground. The results are shown in Fig. 7. It is seen that the rate is predicted to peak at 2.7×10^{-20} rem/proton about 9 m above the ground, and falls to $(0.2\pm0.1)\times10^{-20}$ rem/protons at ground level. The reason for this peak is that a large number of muons emerge from the ground in the low region between 150 and 700 meters from the dump (see Fig. 6). The angle which these muons must have to emerge in that region points them well up into the air, through which they coast with negligible deflection or attenuation. For a muon to reach the site boundary at ground level, much more earth must be penetrated, so the attenuation is large.

The limit prescribed by Federal regulations[13] is that the dose rate at any point at the site boundary must be less than 170 mrem/yr. If the dump received the maximum number of protons annually allowed by the ground water activation limit, 7.7×10^{17} protons/yr (see Section VI-A), the dose rate nine meters above Butterfield Road would be 21 mrem/yr, and 1.5 mrem/yr at ground level.

We conclude that the site boundary hazard created by muons from this dump is negligible. Nonetheless, measurements are warranted because of the lack of empirical tests of CASIM's predictions at these energies.

D. Neutron Dose Rate Above Ground

The beam abort dump is covered with about 20 feet of earth. The shortest path from the top of the concrete to ground level is to the "toe" of the berm (see Fig. 1) through 21.4 feet of earth, based on the architectural prints which may be wrong by a foot. The results from two CASIM runs with different random number seeds are 6×10^{-15} and 8×10^{-15} stars/(cm^3-incident proton) after 20 feet of earth for 1 TeV incident protons. The agreement of the two runs is better than expected for such a thick shield. Using the well-established conversion factor[14] of 9×10^{-6} rem/(stars/cm^3) for concrete, we predict a dose rate of 6.3×10^{-20} rem/incident proton, or 0.0019 mrem/pulse for 3×10^{13} protons incident per pulse, which is barely measurable on instruments owned by the Lab. At the maximum rep rate of 23 secs/cycle the hourly dose would be 0.3 mrem/hour. At lower energies, we assume that this prediction scales as $E^{3/4}$.

Measurements should still be made, in view of the poor statistics of the CASIM runs and the uncertainty about the thickness of the berm.

E. Core Box Removal

The core of the dump (the aluminum box) might fail in a manner which requires digging up the dump and replacing the box. This brings up the questions of how radioactive the surface of the box and the neighboring steel might be after a few years of usage (for the purpose of estimating doses to personnel removing the box), and what design steps were taken to make the box quickly removable.

The level of activation of the surface of the aluminum box and the adjacent steel at some future time will of course depend upon many variables which are not known now, such as the protons dumped per year, the irradiation time, and the cooldown time. We present a sample calculation making worst-case assumptions about the above unknowns. If the dump ever has to be dug up, the calculation should be repeated with our assumptions replaced by data.

We conclude that if the dump is used at the maximum allowed rate, 7.7×10^{17} protons per year at 1 TeV, then after five years of irradiation and a month cooldown, the residual radioactivity would be of the order of 5 rad/hr a few inches from the aluminum box or a few inches from the piece of steel in immediate contact with the aluminum. This potential dose rate is sufficiently high to warrant careful planning and control by radiation safety personnel if the dump ever has to be removed.

The invariant input to any prediction of the future residual radioactivity are the predictions of the program CASIM for the star density per incident proton at various relevant radii from the beam. We call these predictions "invariant" because we do not expect CASIM to change radically even in the distant future. These predictions, at the shower maximum along the beam, are:

$S = 1\times10^{-3}$ stars/cm^3/incident proton at outer surface of aluminum box.

$S = 0.7\times10^{-3}$ stars/cm^3/incident proton at the surface of the steel adjacent to the box.

$S = 2\times10^{-7}$ stars/cm^3/incident proton in the concrete at the top of the steel pile which must be chipped out to remove the steel and the aluminum dump.

$S = 1\times10^{-6}$ stars/cm^3/incident proton at the upstream end of the aluminum box.

The star density at the top of the aluminum box as a function of z, the distance along the beam from the beginning of the graphite, is shown in Fig. 8.

To convert these CASIM star densities into predictions of residual radioactivity, both a model and assumptions about the rate of irradiation and cooldown time, mentioned above, are required. For a model we use that of Barbier as summarized in the Fermilab Radiation Guide.[15] The residual dose is given by:

$$\dot{D} = \frac{\Omega}{4\pi} \cdot \phi \cdot d$$

where d is the "danger parameter" given by Barbier's graphs as a

function of irradiation and cooldown times, in mrad/hr; Ω is the solid angle subtended by the source at the observer; and ϕ is the activating flux in hadrons/(cm^2-sec).

We assume an irradiation time of 1800 days (five years) and a cooldown time of 30 days. This cooldown time is our guess at the minimum time necessary to mobilize for digging; waiting longer than 30 days buys no decrease in the activation of the aluminum and only a slow decrease in the activation of the steel. Irradiation times of more than five years would increase the residual dose by at most a factor of two. The resulting "danger parameters," from p. 12.2-8 of the Radiation Guide, are 2×10^{-5} mrad/hr for steel and 5×10^{-6} mrad/hr for aluminum. We assume that concrete is the same as aluminum as the average atomic number is similar.

We take $\Omega/4\pi$ to be 1/4; the maximum possible value is 1/2, corresponding to "on contact." The hadron flux, ϕ, is related to the star density, S, and the incident primary proton flux, p, by:

$$\phi = \lambda(r) \cdot S \cdot p$$

where $\lambda(r)$ is the ratio of incident hadrons/cm^2 to the number of stars/cm^3. Early in the shower, this ratio is obviously the absorption length of the material; however, as the shower develops, λ increases by an order of magnitude, largely because of the 300 MeV/c cutoff in CASIM. This parameter has been calculated by VanGinneken as a function of radius and other parameters.[16] From his graphs, we obtain λ = 70 cm for the steel next to the core box, 150 cm for the outer surface of the

aluminum core box, 400 cm for the concrete at the top of the dump and 480 at the upstream end of the aluminum box.

We assume that p is the maximum allowed by the ground water activation limit, 7.7×10^{17} protons per year, or 2.4×10^{10} protons/sec. Multiplying all these factors together, we obtain:

$\dot{D}$ = 4500 mrad/hr for the top of the aluminum box.

= 5800 mrad/hr for the steel next to the aluminum box.

= 2.4 mrad/hr for the concrete at the top of the dump.

= 14 mrad/hr for the upstream end of the aluminum box.

If the dump does have to be dug up sometime and these calculations are repeated, the number which we hope will be much smaller is p, the number of primary protons incident per year. It should be remembered that the incident protons can be "weighted" according to their energy (see p. 18).

Some steps were taken in the design to make the core box removable with ease and with minimal radiation doses to the personnel involved. The core box can be removed without disturbing most of the steel shielding and concrete box (see Fig. 9). After chipping out a section of the concrete roof (16'×2'), ten steel "B" blocks (3300 lbs each, 18"×18"×36") must be removed directly above the core box. A crane with a pair of electromagnets is required.

To lift out the core box, two lifting brackets (Fig. 10) must be attached to the aluminum box with 1/2"×13 bolts. After disconnecting the instrumentation leads (a major complication which is discussed in Appendix VI), the box can be lifted straight up and out.

Some obvious precautions can be taken in the above steps to minimize doses to personnel. The bottom surface of the steel "B" blocks in contact with the aluminum box is expected to be quite radioactive. They can be dropped immediately into a nearby concrete blockhouse made of shielding blocks. Necessary handling of the blocks by ironworkers while being moved by the crane can be done with long poles instead of with hands. Bolting the lifting brackets to the aluminum box is the most time-intensive task in close proximity to the box. The rest of the top of the box can be draped with lead sheets, except where the brackets are attached. The box then is disposed in its entirety; i.e., dropped into some lead lined coffin and stored at the boneyard.

F. Activation of the LCW Cooling Water

The dump is cooled by the Main Ring LCW system. The volume of water in the channels of the aluminum box is 16.4 gal, which we consider to be the amount of water under irradiation at any one moment. The flow rate is about 140 gal/min, so the "dwell" time of any water molecule is 11 secs.

The long-range hazard is tritium build up, with a half-life of 12 years. An experiment[17] on a bag of water very close to the extinct DØ abort dump yielded a tritium concentration of 87 pCi/mℓ per 10^{17} protons dumped. We assume that this result is also correct for our dump, at least to within an order of magnitude. However, the 16.4 gal of water in our dump is mixed continuously with the 60,000

gal inventory of the whole system, a dilution factor of 3700. With 7.7×10^{17} protons dumped per year, the tritium build up is only 1.8 pCi/mℓ in ten years, far below the EPA standard[18] of 20 pCi/mℓ for drinking water.

A possible short-term problem is carbon-11 (half-life 20 min) production. Water from the dump reaches the C-1 Service Building, outside of the interlocked area, seven minutes later. There have been instances in the Proton area in which this effect led to high radiation rates near the water pipes and resin bottles, in small volume closed-loop systems which cooled only a beam dump.

However, we have done a calculation which indicates that the effect is small for this system. We assume that the production cross section for carbon-11 is the same as for tritium, but the radioactivity is a factor 3.15×10^{5} greater (the ratio of the decay rates). The proton abort rate is assumed to be 3×10^{13} every 23 secs. The water entering the dump from the 60,000 gal inventory is free of carbon-11 because all but 10% of it has not been through the dump for more than an hour. The flow rate and instantaneous irradiated volume are given in the first paragraph of this section. On the way from the dump to C-1, the water from the dump is diluted by a factor two by water emerging from Main Ring magnets and power supplies.

The resulting activation of the water from carbon-11 in the C-1 building is 1300 pCi/mℓ, ignoring the seven minute decay time. The resulting exposure rate from the 5-5/8" o.d. aluminum pipes has been

calculated[19] to be 0.04 mrem/hr at one foot, ignoring self-attenuation in the water.[20]

[Note added in 1984: the above prediction was very wrong. Rates of 500 mrem/hr (scaled to 3 E13) were measured, and water from the dump had to be first sent to a large "holding tank" at C0.]

Even though the above calculations can be trusted only within an order of magnitude, the conclusion is that water activation will not be a problem. Nonetheless, tritium concentration in the Main Ring LCW system will continue to be measured periodically by the Environmental Safety Group, and the Accelerator Safety Group will do radiation surveys inside the C-1 Service Building as soon as the intensity reaches 10^{13} protons per pulse and can be sent to the abort dump every pulse for an hour. These empirical tests are cheap and essential checks for gross conceptual oversights or order-of-magnitude mistakes in the calculations presented here.

G. Absorbed Dose and Residual Radioactivity in the Tunnel

Excessive leakage of particles out the side of the dump into the tunnel could cause enough energy deposition to quench the superconducting magnets. For that reason, an extra 18" of steel was set between the abort dump and the tunnel (see Fig. 3). Subsequently, we have done an energy deposition calculation using CASIM which predicts that 1.1×10^{4} GeV/cm^3 will be deposited in magnets in the tunnel for each aborted pulse of 3×10^{13} protons. This energy is three orders of magnitude lower than the energy density believed to be necessary to quench magnets during 20 μsec spill,[21] namely 2.5×10^{7} GeV/cm^3.

Residual activity in the tunnel from leakage through the side of the dump will be immeasurably small. In Section E above, a prediction of 2.4 mrem/hr was made for the residual activity at the top of the concrete surrounding the dump after five years of maximum usage. As seen in Fig. 3, the inside of the tunnel is separated by an additional 34" of dirt or concrete, leading to a prediction of 0.2 mrem/hr residual radioactivity on the inside wall of the tunnel.

H. Avoiding Beam Loss on Hidden Flanges

Any beam lost on apertures within the CØ straight section will be detected by the many loss monitors in CØ. However, either of the beams could scrape on flanges buried underground between C12 and C13 without being detected. Furthermore, some of these flanges form apertures which are narrower than the 6"×6" graphite blocks, so it is not adequate to require simply that the beams each appear somewhere in the appropriate half of the 12"×6" beam position detector (labeled "ion chamber" in Fig. 1). The position detector masks exactly the Main Ring graphite on the left (see Fig. 2) and the Tevatron graphite on the right.

Figure 11 shows the hidden apertures between C-12 and C-13 for both beams,[22] in both the vertical and horizontal planes. The crooked path of the beam pipes through the tunnel wall is a construction error. In Figure 12, these apertures are "masked" onto the position detector at the dump. The solid contours delineate the restricted area within which the entire Main Ring or Tevatron beam must lie to

guarantee missing hidden flanges, independent of the position of the beams within the magnet apertures back in CØ. The dotted contours show the limits for the beam centroid, taking into account the finite size of the 8 GeV Main Ring Beam and the 150 GeV Tevatron beam.

The aborted Tevatron beam has no ability to be steered by magnets independent of the Tevatron bus except the abort kickers at B-48. If the kickers are mistuned, the beam will scrape on the Lambertsons before it will hit any of the hidden flanges. Therefore, failure of the Tevatron beam to appear within the limits shown in Fig. 12 would be an unexpected mystery requiring high-level detective work.

However, the aborted Main Ring beam can be steered both by the abort Lambertsons (vertical plane) and EPB dipoles (mostly a horizontal bend), both of which are independent of the Main Ring bus. The response of MCR operators to Main Ring aborted beam appearing outside of the limits shown in Fig. 12 should be to check the Lambertsons and EPB dipoles for proper behavior, cut back the intensity if the problem is not cured, and then call experts.

Beam scraping on the hidden flanges is a radiation safety matter for two reasons. Minor scraping on the hidden flanges irradiates the ground water in a manner which we have not calculated. Full beam irradiation of these hidden flanges can melt holes in the vacuum system.

VII. Conclusions

We conclude that the abort dump is safe to use at an energy of 1 TeV up to an intensity of 3×10^{13} protons per pulse, provided that the monitoring program presented here is enforced. In order to exceed this intensity at 1 TeV, aborted beam sweeping in the vertical plane during the 21 μsec spill must be implemented in order to prevent melting the graphite at the core of the shower.

In addition, we strongly recommend that the intensity limit of 3×10^{13} protons per pulse not be exceeded until there has been a thorough review of both this paper and empirical data about dump performance at 3×10^{13} which are not yet available. These data are the temperature rises in the seven RTD's, the measured muon rates, and ground water activation.

VIII. Other Resources

The abort dump photo album is an invaluable aid in seeing how the dump went together and where all the underground pipes and cables really are. It will be essential if the dump ever has to be dug up. This album, a thin black loose leaf notebook, is held by the Accelerator Safety Group, and locked up because it is irreplaceable.

The civil construction prints are held by the Architectural Engineering Group, Job No. 6-1-64. The blueprints for the aluminum box are held by the Accelerator Design Group, with numbers in the vicinity of 0451-ME-85009 (the assembly print).

IX. Acknowledgements

We are grateful to Nicolai Mokhov for his participation in the design phase of this project. His contribution is enclosed as

Appendix IV. We thank Max Palmer and Don Breyne both for their design work and for help in preparing this document. Sam Baker and Peder Yurista provided frequent assistance in the radiation safety estimates. Marion Richardson typed the paper with patience and accuracy.

REFERENCES

1. J.Kidd et al., "A High Intensity Beam Dump for the Tevatron Beam Abort System," IEEE Trans. Nucl. Sci., NS-28, No. 3, 2774 (June 1981).

2. E.Harms et al., "Instrumentation for the Tevatron Beam Dump," IEEE Trans. Nucl. Sci., N5-28, No. 3, 2771 (June 1981).

3. Michael Harrison, "The Tevatron Abort System," Fermilab publication, UPC-153, (November 1981).

4. F. Turkot, "The New Main Ring Abort System," Fermilab publication, TM-1049, (May 1981).

5. N.V.Mokhov and A.VanGinneken, "Calculations of Energy Deposition Densities in High Energy Accelerator Targets," Fermilab publication, TM-977, (1980).

6. W.Kalbraier, W.C.Middelkoop, P.Sievers, "External Targets at the SPS," CERN Lab II/BT/74-1 (1974); K.Teutenberg, P.Sievers, W.C.Middelkoop, "Absorber Blocks for Internal and External Beam Dumping at the SPS," CERN Lab II/BT/74-4 (1974); C.Hauviller, H.Schonbacher, A.VanSteenbergen, "Beam Dump Absorber for the 400×400 GeV^2 $\bar{p}p$ Superconducting Large Storage Rings," CERN-ISR-GE/79-4 (1979).

7. R.D.Brown and D.L.Grisham, "Graphite Targets at LAMPF," IEEE Trans. Nucl. Sci., to be published (June 1983), and private communications.

8. A.VanGinneken and M.Awschalom, "High Energy Particle Interactions in Large Targets," Vol. 1, Fermilab (May 1975).

9. J.D.Cossairt, N.V.Mokhov, C.T.Murphy, "Absorbed Dose Measurements External to Thick Shielding at a High Energy Proton Accelerator: Comparison with Monte-Carlo Calculations," Nucl. Instrum. Methods 197, 465-472 (1982).

10. Peter J. Gollon, "Soil Activation Calculations for the Anti-Proton Target Area," Fermilab publication TM-816 (September 1978).

11. A.M.Jonckheere, "Acquifer Dilution Factors of Ground Water Activity Produced Around Fermilab Targets and Dumps,", Fermilab publication TM-838, (December 1978).

12. R.H.Thomas and S.V.Thomas, "Variance and Regression Analyses of Moyer Model Parameter Data - A Sequel," preprint LBL-16025, Lawrence Berkeley Laboratory (April 1983); submitted to Health Physics.

13. Department of Energy Manual 5480.1, Chapter XI.

14. See Reference 8, p. 50.

15. Suzanne A. Gronemeyer, ed., "Radiation Guide," Fourth Edition, Chapter 12.2, Fermilab (April 1983).

16. See Reference 8, p. 42-43.

17. Sam Baker, private communication.

18. Environmental Protection Agency National Interim Primary Water Regulations; Code of Federal Regulation, Title 40, Part 141.

19. Peder Yurista, private communication.

20. However, the β^+ stops in the aluminum wall and produces two gamma rays.

21. Design Report, Superconducting Accelerator, Fermilab, p. 226, (May 1979).

22. C.T.Murphy, "Geometry and Coordinates of the Abort Dump and Beam Pipes," Fermilab publication TM- , (August 1983).

TABLE I. Summary of limits on proton intensity to the abort dump resulting from various radiation hazards. The column "Ref." refers to the section of this paper which discusses the problem.

Hazard	Ref.	Limit	Proton Intensity Limit
1. Ground water activation	VI-A	2.44×10^{17} stars/year	7.7×10^{17} protons/yr
2. Off-site muons	VI-C	170 mrem/yr	63.0×10^{17} protons/yr
3. On-site muons	VI-C	2.5 mrem/hr for unposted regions	2.5×10^{15} protons/hr
4. Neutron dose rate	VI-D	2.5 mrem/hr	4.0×10^{17} protons/hr
5. Tritium activation of LCW water	VI-F	20 pCi/mℓ in 10 yrs.	85.5×10^{17} protons/yr
6. Quenching magnets in tunnel	VI-G	2.5×10^{7} GeV/cm^3	6.8×10^{16} protons/pulse
7. Cracking the graphite	II	$\Delta T<2290°C$	5.9×10^{13} protons/pulse

Table II. Breakdown of distribution of star density from abort dump in various regions of controlled and uncontrolled soil. See Fig. 3.

Region	Stars/Incident Proton	
	Run I	Run II
All controlled granular fill	0.404	0.394
Uncontrolled fill and soil:		
Upstream	0.005	0.006
Downstream	0.002	0.0002
Above	0.021	0.105
Below	0.235	0.212
Outside	0.005	0.002
Inside	0.007	0.030
Sum, uncontrolled fill and soil	0.275	0.356

FIGURE CAPTIONS

1. Isometric overview of entire abort dump shielding mass. Inset: Cross section of upstream end of dump illustrating its position with respect to the tunnel and berm.
2. Isometric cutaway view of the aluminum-graphite core box.
3. Scale cross section of dump at the upstream end of the graphite.
4. Scale cross section of dump along the beam direction.
5. Star density as a function of energy at various radii in the dump, at the shower maximum in z (the coordinate along the beam direction), as predicted by the program CASIM.
6. Muon dose rate per incident proton at ground level as a function of distance from the dump along the projected beam direction. Lower insert: Elevation of the earth with respect to the projected beam.
7. Muon dose rate as a function of elevation above the surface of the earth at the site boundary.
8. Star density as a function of z (distance along the beam beginning at the first piece of graphite) at two radii in the core box.
9. Cross section of the dump at the upstream end illustrating the details of the steel shielding blocks.
10. Blueprint of lifting fixtures necessary to remove the core box from the shielding mass.
11. Scale drawing of the aborted beam apertures between C-12 and C-13 for the Main Ring and the Tevatron, in the vertical and horizontal planes.
12. Beam apertures of Fig. 11 masked onto the position detector just upstream of the abort dump. Solid lines: Outer limit permitted for all particles to avoid scraping on apertures. Dotted lines: Outer limit allowed for beam centroids.

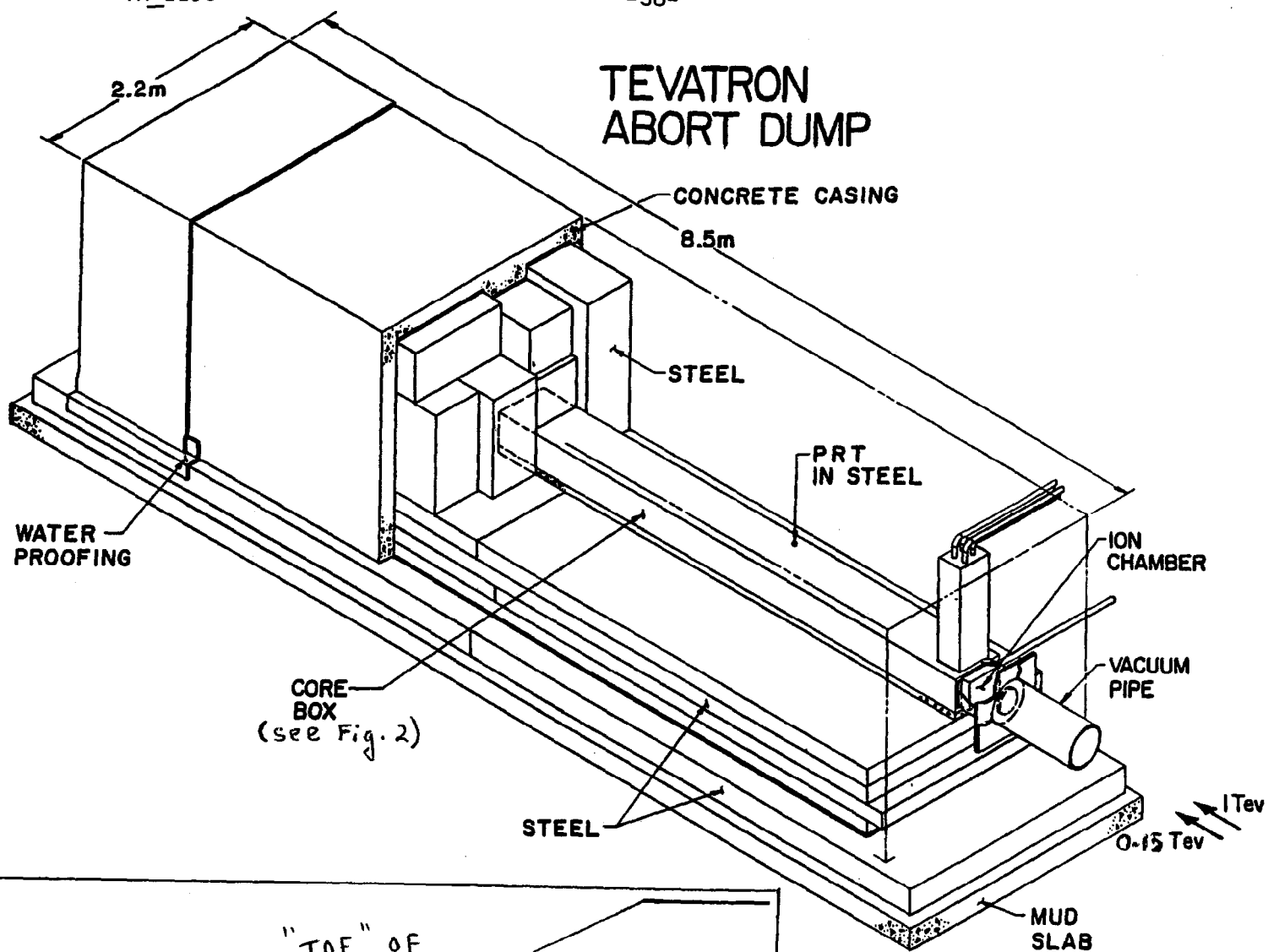
TEVATRON
ABORT DUMP
2.2m
8.5m
CONCRETE CASING
STEEL
PRT
IN STEEL
WATER
PROOFING
ION
CHAMBER
VACUUM
PIPE
CORE
BOX
(see Fig. 2)
STEEL
1 Tev
0-15 Tev
MUD
SLAB

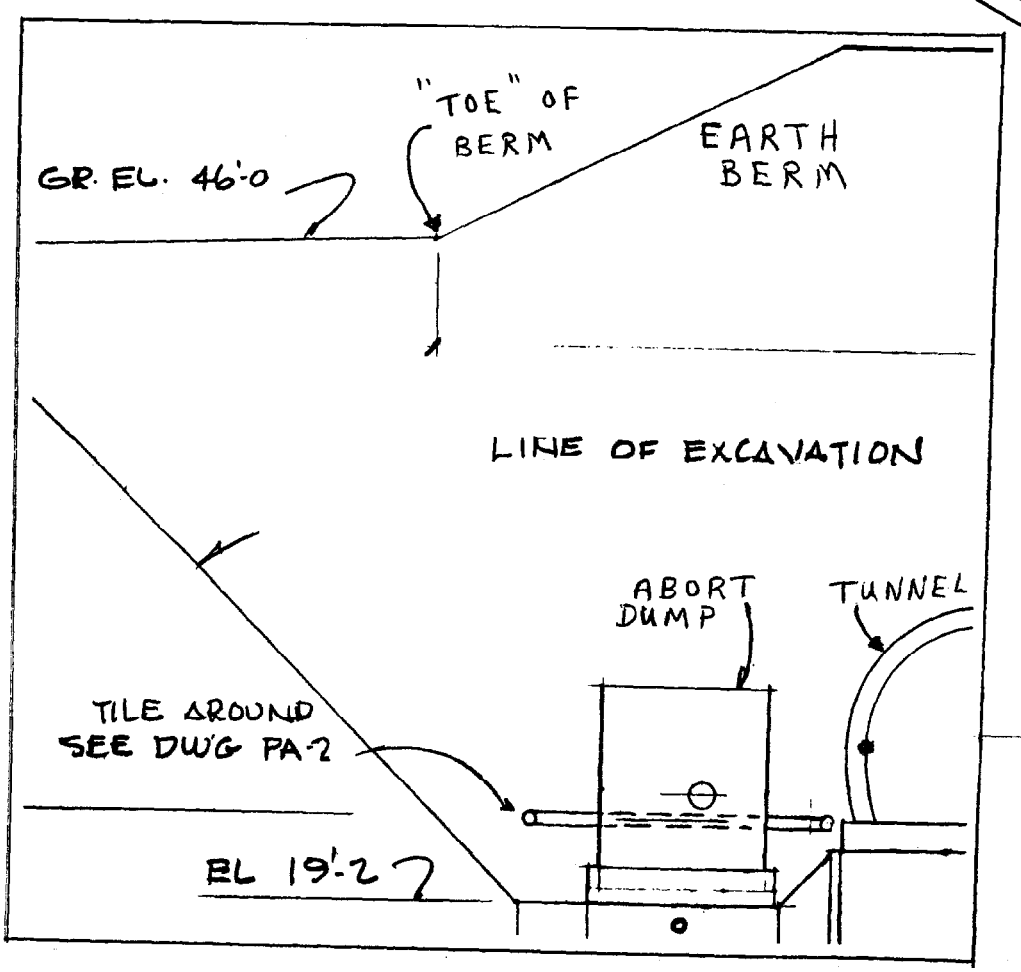
"TOE" OF
BERM
EARTH
BERM
GR. EL. 46'-0
LINE OF EXCAVATION
ABORT
DUMP
TUNNEL
TILE AROUND
SEE DWG PA-2
EL 19'-2"

Fig. 1

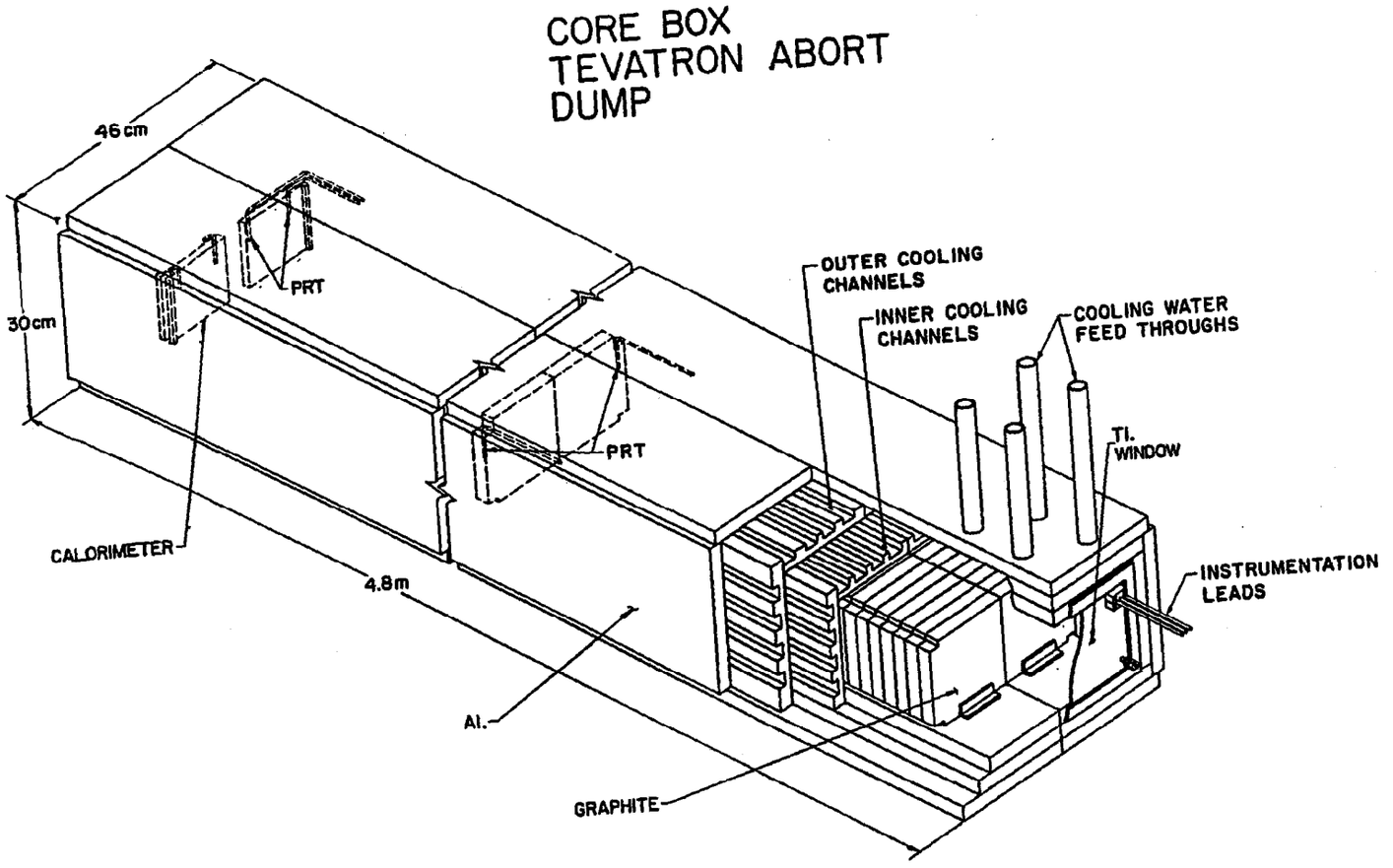
CORE BOX
TEVATRON ABORT
DUMP
46cm
30cm
PRT
PRT
OUTER COOLING
CHANNELS
INNER COOLING
CHANNELS
COOLING WATER
FEED THROUGHS
Ti.
WINDOW
INSTRUMENTATION
LEADS
CALORIMETER
4.8m
Al.
GRAPHITE

Fig. 2

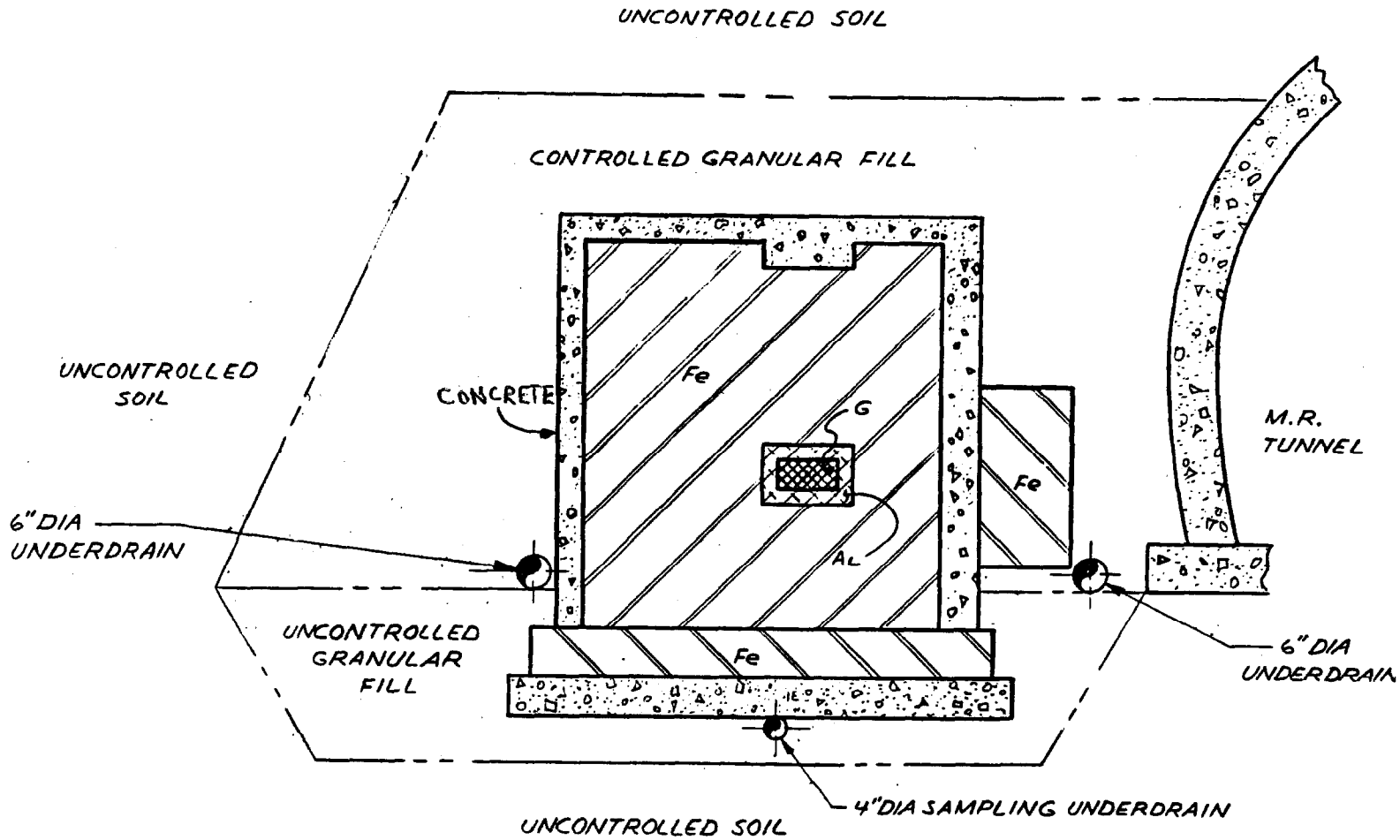

TEV ABORT DUMP

CROSS SECTION LOOKING DOWNSTREAM

Fig. 3

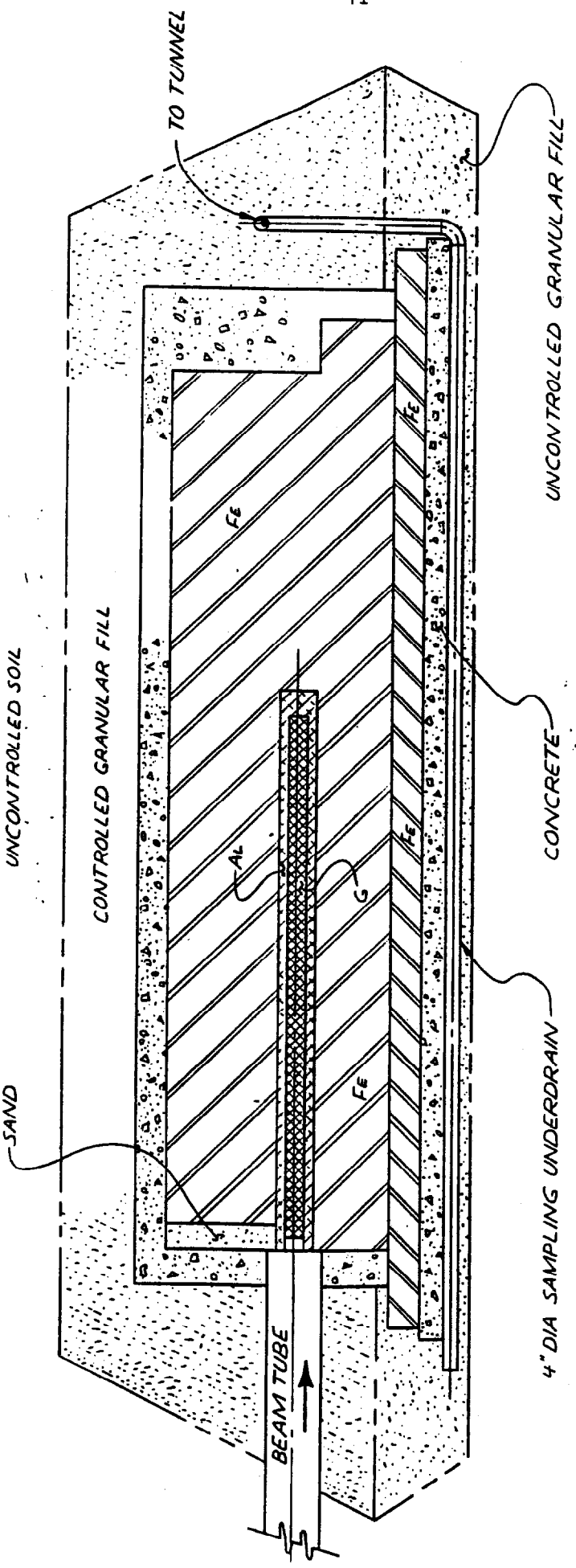

T_{EV} ABORT DUMP
CROSS SECTION ALONG BEAM

Fig. 4

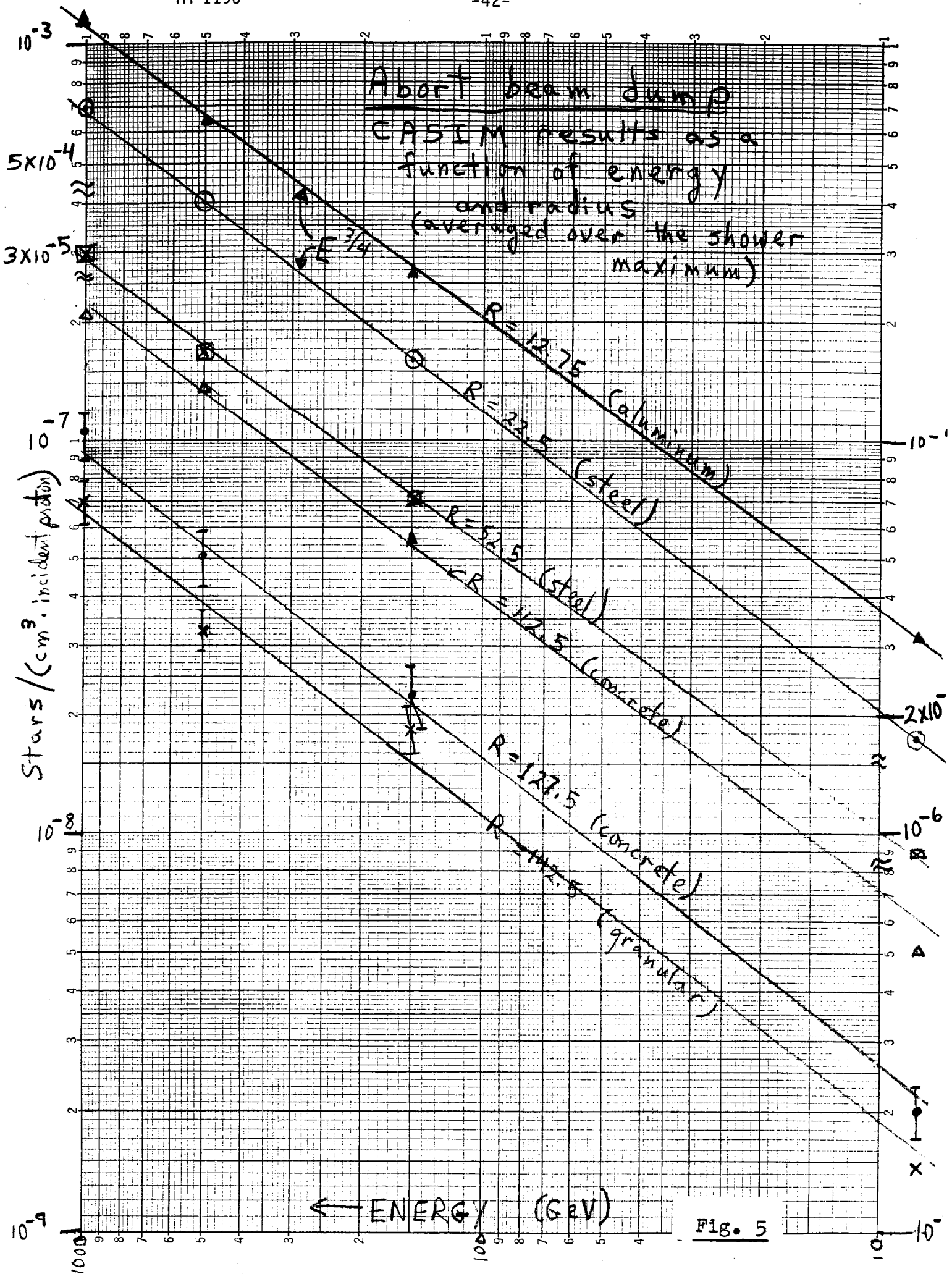
Abort beam dump
CASIM results as a function of energy and radius (averaged over the shower maximum)
$E^{3/4}$
R = 12.75 (aluminum)
R = 22.5 (steel)
R = 52.5 (steel)
R = 127.5 (concrete)
R = 177.5 (concrete)
R = 477.5 (granular)
Stars/(cm³ · incident proton)
ENERGY (GeV)
10^{-3}
5×10^{-4}
3×10^{-5}
10^{-7}
2×10^{-7}
10^{-8}
10^{-9}
10^{-6}
1000
100
10
1

Fig. 5

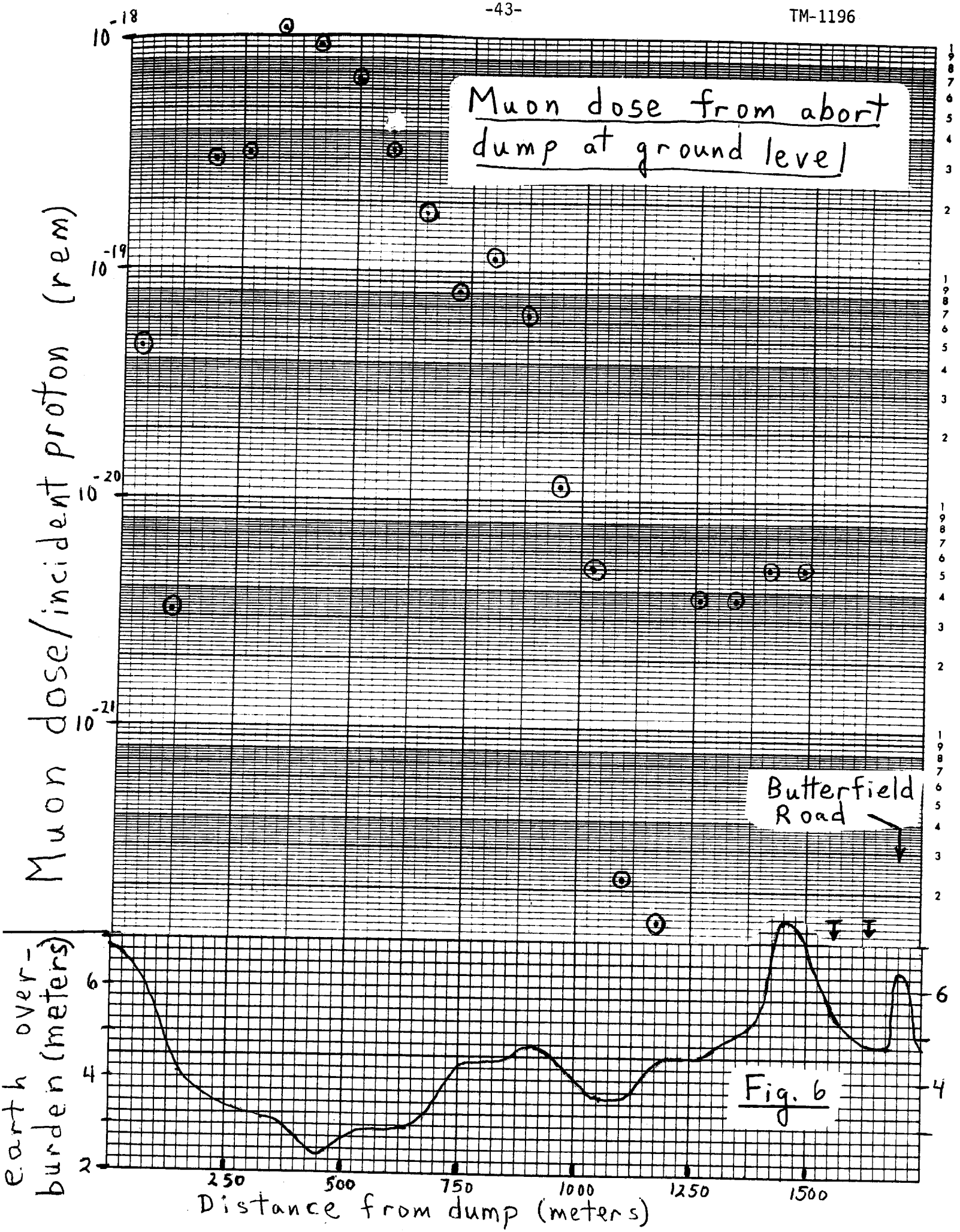
Muon dose from abort dump at ground level
Muon dose/incident proton (rem)
10^{-18}
10^{-19}
10^{-20}
10^{-21}
Butterfield Road
earth over-burden (meters)
2
4
6
250
500
750
1000
1250
1500
Distance from dump (meters)

Fig. 6

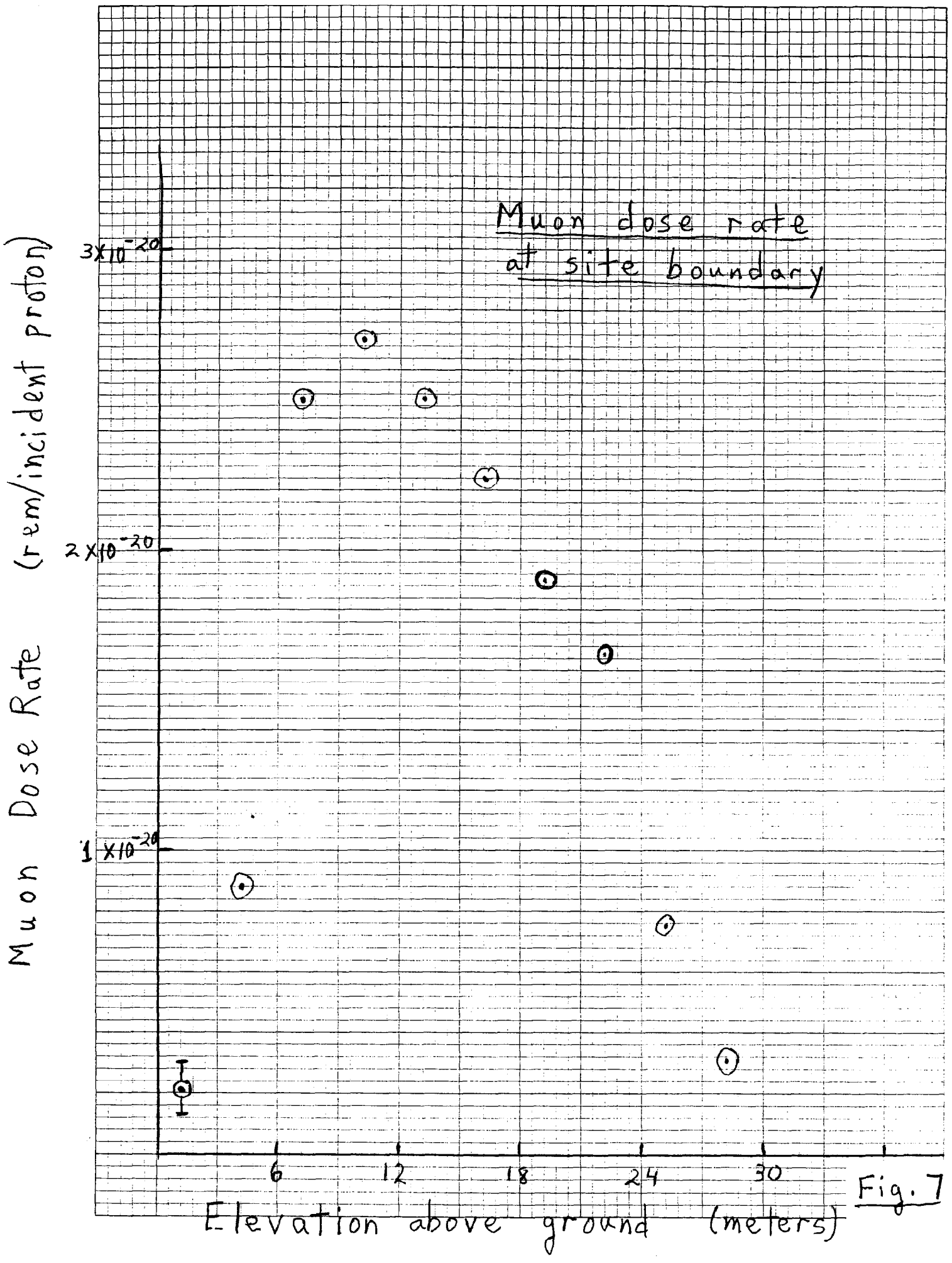
Muon dose rate
at site boundary
Muon Dose Rate (rem/incident proton)
3X10^-20
2X10^-20
1X10^-20
6
12
18
24
30
Elevation above ground (meters)

Fig. 7

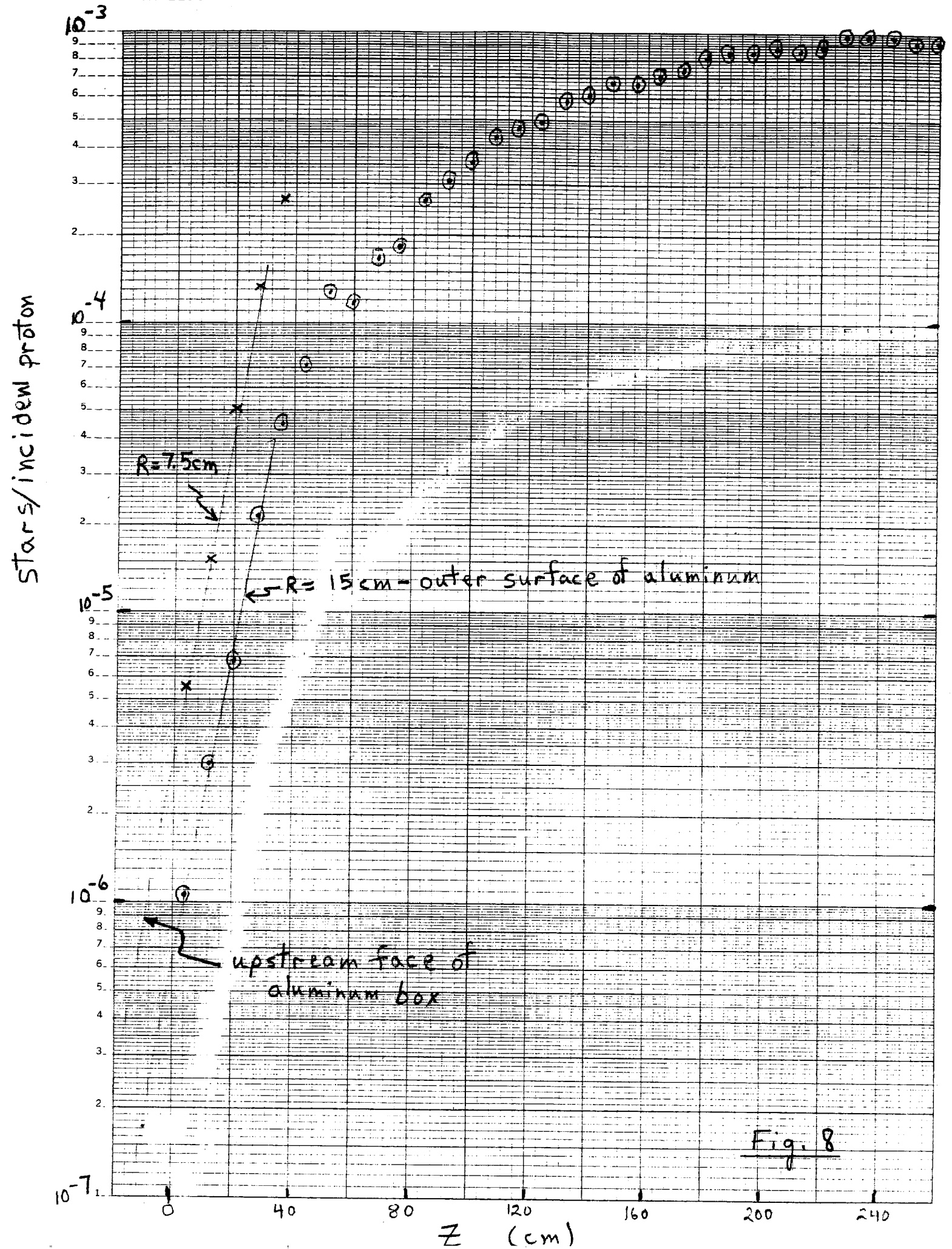
Stars/incident proton
10^{-3}
10^{-4}
10^{-5}
10^{-6}
10^{-7}
R = 7.5 cm
R = 15 cm - outer surface of aluminum
upstream face of aluminum box
0
40
80
120
160
200
240
Z (cm)

Fig. 8

3A CROSS SECTION (CONST'N SIMILAR TO
1/2"=1'0

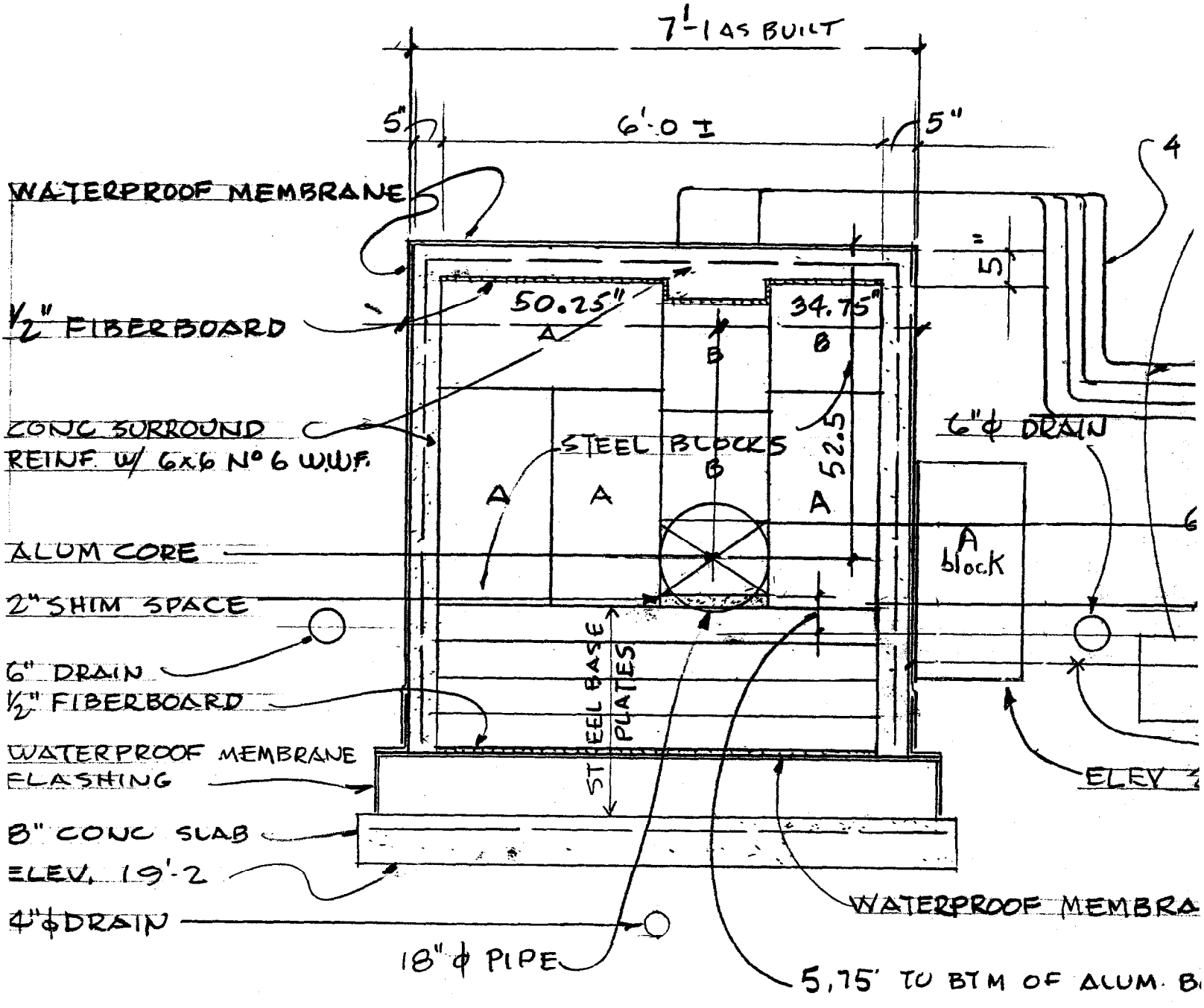

2A CROSS SECTION
1/2"=1'0

Fig. 9

REV.	DESCRIPTION	DRAWN	DATE	APPD.	DATE

ITEM NO.	PART NO.	DESCRIPTION OR SIZE	QTY. REQ.
		PARTS LIST	

UNLESS OTHERWISE SPECIFIED
FRACTIONS ± 1/16 | DECIMALS ± | ANGLES ±
1. BREAK ALL SHARP EDGES 1/64 MAX.
2. DO NOT SCALE DWG.
3. DIMENSIONING IN ACCORD WITH ANSI Y14.5 STD'L.
MAX. ALL MACHINED SURFACES

ORGINATOR
DRAWN BREYNE 5-13-80
CHECKED
APPROVED
USED ON
MATERIAL- STEEL

FERMI NATIONAL ACCELERATOR LABORATORY
UNITED STATES DEPARTMENT OF ENERGY

BRACKET-LIFTING BEAM ABORT CORE ASSEM. MAIN RING

SCALE FULL | PLANED | DRAWING NUMBER 0451MC84975 | REV.

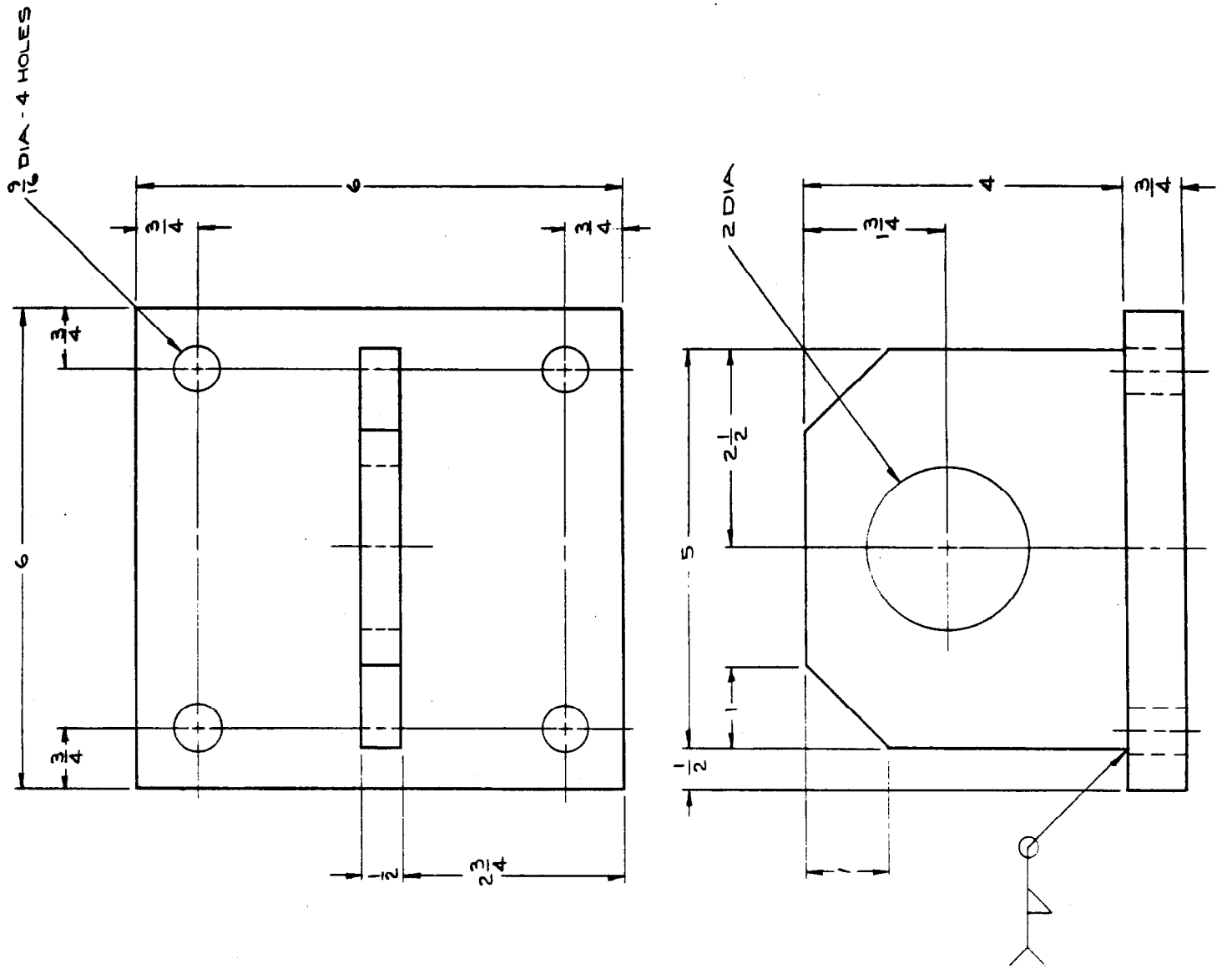

Fig. 10

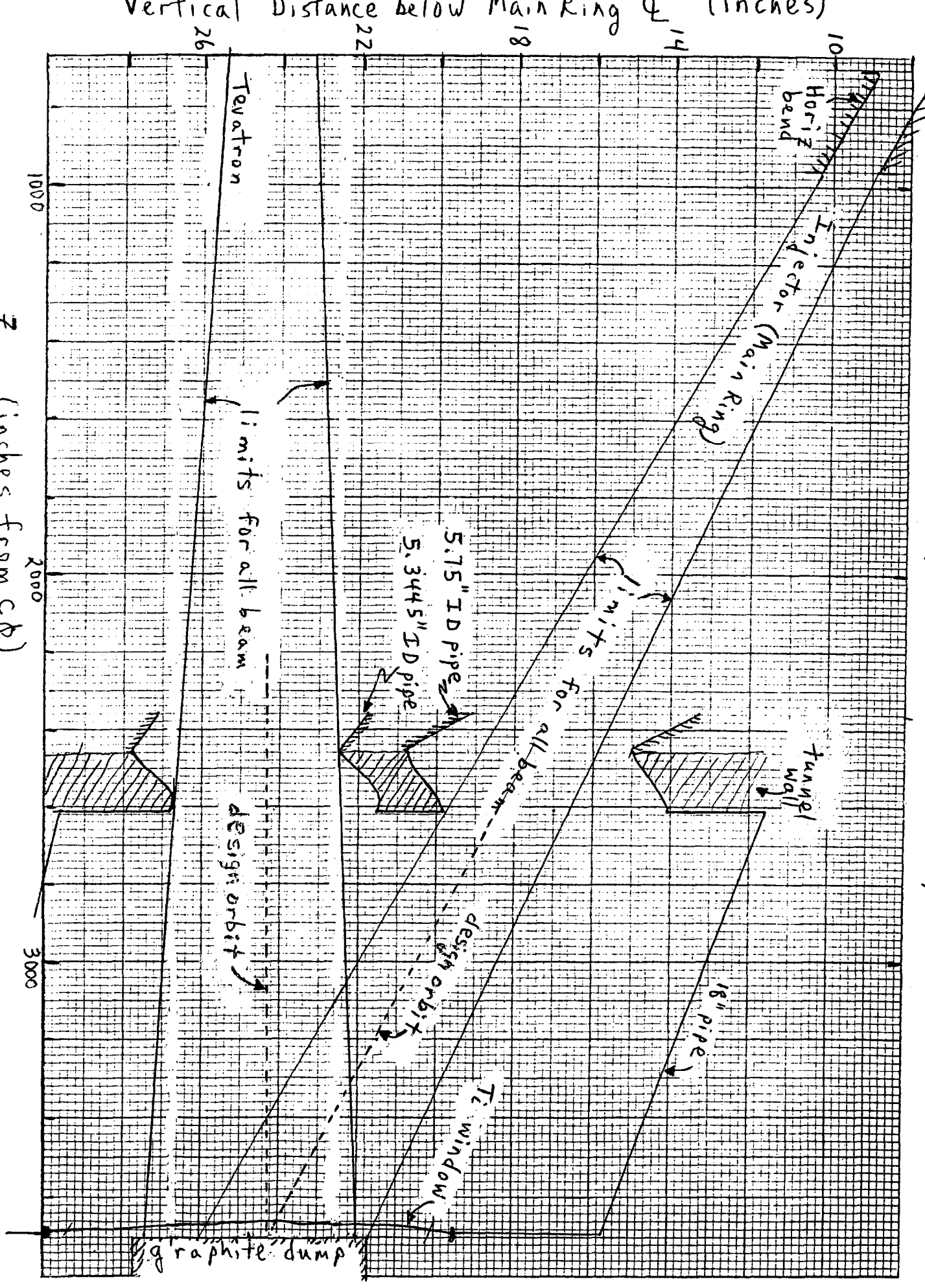
Vertical Distance below Main Ring ℄ (inches)
26
22
18
14
10
Z (inches from C℄)
1000
2000
3000
Tevatron
limits for all beam
design orbit
5.345" ID pipe
5.75" ID pipe
limits for all beam
design orbit
Tc window
graphite dump
Horiz bend
Injector (Main Ring)
tunnel wall
18" pipe
Hidden vertical apertures, abort system

Figure 11

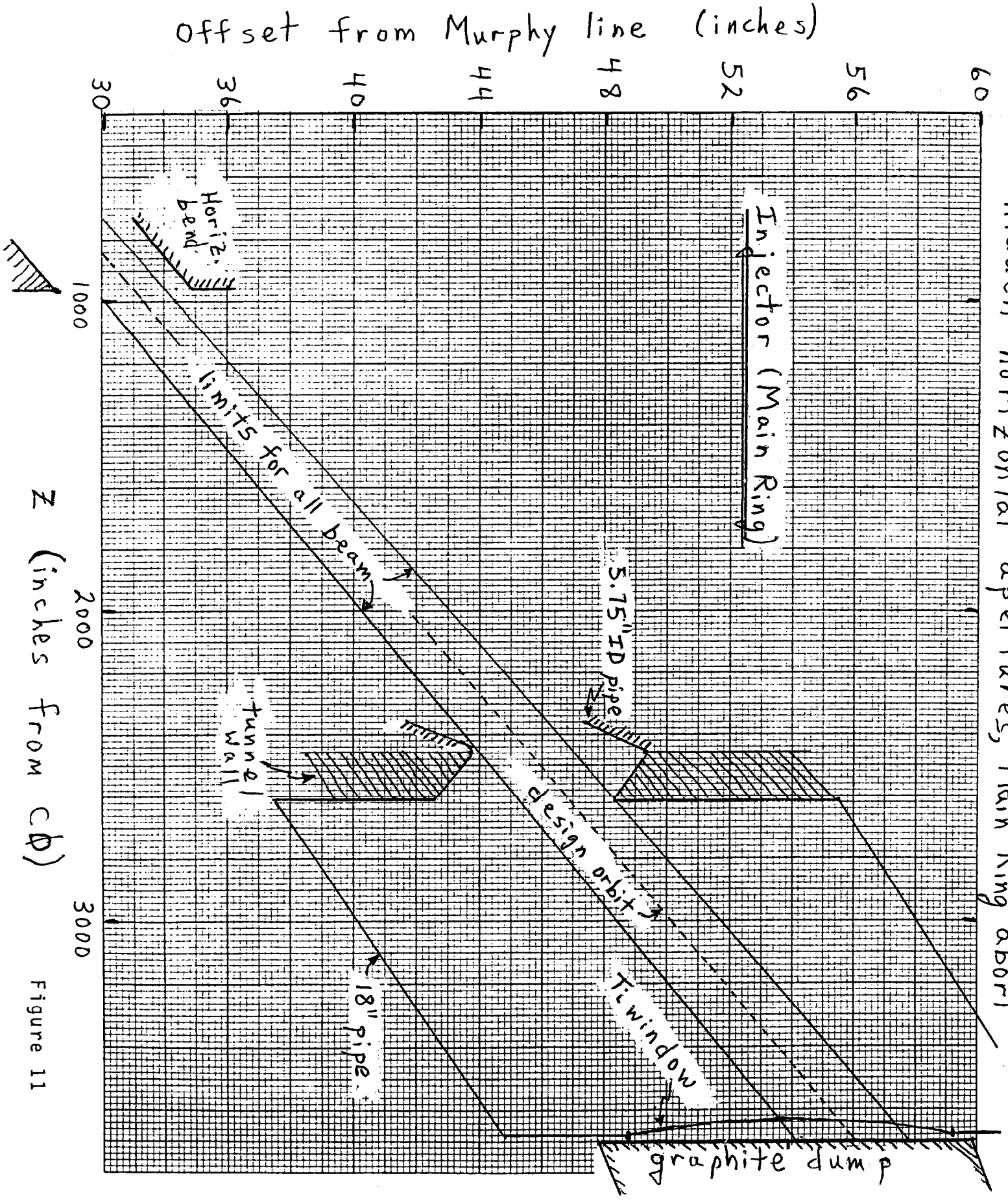
Hidden horizontal apertures, Main Ring abort
Offset from Murphy line (inches)
30
36
40
44
48
52
56
60
Injector (Main Ring)
Horiz. bend
limits for all beam
5.75" ID pipe
tunnel wall
design orbit
Ti window
graphite dump
18" pipe
1000
2000
3000
Z (inches from CØ)

Figure 11

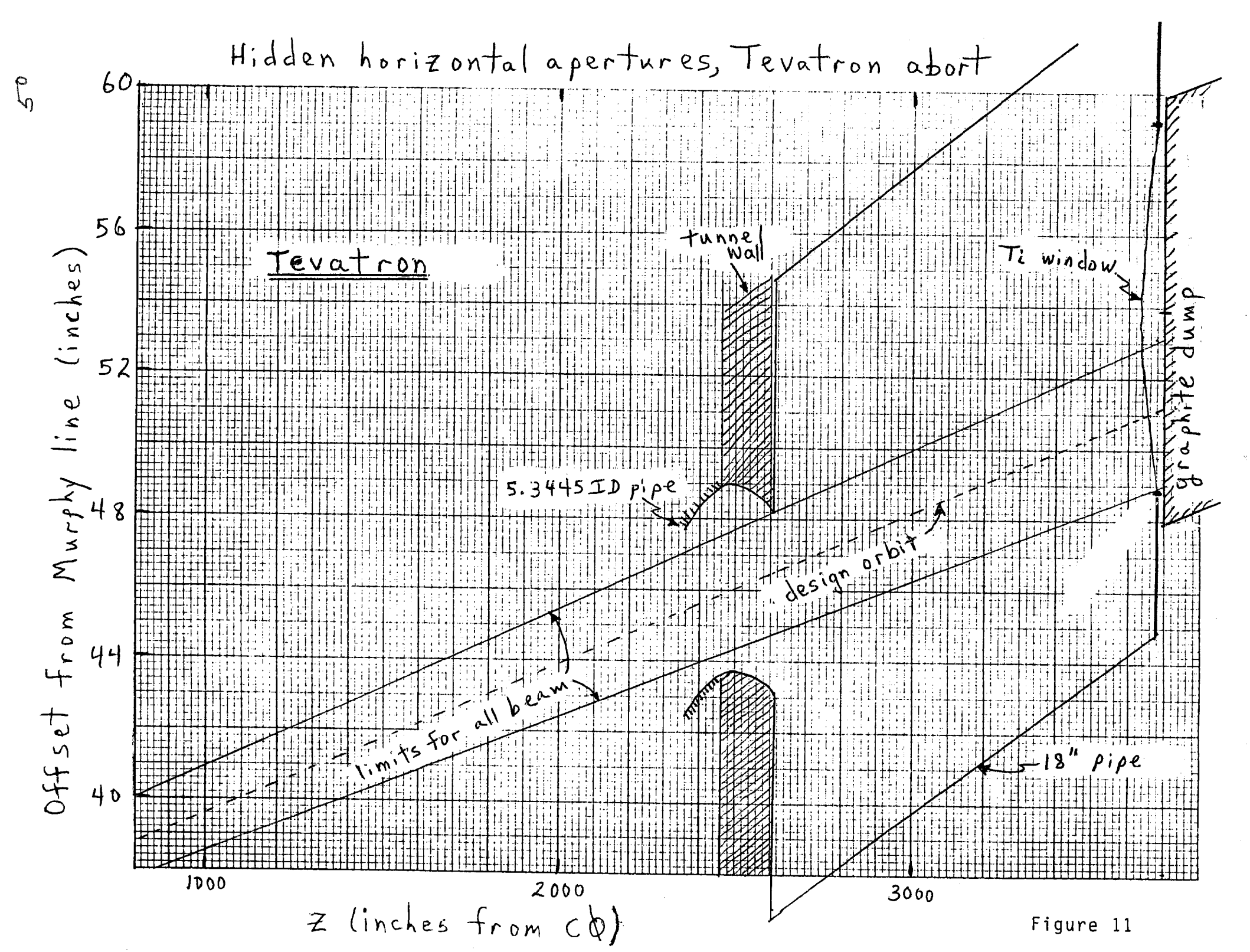
Hidden horizontal apertures, Tevatron abort
Tevatron
tunnel wall
Ti window
graphite dump
5.3445 ID pipe
design orbit
limits for all beam
18" pipe
Offset from Murphy line (inches)
60
56
52
48
44
40
1000
2000
3000
z (inches from C0)

Figure 11

Projection of abort pipe apertures onto upstream face of graphite dump and ion chamber

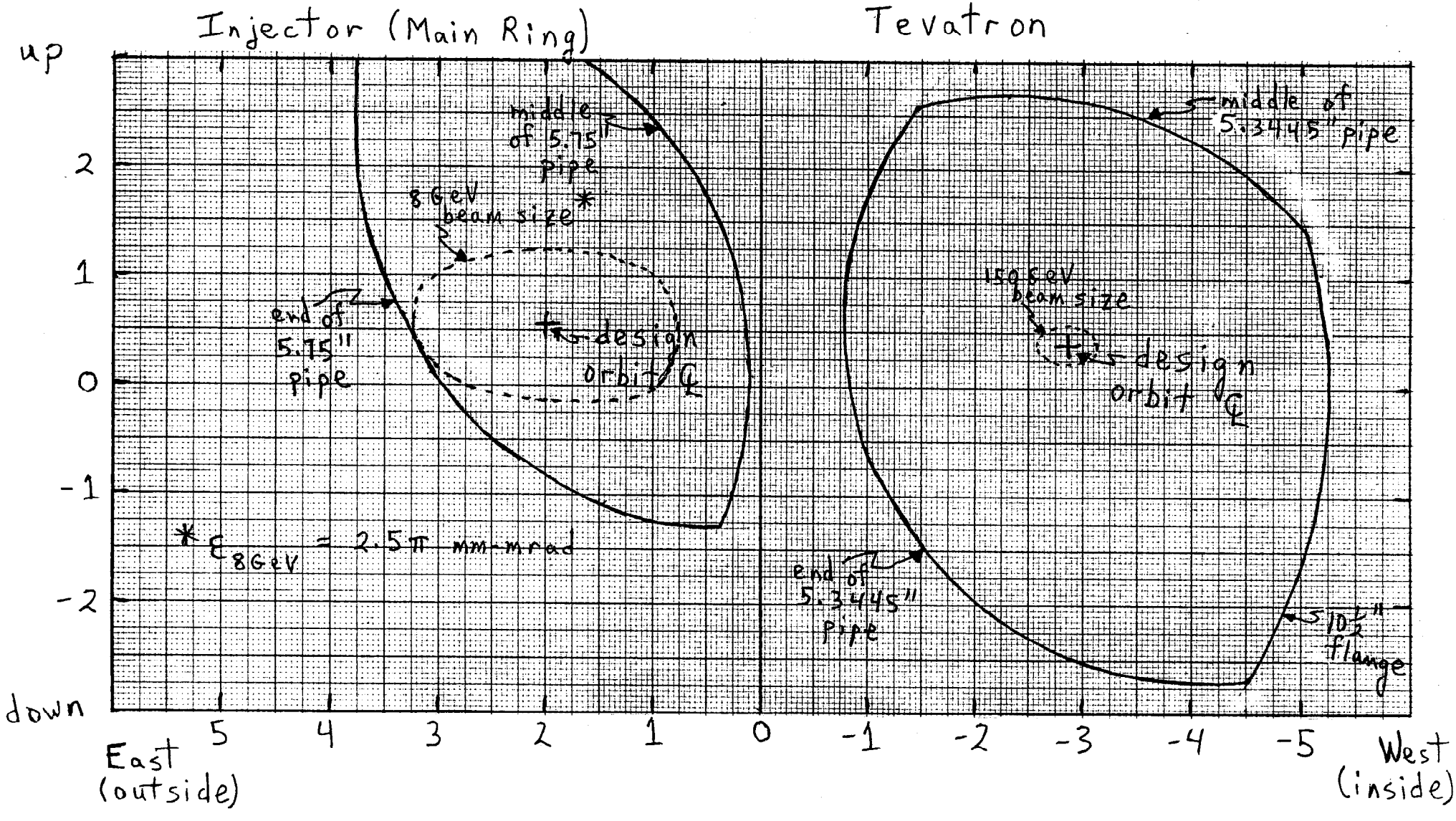

Figure 12

APPENDIX I

Submitted to the 1981 Particle Accel. Conf., March 11-13, Washington DC

A HIGH INTENSITY BEAM DUMP FOR THE TEVATRON BEAM ABORT SYSTEM

J.Kidd, N.Mokhov,† T.Murphy, M.Palmer, T.Toohig, F.Turkot and A.VanGinneken
Fermi National Accelerator Laboratory,* Batavia, Illinois 60510

Introduction

The beam abort system proposed[1] for the Fermilab Tevatron Accelerator will extract the proton beam from the ring in a single turn (~20μs) and direct it to an external beam dump. It is the function of the beam dump to absorb the unwanted beam and limit the escaping radiation to levels that are acceptable to the surrounding populace and apparatus. In addition, it is clearly desirable that it be maintenance free and have a lifetime equal to that of the accelerator, 10-20 years. A beam dump that is expected to meet these requirements has been designed and constructed. We describe below the detailed design of the dump, including considerations leading to the choice of materials.

Parameters of the Beam and Dump Specifications

The extreme values of the parameters of a single aborted beam pulse are:

1. energy of protons 1 TeV
2. number of protons 2×10^{13}
3. total kinetic energy 3.2 MJ
4. time duration 20μs
5. transverse beam size (σ of a Gaussian in mm) as a function of drift distance, s (in m), from the downstream end of the CØ long straight section

$$\sigma_x = 0.520\sqrt{1+\frac{(s+55)^2}{60^2}}\ ,\quad \sigma_y = 0.455\sqrt{1+\frac{(s-1.3)^2}{60^2}}$$

$\sigma_{x'} = \sigma_{y'} = 7.5$ μrad.

6. transverse variation of beam position ±1.5 cm.

With regard to repeated beam aborts and the yearly average beam we have the following specifications:

7. Short term continuous operation: 2×10^{13} ppp at 1 TeV with a 23s cycle time for 4 hours duration <power input> = 139 kW
8. Yearly proton flux: 3.5×10^{17} p/yr at 1 TeV.

The aborted beam line geometry is such that at the end of the CØ long straight section it is directed radially outward by 8.1 mr with respect to the tangent to the circle of the Tevatron and is 2.5 cm above and parallel to the plane of the closed orbit. On average this plane is ~6m below ground level. Given this geometry, there is a minimum distance (s) from the end of the CØ straight section to the dump, dictated by the need to have sufficient transverse separation (2.1 m) between the dump and the superconducting magnets of the Tevatron ring to avoid quenches induced by transient radiation from the dump during beam aborts; $s_{min} = 55$m. The cost of civil construction for the dump argues for keeping s close to s_{min}; the incremental cost was estimated at 10K$/m.

Choice of Material for Dump Core

The reliability of the dump depends critically on the integrity of the material which makes up the upstream five hadronic absorption lengths (λ_a) of the core. Operating experience both at CERN and Fermilab has clearly demonstrated the capability of 400 GeV proton beams of similar size and intensity to fracture or melt solid materials in the immediate vicinity of the line of the beam as a result of high local energy deposition and large temperature gradients. The peak energy density can be reduced by: (a) enlarging the transverse size of the incident beam, (b) going to materials of lower mass density and lower atomic number, and (c) inserting matter-free drift spaces in the absorber. The chance of harmful material damage is reduced by using materials with high melting points and high thermal shock resistance. A measure of the thermal shock resistance of a solid material is given by the temperature differences ΔT_{cc} and ΔT_{ct}:

$$\Delta T_{cc} = \frac{\sigma_c}{\alpha E}(1-\nu);\qquad \Delta T_{ct} = \frac{6\sigma_t}{\alpha E}(1-\nu) \qquad (1)$$

where α = linear thermal expansion coefficient, E = Young's modulus, ν = Poisson's ration, and σ_c and σ_t are the compressive and tensile strenghts of the material. Given a localized temperature spike in the material with maximum temperature difference ΔT, then ΔT_c is the temperature difference at which the stress in the material equals the strength of the material.

For a given beam and a given absorber material and geometry (including possible drift spaces), ΔT is calculated using a Monte Carlo nuclear cascade program called MAXIM[2]; more precisely the program calculates the spatial distribution in the absorber of the energy density, ε, deposited by ionization from the charged particles produced in the cascade. The specific heat, C_p, of the material is then used to calculate the temperature distribution corresponding to ε(r) (ε_{max} is the significant quantity); idealy if $(T_{max} - T_{initial}) < \Delta T_c$, then the material will not be damaged. For ductile materials, such as Al, Cu, and Fe, it may be permissible to exceed the criterion; however, for

TABLE I. Properties (T = 25°C)

Material	ρ g/cm³	λ_a cm	λ_{rad} cm	C_p CAL/°C-g	α 10^{-6}/°C	E 10^6 psi	σ_c 10^3 psi	σ_t 10^3 psi	λ w/cm-°C
Graphite (H-489)	1.71	45.1	25.0	0.19	2.3+ 3.0Δ	1.2 0.95	6.5 6.5	2.1 2.0	1.42
BeO	2.85	27.0	14.6	0.25	9	53	225	25	2.6

+with grain, Δacross grain. Graphite softens at 2600°C, BeO softens at 1800°C.

*Operated by Universities Research Association, Inc. under contract with the U.S.Department of Energy.

†Institute for HEP, Serpukhov, USSR

TABLE II. $N_p = 2\times10^{13}$, $\sigma_x = 1.20$ mm, $\sigma_y = 0.68$ mm

Material	ΔT_{cc} °C	ΔT_{ct} °C	ρH^* kJ/cm³	ε_{max} kJ/cm³	$\Delta T(\varepsilon_{max})$ °C	$\frac{\varepsilon_{max}}{\rho H}$	N_{pmax} 10^{13}
BeO (I)	471	314	2.08	7.15	1400	3.44	0.6
BeO (II)	471	314	2.08	3.53	750	1.70	1.2
Graphite	2280	4210	6.89	2.40	880	0.35	5.7

(I) solid BeO

(II) 90 cm of BeO spaced over 215 cm

* $\rho H = \rho \int_{298}^{298 + \Delta T_{cc}} C_p \, dT$

brittle materials which do not tolerate plastic deformations, it would appear to be a reasonable criterion.

A number of studies[3] have been made of the suitability of various materials; only solid forms were considered because of the additional problem of conducting away the maximum average power input of 139 kW. The best candidates were Be, BeO ceramic, and graphite; they all fall in the brittle category. The approach adopted was to explore what absorber geometry would be required for BeO and graphite for the natural beam size at s = 70 m (the first logical location beyond $s_{min} = 55$ m from the point of view of interconnections between dump and existing tunnel). Some properties of these materials[4] are given in Table I. The results of the nuclear cascade calculation are given in Table II.

Calculations with a graphite absorber were made[5] for a range of incident proton energy, E, (0.1 to 5.0 TeV) and as a function of $B(\equiv 4\pi \sigma_x\sigma_y$, an area which contains 86.5% of the beam for $\sigma_x = \sigma_y$; range 10^{-2} to 10^{4} mm²). The dependence of ε_{max} on E and B were found as follows:

$$\varepsilon_{max}(B = 12 \text{ mm}^2) = C_1 E^{1.44}, \quad E = .3 - 3 \text{ TeV}$$

$$\varepsilon_{max}(E = 1 \text{ TeV}) = \frac{C_2}{B^{.34}}, \quad B = 3 - 100 \text{ mm}^2 \qquad (2)$$

ε_{max} approaches a $(B)^{-1}$ behavior only for rather large $B(>10^{4}\,\text{mm}^2)$. As a consequence one gains rather slowly in reducing ε_{max} by increasing s; e.g. to decrease ε_{max} by a factor of 2 requires changing s from 70 m to 275 m (B increases by a factor 7.4).

The results in Table II clearly indicate the superiority of a solid graphite absorber; if taken literally, this material has the capability of absorbing 5.7×10^{13} ppp without fracturing. It should not be taken literally for several reasons: (1) the calculation of ε_{max} is uncertain to at least ±30%, (2) the quasi-static stress analysis is clearly a crude approximation to the real situation.

Several of its physical properties must be taken into account in utilizing graphite as an absorber. Firstly, it oxidizes at elevated temperatures, losing 1% of its weight per day at 450°C; the presence of radiation or radiation damage enhances the oxidation rate. This argues for a dry argon atmosphere at the graphite. Secondly, graphite undergoes dimensional change under irradiation; e.g., if subjected to a flux of 1×10^{20} neutrons/cm² (~1 MeV) at 30°C, some graphite expands ~1% in the "across grain" direction. If the exposure takes place at 200°C, the expansion is a factor 10 smaller. In the neighborhood of ε_{max}, the probability of an interaction of a carbon nucleus with a high energy hadron summed over the dump lifetime (5×10^{18} p's) is comparable to that ($\sim10^{-4}$) for a 1×10^{20} n/cm² flux at 1 MeV. It seems plausible that there will be significant radiation damage effects near ε_{max}, but that they will be confined to a few mm from the beam axis, and are unlikely to cause a large-scale change in volume. In an absorber of close packed blocks, the graphite has "no place to go" even if it should become pulverized along the beam axis; heat conductivity would clearly decrease.

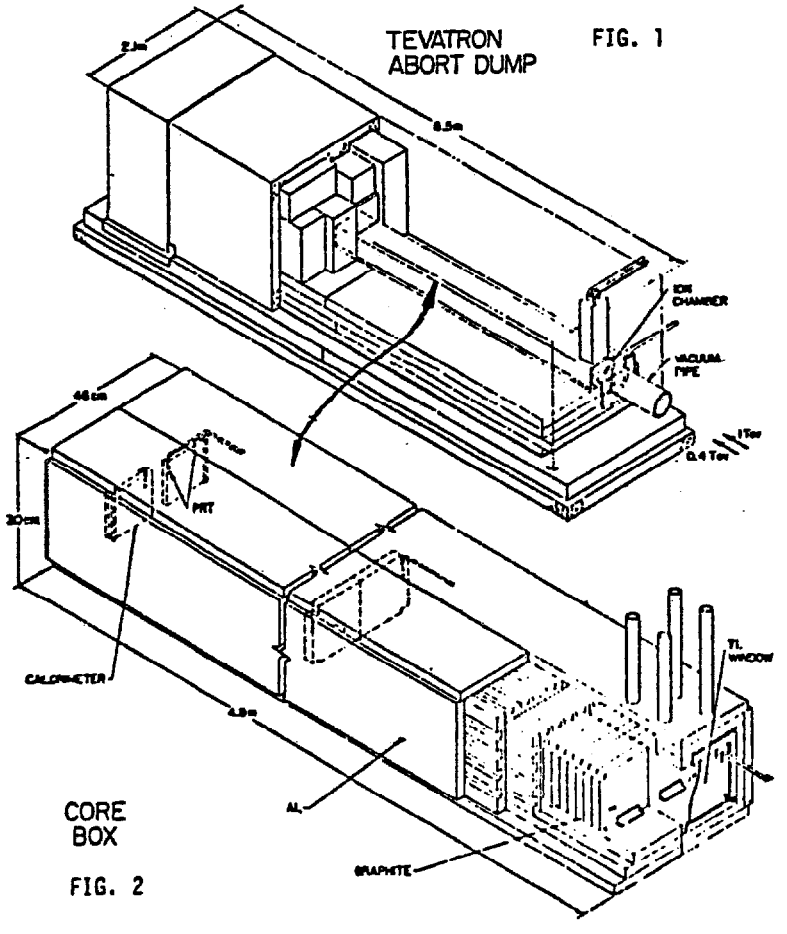

FIG. 1

FIG. 2

Overall Dump Design

The internal structure of the dump is seen in Fig. 1. The core consists of two identical side-by-side stacks of graphite blocks; a block has dimensions 15.2×15.2×2.54 cm³; 350 blocks make up the core. Longitudinal segmentation of the graphite helps reduce dynamic stress enhancement[3] that could occur from the shock wave propagating in a single long block ($v_{sound} \times 20\ \mu s$ = 3.9 cm in H489). Main Ring aborted beam impinges on the left-hand stack, Tevatron beam on the right. The graphite is contained in an aluminum box (see Fig. 2) which has cooling water flowing through its walls. The concrete "skin" which covers the steel is itself covered with a watertight Molnar (plastic) membrane. The asymmetric horizontal location of the core box in the dump is compensated by an extra row of steel blocks between dump and tunnel; this stratagem was adapted in order not to undercut the existing tunnel during excavation for foundation work.

Graphite-Filled Aluminum Core Box

Some details of the core box are given in Fig. 2. It is welded up out of 2.54 cm thick, 4.8 m long aluminum plate (type 5083 H112[6]). The wall is made of three plates; water passages are milled in the inner two. The left and right halves of the box were fabricated separately and leak tested. The horizontal inside surfaces were then milled flat and parallel to ±0.05 mm. The transverse dimensions of the graphite blocks were milled to fit the transverse dimensions of the box; the 15 cm × 15 cm surfaces of the graphite were saw-cut (as provided by the manufacturer). The inner surfaces of the box were given a thin coating of graphite paint (alcohol base) and then the two half-boxes were stacked with graphite. The two halves were then clamped together and the outside center welds made. The interior of the box is hermetically sealed; a 2 cm thick plate closes the downstream end, a 0.6 mm titanium window closes the upstream end. Two gas lines and six temperature transducer leads exit through the titanium window.

Thermal Considerations

The cascade calculations by MAXIM on the spatial distribution of heat energy deposition in the graphite (let Z = distance into graphite from front face) yields:
1. When integrated over transverse dimension, the distribution has a broad maximum at Z = 2.2 m (Z_M), FWHM = 2.5 m; the energy per graphite block at Z_M is 16.0 kJ (a ΔT = 20°C if uniform over the block) corresponding at 700 w per block average power at a 23 s cycle.
2. The maximum, ΔT = 880°C, occurs on axis at Z = 1.2 m.

Measurements were made of the heat transfer properties of the graphite-to-aluminum interface. A saw-cut graphite surface on a smooth aluminum surface under low pressure (3.5 psi) gave a thermal transfer coefficient, K, of 0.03 w/cm²-°C; milling the graphite to a flat finish increased K to .08 w/cm²-°C. With increasing pressure, K rises smoothly reaching 0.16 w/cm²-°C at 35 psi; a thin coat of graphite paint increased K by 11%.

In order to make an estimate of temperature build up under continuous beam aborts with a 23 s cycle, a steady-state analysis (see Ref. 3) with a cylindrical geometry model of the core box was made. Assuming K = 0.15 w/cm²-°C, heat transfer over 54% of the edge area of the block, and a cooling water temperature of 35°C, this calculation gives a central temperature of 140°C. Immediately following the next abort pulse, the peak temperature becomes 790°C (at Z_M). Using the thermal diffusivity of graphite at 800°C (0.15 cm²/s) and a 1 mm length, the thermal spike will halve in about 30 ms. The unconstrained thermal expansion of a graphite block in the 15 cm dimension is estimated to be 0.04 mm.

Each of the two independent water cooling circuits in the aluminum core box has a measured flow rate of 72 gpm (110 psi drop). An average power input of 139 kW into one cooling loop at this flow rate makes a 7.2°C temperature rise.

Radiation Considerations

The basic dump block in Fig. 1 has dimensions 2.1×2.6×8.5 m³ (W×H×L); in terms of hadronic absorption lengths it is equivalent to a block of Fe 1.67×2.08×4.77 m³ with an additional 0.46 m at beam level on the tunnel side. Hence in units of λ_a, it has 6.1 λ_a transverse to the beam and 27.9 λ_a along the beam (15 of the 2×10^{13} protons make it through unscathed). The program CASIM was used to evaluate pulsed and residual radiation levels in various locations.

1. Tunnel Radiation - The superconducting wire of the Tevatron dipoles is 2.5 m distance from Z_M. At full field, fast (<1 ms) heat energy deposition of ~0.5 mJ/g will induce a quench. Calculations give an energy dump of only 2 μJ/g at the inner edge of the tunnel wall. The residual radiation in the tunnel after a 30 d irradiation (average of 1.1×10^{10} p/s) and a 1 d cooldown is calculated to be 5 mrem/hr.
2. Soil Activation - The program computes the total number of "stars," nuclear interactions, produced in the "unprotected" soil (soil below the level of the drain tile). It yields 3.2×10^{16}/yr, about 13% of the limit for the total Fermilab site. A 10 cm diameter drain pipe has been placed in the soil beneath the dump for the purpose of monitoring the activity level in the ground water there.
3. Above Ground Dose Rates - The earth coverage directly above the dump is 6 m; the maximum expected dose rate there is 1 mrem/hr. A substantial beam of muons, about 2×10^{11} (E>1 GeV) per abort, emerges from the downstream face of the dump. A modified version of CASIM was used to calculate the dose rate of the Fermilab site boundary, a horizontal distance of 1.7 km beyond the dump, taking into account the existing earth overburden along the 1.7 km. At the boundary it predicts dose rates of 14 mrem/yr at grade level and 70 mrem/yr for 15 m above grade. The self-imposed Fermilab limit is 10 mrem/yr. The problem arises from muons scattering out of the earth and propagating in the atmosphere; about 450 m downstream of the dump the earth overburden falls to 2.4 m; it will probably be necessary to increase the overburden for a distance of ~1 km beyond the dump.

Dump Instrumentation

The position of the incident beam is measured by a segmented ion chamber placed at Z = -15 cm. Temperature is measured at five points in the dump using platinum resistance transducers (PRT).

In order to measure the integrity of the graphite with respect to beam absorption a thermal calorimeter is placed just beyond the end of the stack at Z = 4.47 m. A ΔT in the calorimeter of ~4°C is expected from a single 1 TeV beam abort; a larger ΔT would signal a "hole" in the upstream graphite absorber. A more complete description of the instrumentation is given in a following paper.

Acknowledgement

We thank H.Edwards, P.Sievers, S.Baker, and D.Cossairt for helpful discussions; the invaluable work of D.Breyne and the Fermilab machine shops also merits mention.

References

1. Design Report, 1979 Superconducting Accelerator, Fermilab (1979).
2. N.V.Mokhov and A.VanGinneken, "Calculations of Energy Deposition Densities in High Energy Accelerator Targets," TM-977, Fermilab (1980).
3. W.Kalbraier, W.C.Middelkoop, P.Sievers, "External Targets at the SPS," CERN Lab II/BT/74-1 (1974); K.Teutenberg, P.Sievers, W.C.Middelkoop, "Absorber Blocks for Internal and External Beam Dumping at the SPS," CERN Lab II/BT-74-4 (1974); C.Hauviller, H.Schonbacher, A.VanSteenbergen, "Beam Dump Absorber for the 400×400 GeV² $\bar{p}p$ Superconducting Large Storage Rings," CERN-ISR-GE/79-4 (1979).
4. The BeO ceramic is "Berlox K-150" of the National Beryllia Corp; H-389 graphite is a fine grain (0.08 mm), isostatically molded graphite made by Great Lakes Carbon Corp.
5. N.V.Mokhov, "Energy Deposition in Targets and Beam Dumps at 0.1-5 TeV," FN-328, Fermilab (1980).
6. An alloy with good corrosion resistance, typically used in marine welded structures.

APPENDIX II

INSTRUMENTATION FOR THE TEVATRON BEAM DUMP

E.Harms, B.Hendricks, G.Lee, and T.Williams
Fermi National Accelerator Laboratory*, Batavia, Illinois 60510

Introduction

A graphite core beam dump designed to accept aborted protons from both the Main Ring and the Tevatron has been installed at Fermilab. Instrumentation was designed and constructed to monitor the integrity of the dump, the temperature at various locations about the core, and the position of the beam at the front face of the dump. These devices include calorimeters, temperature sensing devices, and an ionization chamber. Constraints were placed on the choice of materials used due to expected maximum temperatures of 400°C and accumulated doses over 10 years of up to 10^{10} R. Presented in this paper are details of the choice of materials for and the design and construction of the desired instrumentation.

x-y Position Detector

The x-y position detector is a segmented ionization chamber having an effective area of 30.5 cm x 15.2 cm and a resolution of ± 1.3 cm in both planes. The active portion of the detector consists of two planes of titanium strips separated by a titanium high voltage plate which has a thickness of 1.58 mm. The horizontal beam position is measured by twelve equally spaced strips, six for the Main Ring beam and six for the Tevatron beam. Because the Main Ring and Tevatron beams will not be aborted simultaneously, their corresponding strips are jumpered together thus reducing the number of cables needed. The vertical beam position is measured by six equally spaced strips. The aforementioned strips are all 4.44 cm wide and are separated by .635 cm. Commercial high voltage ceramic feedthroughs are used to carry the signals and high voltage from the detector plates to the external environment. The signal plates employ 10-pin nickel conductor feedthroughs, while the high voltage plate uses a 1-pin copper conductor feedthrough. Because of possible oxidation each feedthrough is protected by a titanium cover box which may be flooded with dry argon.

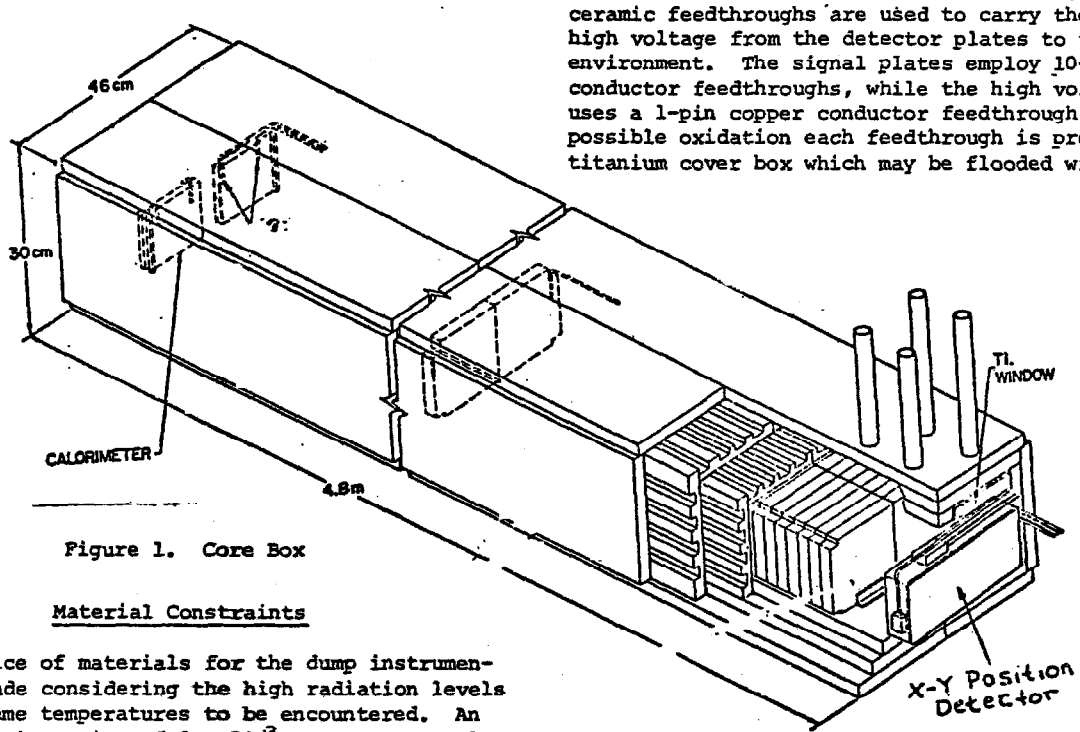

Figure 1. Core Box

Material Constraints

The choice of materials for the dump instrumentation was made considering the high radiation levels and the extreme temperatures to be encountered. An expected beam intensity of 2×10^{13} protons per pulse gives an estimated 10 year lifetime absorbed dose of 10^{10} Rads. Another constraint was an estimated temperature in excess of 400°C at the shower maximum. These conditions precluded the use of any organic compounds as insulation material. Ceramics however did meet these criteria and were commercially available. As a result, magnesium oxide was chosen for the cable insulation, and alumina was chosen for the position detector vacuum feedthroughs.

Table 1. Material Data[2,3,4]

	Teflon	Alumina	Magnesium Oxide
Radiation dose	3.7×10^4 Rads	2×10^{19} n cm^{-2}	3.5×10^{18} n cm^{-2}
Melting point in degrees C	400	2000	2700

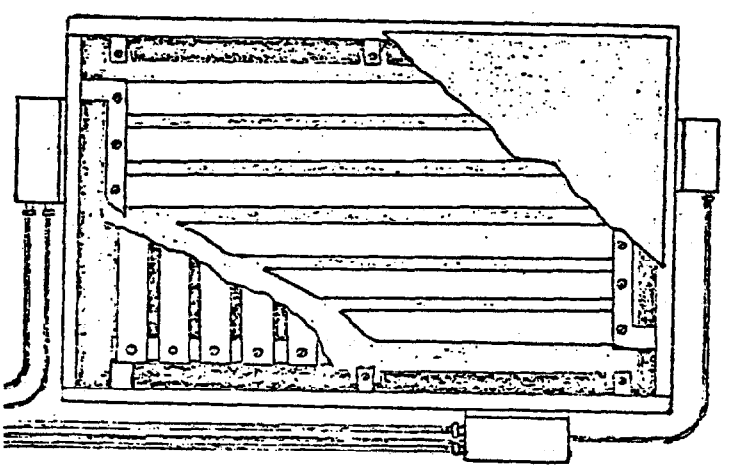

Figure 2. x-y Position Detector

*Operated by Universities Research Association, Inc. under contract with the U.S.Department of Energy.

Temperature Transducers

The primary instrumentation for the thermal measurements of the abort are platinum element resistance temperature detectors (RTD). These were chosen for their high radiation resistance and measurement accuracy and stability. These devices consist of fine platinum wire wound around an alumina core and encapsulated in a stainless steel sheath. The element comes equipped with three leads making possible balanced bridge measurements. The element leads are then welded to a three-constantan-conductor cable which was described earlier in this paper.

The electronics required to measure the resistances of the RTDs will reside above ground in a Main Ring service building. The detection circuitry will consist primarily of a constant current source. The resulting measurements will be sent back to the main control room via a computer link.

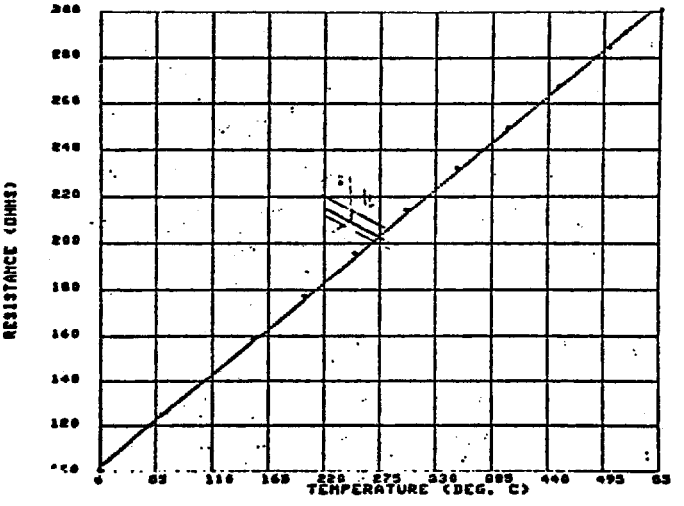

Figure 3. Plot of Resistance vs. Temperature

RTD Specifications:

1.	Element resistance	100 @ 0°C
2.	Resistance per degree	.1
3.	Temperature range	-200°C to 540°C
4.	Measuring current	10 milliamps DC max.
5.	Response time constant	4.5 seconds
6.	Power dissipation	50 milliwatts max.

There are seven RTDs located in the abort. Two are located near T max (z=2.2 m) as calculated by a Monte Carlo nuclear cascade program called MAXIM. The danger of the graphite expanding sufficiently to crack the aluminum shell necessitates temperature monitoring at that location. As a result, attempts will be made to maintain these temperatures below 200°C.

There is another RTD in one of the steel shielding blocks surrounding the sluminum shell. It is located downstream of the secondary particle shower maximum (z=2.4 m) and will provide temperature monitoring of the blocks. The concern here is that the steel may expand sufficiently to crack the surrounding concrete skin. Attempts will be made to maintain temperatures to approximately 50°C. There are four additional RTDs located in the calorimeters, which are described below.

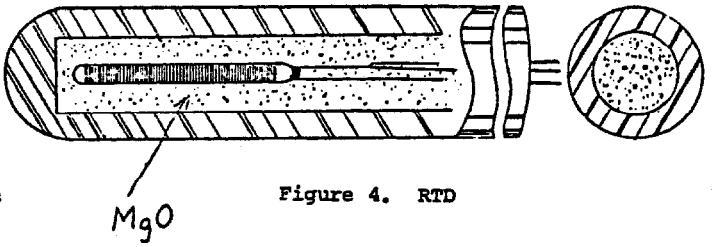

Figure 4. RTD

The Calorimeters

The calorimeters are two aluminum blocks (11.4 cm x 13.3 cm x 1.27 cm) located at the end of the graphite core (see Figure 5). There is one for Main Ring beam and one for Tevatron beam. Each is insulated with asbestos and equipped with two RTDs, one located in the top of the block, the other in the bottom. The base of each calorimeter is welded to the aluminum box so that it will reach thermal equilibrium with the box in about 30 seconds. This time constant is roughly equivalent to the proposed cycle time for the Tevatron. The purpose of the calorimeters is to monitor the integrity of the dump materials by measuring the temperature rise of the calorimeter at each aborted beam pulse. By means of the calorimeters, long-term changes in the temperature rise of the dump per abort, and ultimately the integrity of the dump core material can be noted. A rise in temperature per abort would indicate the possibility of cracked or broken graphite blocks upstream.

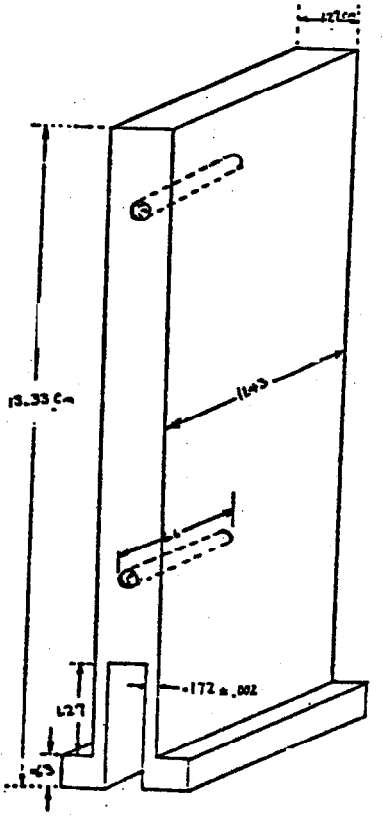

Figure 5. Calorimeter

Acknowledgements

We wish to thank F.Turkot for his invaluable assistance. The efforts of M.Syphers, M.Utes, and the Fermilab Machine Shop are also appreciated.

References

1. N.V.Mokhov and A.VanGinneken, "Calculations of Energy Deposition Densities in High Energy Acceleration Targets," TM-977, Fermilab (1980).

2. Collins, C.G. and Calkins, V.P., "Radiation Damage to Elastomers, Organic Liquids, and Plastics," APEX-261, General Electric Company, Cincinnati, Ohio, September 1956.

3. Wheeler, R.G., "Neutron Irradiation of Sapphire (Al_2O_3)," HW-42022, March 1956.

4. Monk, G.W., "Refractory Dielectrics in a Reactor," WADC-TR-57-599 (1957).

APPENDIX III

PROPERTIES OF GRAPHITE

GREAT LAKES CARBON CORPORATION
Graphite Products Division
Specialty Products Department
6200 Pine Ave., Niagara Falls, N. Y., 14304

Grade: H-489

Size range: 13 x 13 in. and 11 1/2 in. x 26 in. cross sections, up to 76 in. long. Up to 19 in. diameter, up to 76 in. long.

Application: Similar to H-440 but where smaller grain size and lower density are required.

Typical Properties

		English Units	Metric Units
Maximum Grain Size		3×10^{-3} in	8×10^{-2} mm
Apparent Density		107 lb/ft^3	1.71 Mg/m^3
Resistivity	W. G.	42×10^{-5} ohm in	11 μ ohm m
	A. G.	50×10^{-5} ohm in	13 μ ohm m
Flexural Strength	W. G.	3600 psi	24800 k Pa
	A. G.	3000 psi	20700 k Pa
Compressive Strength		6500 psi	44800 k Pa
Tensile Strength	W. G.	2100 psi	14500 k Pa
	A. G.	2000 psi	13800 k Pa
Modulus of Elasticity (sonic)	W. G.	1.2×10^6 psi	8.3×10^6 k Pa
	A. G.	0.95×10^6 psi	6.6×10^6 k Pa
Coeffecient of Thermal Expansion	W. G.	13×10^{-7} per deg F	23×10^{-7} per deg C
	A. G.	17×10^{-7} per deg F	30×10^{-7} per deg C
Thermal Conductivity		82 BTU/ft·hr·deg F	142 W/m·C
Permeability	W. G.		1.4×10^{-2} darcy
	A. G.		1.1×10^{-2} darcy
Hardness, Scleroscope		33	33
Average Pore Size		2×10^{-4} in	5×10^{-3} mm
Available Porosity		20% of bulk volume	20% of bulk volume
Ash		0.05%	0.05%

Note:

W. G.--test specimens cut with their long dimension with the grain; i.e., in the 12 x 12 in. plane.

A. G.--test specimens cut with their long dimension against the grain; i.e., in the 72 in. direction.

Properties are measured at room temperature unless otherwise noted.

Fermilab

July 2, 1980

TO: Helen Edwards

FROM: Frank Turkot
Thornton Murphy

SUBJECT: Selection of Graphite for the Core of the Abort Dump

We have decided to switch from BeO to graphite, and a particular graphite (Union Carbide grade CS), for the core of the dump for several reasons, the most important of which is that stress calculations indicate that it will not crack under the thermal shock of 2×10^{13} ppp at 1000 GeV, nor under the shock of 1×10^{14} ppp if ±9 mm of vertical sweeping is added to the aborted beam. By contrast, the spaced-out arrangement of BeO (by which we mean the alternation of BeO and air gaps along the beam direction of equal length) which Mokhov arrived at just to keep the temperature well below the softening point of BeO produces stresses which exceed the yield strengths (compressive and tensile) of BeO by a factor of 2 at 2×10^{13} ppp (no sweeping) and by a factor of 2½ at 10^{14} ppp (with ±9 mm of sweeping).

A quantitative comparison of the two materials is shown in the enclosed table. Some explanation is necessary. ΔT under various beam conditions are listed. This ΔT is based on VanGinneken's program MACSIM at the core of the shower ($r<0.35$ mm). This program has been cross-examined and "much improved" in the last few months for effects at small radii by Mokhov and VanGinneken, both because of our interest and the interest of the $\bar{p}p$ people. Conversion from energy deposition per gram to ΔT takes into account the temperature dependence of the specific heat. The net result of these improvements is that temperatures at small radii are larger than the programs predicted in January by about a factor of 2.

For comparison with these maximum temperature rises, we list two "cracking temperatures", based on textbook thermal stress analysis, which is valid in a two-dimensional approximation at the center of a block of material; the analysis does not deal with the stresses at the ends (along the beam) where the problem becomes three-dimensional. The first limit listed, $T = S_c/\alpha Y$, is based on the limit of compressive strength under longitudinal (along the beam) stress. The second limit, $\Delta T = 8S_t/\alpha Y$, is based on the limit of tensile strength under azimuthal stress which is maximum at about 2.5 times the beam radius (σ); the temperature refers to the temperature at $r = 0$, however. Taken literally, these data imply that BeO will crack, even at 2×10^{13} ppp, while graphite will not. However, one should assume that both the shower Monte Carlo and the simple-minded stress analysis have large uncertainties in them. We note that with graphite the operating temperatures predicted by the Monte Carlo are a comfortable factor of three below the predicted cracking temperatures. At 10^{14} ppp, we recommend sweeping the beam because the predicted temperature without sweeping is getting too close to the sublimation point.

Other factors have also been considered. The graphite will cost only $4,700. The aluminum box will be filled entirely (no large air gaps) with graphite, which makes the assembly easier and leaves the graphite no place to "fall" if it does crack or pulverize. The thermal expansion coefficient is much smaller than that of BeO, so that there is less working of the aluminum box during thermal cycles. However, we have bought one complication: a nitrogen or helium purge of the aluminum box might be required to prevent losing the graphite to CO_2 information which is significant above 400°C.

In addition to making these stress calculations, one of us (FT) has consulted the experience of a number of experts from CERN, SLAC and several of the graphite corporations. These experiences will perhaps be recorded in a separate memo. One additional concern learned from these conversations is the propensity of graphite to swell from neutron capture (a reactor discovery). The magnitude of this effect is still being pursued.

Since drafting this memo the lack of availability of "CS" graphite has forced us to switch to Great Lakes H-489, whose properties are also shown in Table I. It is not as good as "CS", but much better than BeO.

mhr
cc:P.Limon
N.Mokhov
M.Palmer
T.Toohig
R.Vanecek
A.VanGinneken

TABLE I

PROPERTIES OF BeO AND GRAPHITE

Property	BeO	Graphite "CS"		Graphite H-489	
		With Grain	Across Grain	With Grain	Across Grain
ρ, density (gms/cc)	2.85	1.65	1.65	1.71	
C_p, specific heat (cal/gm°C) at 20°C	0.25	.19?		.19?	
k, conductivity (cal/sec cm°C)	0.62	0.29?		.34	
S_c, compressive strength (10^3 psi)	225	~6.75	~7.47	6.5	6.5 ?
S_T, tensile strength (10^3 psi)	25.	2.5	1.8	2.1	2.0
Y, Young's modulus (10^6 psi)	53.	1.6	0.9	1.2	0.95
α, thermal expansion coefficient (10^{-6}/°C)	9.	1.2	1.8	2.3	3.0
$T_{crack} = S_c/\alpha Y$ (°C)	471.	3,515	4,611	2,314	2,235
$T_{crack} = 8\ S_T/\alpha Y$ (°C)	419.	10,416	8,888	5,983	5,504
T_{melt}, (°C)	2,530.	3,500 (sublimes)		3,500	
Predicted temperature rises (MACSIM):					
ΔT - 2×10^{13} ppp (°C) at 1000 GeV	750	780		780	
ΔT - 1×10^{14} ppp, no sweeping (°C)	2,616	3,180		3,180	
ΔT - 1×10^{14} ppp, ±9mm sweep (°C)	908	1,113		1,113	
ν (Poisson's ratio)				.14-.16	

APPENDIX IV

TM-1196

FN-328
1111.140

ENERGY DEPOSITION IN TARGETS AND BEAM DUMPS AT 0.1-5 TeV PROTON ENERGY

N.V.Mokhov*

Institute for High Energy Physics

Serpukhov, USSR

August 8, 1980

ABSTRACT

Modifications of the Monte Carlo program MARS and comparisons with other programs are described. Regularities of energy deposition formation in targets and beam dumps irradiated by 0.1-5 TeV protons are investigated. Enthalpy reserves and admissible energy deposition densities are calculated for some materials. Tolerable beam sizes in the 10^{12} to 10^{15} intensity range are determined.

*Visiting Scientist at Fermilab, December 1979 to September 1980

I. INTRODUCTION

The complex accelerator projects of the generation to come, Tevatron, UNK and Pentevac for example, assume extremely high values of proton energy (up to 5 TeV) and beam intensity (up to 6×10^{14} ppp). The behavior of matter struck by such beams results in a number of macroscopic features; e.g., instantaneous melting, explosion, cracking and long-term effects. The cause of these features, energy deposition during hadronic and electromagnetic shower development, is the subject of this paper. Throughout the paper we assume beam spill times which are short compared to the conduction time constant of the struck material.

II. MARS-7 AND MARS-8 PROGRAMS

The three-dimensional nuclear-electromagnetic cascades are calculated exclusively with Monte Carlo programs. The present study is performed with the MARS computing complex[1-3] which uses phenomenological formulas for inclusive hadron production in the energy region from a few MeV up to a few TeV. Other features of the MARS programs are absorption cross section energy dependence, an exact description of hadron-proton interactions, the possibility for point-like detectors, and the analytical geometry methods used for particle transport and three-dimensional geometry description.

MARS-4[3] is the basic program. MARS-5[4] was designed for calculations of p, n, π^+, π^-, k^+, k^-, $\bar{p}$ distributions from a target as well as the stopping densities of negative hadrons (π^-, k^-, $\bar{p}$, Σ^-). MARS-6[5] makes it possible to consider in a convenient way the effect of magnetic and electric fields and also the azimuthal

structure of the constructions. Note also the special ultra-relativistic version for DUMAND acoustic studies.[6]

In general the results of the calculations agree well with experimental data as well as with CASIM[7,8] predictions.[3,9] However recent study[9] has shown the great importance of precision in the description of the energy deposition from low energy hadrons and electromagnetic showers from π^0 decays. The program MAXIM was created[10] which is the combination of CASIM[7] and the electron-photon shower program AEGIS,[8] and which also considers the transport of low energy protons.[9]

Similar features were introduced in the MARS programs. The main modifications in creating MARS-7 and MARS-8 programs are:

1. A new description of electromagnetic showers from neutral pion decays, radial dependent empirical formula from Ref. 7 in MARS-7 and quasianalog simulation of electron-photon showers from Ref. 8 in MARS-8.
2. The transport of evaporated protons and neutrons, nucleons from π^- capture and subthreshold nucleons; it gives in some cases a factor of two because the range of such particles can exceed the small beam and radial bin sizes.
3. A better description of Coulomb and elastic scatterings for initial hadrons.
4. A slight improvement in the energy dependence of absorption cross sections at the highest energies.

III. RESULTS: COMPARISONS AND REGULARITIES

In this section we present the results of the calculations of energy deposition density distributions, $\mathcal{E}$, in the central parts of targets and beam dumps irradiated by 0.1-5 TeV proton beams of various sizes. Graphite with density $\rho = 1.71$ g/cm^3 has been chosen as the most appropriate (from melting and cracking points of view) material for such applications. In one case BeO ceramic has been considered.

The beam distribution is Gaussian in both vertical and horizontal profiles with standard derivations of σ_v and σ_h, respectively. In all cases the smallest radial bin has been chosen as $0 \le r \le 0.5\sigma_{min}$, which is related to the real maximum energy deposition density $\mathcal{E}_{max}$.[9]

The longitudinal distributions of energy deposition density $\mathcal{E}$ at various radial intervals are shown in Figs. 1-4 for 100, 400, 1000, and 3000 GeV proton energies. These figures show the results of MARS-7, MARS-8, CASIM, and MAXIM calculations (the last two only at $E_0 \le 1000$ GeV where they work). It is remarkable that the data of pairs (MARS-7, CASIM) and (MARS-8,MAXIM) agree very well in spite of very different physical and calculative schemes used. The factor of 1.5-2 disagreement at the shower maximum inside pairs (MARS-7, MARS-8) and (CASIM, MAXIM) arises evidently from the different description of the electromagnetic shower.

Three conclusions result from these comparisons:

1. Since four different programs agree with each other to the extent seen in Figs. 1-4, we feel reassured that the absolute value of the energy deposition is believable within a factor of 1.5-2.
2. We recommend the use of MAXIM (at $E_0 \leq 1$ TeV) and MARS-8 because they incorporate the most accurate description of the electromagnetic shower.
3. A cheaper approximation (factor of two on the average) is achieved by running of CASIM or MARS-7 (compared with MAXIM or MARS-8).

The rest of the results presented in this paper have been obtained with the MARS-8 program.

The spatial distributions of energy density for a large 3 TeV proton beam are shown in Fig. 5. Figure 6 is a collection of longitudinal maximum energy density distributions for incident protons in the 0.1 to 5 TeV energy range. It is interesting to note a transformation of curves with energy.

Figure 7 shows the radial dependence of $\mathcal{E}/E_0$ values at shower maxima for E_0 = 0.4, 1, 3, and 5 TeV for two various beam sizes. There is no radial dependence at $r<0.5\sigma$ min. At $E_0 \geq 1$ TeV and r>1 cm energy deposition divided by E_0 does not depend on initial energy (scaling). In this region the radial dependence can be approximated by the expression

$$\frac{\mathcal{E}}{E_0} = 4.1\times10^{-5}\ r^{-2.32},\ \frac{1}{g\times 1\ \text{inc-proton}} \qquad (1)$$

where $1<r<10$ cm, $\sigma<1$ cm, $E_0 \geq 1000$ GeV, $[\mathcal{E}]$ = GeV×g^{-1}×1 inc-proton^{-1}. For other conditions the slope in Eq. (1) will be slightly changed.

The energy dependences of maximum energy deposition densities $\mathcal{E}_{max}$ are presented in Fig. 8 for various beam sizes. It is remarkable that we can describe these dependences in wide region with simple law

$$\mathcal{E}_{max} = A \times E_0^n, \ \text{GeV} \times g^{-1} \times 1 \ \text{inc-proton}^{-1}, \qquad (2)$$

where E_0 in GeV and parameters A and n for graphite target are listed in the table below:

Beam	σ_v, cm	σ_h, cm	E_0, GeV	A×10^5	n
1	0.07	0.14	400-3000	2.3	1.44
2	0.7	1.4	100-5000	1.3	1.20
3	2	4	100-5000	.48	1.13

Figure 9, which also uses data from a previous paper[9], shows the $\mathcal{E}_{max}$ dependence on beam area defined as

$$B = 4\pi \ \sigma_v \ \sigma_h. \qquad (3)$$

Data are presented for 0.1, 0.4, 1, 3, and 5 TeV. 1 TeV results are shown for three different beam shapes $\sigma_h = \sigma_v$, $\sigma_h = 2\sigma_v$, $\sigma_h = 10\sigma_v$. As was first noted in Ref. 9, results are completely independent of beam shape. At the smallest areas and $E_0 \leq 1$ TeV the data are independent of initial energy.

IV. TEMPERATURE RISE AND LIMITS

The instantaneous temperature rise in the considered bulk of matter can be determined from the calculated energy deposition

distributions and from an enthalpy reserve. The latter is determined as

$$\Delta H(T) = \int_{T_0}^{T} C_p\,(T^1)dT^1, \qquad (4)$$

where T_0 and T are the initial and final temperatures, respectively, and $C_p(T)$ is the heat capacity.

Using thermophysical data from Ref. 11, we have calculated Eq. (4) and results for graphite and BeO are presented in Fig. 10. At T_0 = 20°C and T≥100°C Eq. (4) for graphite gives

$$\Delta H(T) = 0.165 \times T^{1.31}, \ \frac{\text{Joules}}{\text{g}}. \qquad (5)$$

The enthalpy reserve and the energy deposition are related by the equation

$$\Delta H(T) = 1.6\times10^{-10}\times I\times\mathcal{E}, \qquad (6)$$

where I is the number of incoming protons per pulse.

Now we can easily estimate the instantaneous temperature due to a single pulse. Solving Eqs. (5) and (6) for temperature, we obtain:

$$T = \left(\frac{1.6\times10^{-10}\times I\mathcal{E}}{0.165}\right)^{0.76336}, \qquad (7)$$

for T≥100°C.

The next relation must be valid for all parts of the considered systems

$$\Delta H\ (T_{max}) \geq 1.6\times10^{-10}\times I\times\mathcal{E}_{max}, \qquad (8)$$

where the maximum energy deposition can be determined by Eq. (2) and T_{max} is the "melting" or "cracking" temperature, whichever is smaller.

In particular for graphite H-489 we have[12]

$T_{melt} = 3500°C$

$T_{crack} = (2235\text{-}2314)°C.$

We have chosen $T_{max} \simeq 2300°C$ and from Fig. 10 or Eq. (5) we have obtained

$$\Delta H\ (T_{max}) \simeq 4000 \text{ Joules/g.}$$

The admissible energy deposition density must be

$$\mathcal{E}_{max} \leq \frac{2.5\times10^{13}}{I}, \frac{GeV}{g\times 1 \text{ inc-proton}} \qquad (9)$$

For any proton beams and graphite targets or beam dumps, the next fundamental limit follows from Eqs. (2) and (9)

$$E_0^n \times I \leq \frac{2.5\times10^{13}}{A} \qquad (10)$$

where parameters n and A are determined in the previous table.

Now we can get tolerable beam sizes from Fig. 9 and the limitations of this section. Because the maximum energy deposition is independent of beam shape it is very convenient to consider limitations on beam area $B = 4\pi\ \sigma_v\ \sigma_h$ or particularly on $\sqrt{B}$. The minimum possible value of $\sqrt{B}$ as a function of the number of incident protons are presented in Fig. 11 for 0.1, 0.4, 1, 3, and 5 TeV protons. In the specific case $\sigma_h = 2\sigma_v$ the value of $\sqrt{B} \simeq 5\sigma_v$. Note once more that the data of Fig. 11 have been calculated for maximum instantaneous temperature in graphite $T_{max} = 2300°C$. Figure 11 has the parameters of all accelerators of new generation.

Acknowledgements:

Valuable discussions with H.Edwards, T.Murphy, T.Toohig,

F.Turkot, and A.VanGinneken are greatly appreciated. I am especially thankful to T.Murphy for his reading the text and making a lot of suggestions and to A.VanGinneken for introducing me to his programs and for many days of joint work.

References:

[1]N.V.Mokhov, in Proc. IV All-Union Conference on Charged Particle Accelerators, Moscow, 1974, V.2, M., "Nauka", 1975, p.222.

[2]N.V.Mokhov, preprint IHEP76-64, Serpukhov, 1976.

[3]I.S.Baishev, S.L.Kuchinin, N.V.Mokhov, preprint IHEP78-2, Serpukhov, 1978.

[4]A.S.Denisov, et al., preprint LINP-459, Leningrad, 1978.

[5]M.A.Maslov, N.V.Mokhov, preprint IHEP79-135, Serpukhov, 1979. To be published in "Particle Accelerators", 1980.

[6]G.A.Askarian, B.A.Dolgoshein, A.N.Kalinovsky, N.V.Mokhov, Nucl Instr.Meth. 164, 267, 1979.

[7]A.VanGinneken, Fermilab FN-272, 1975.

[8]A.VanGinneken, Fermilab FN-309, 1978.

[9]N.V.Mokhov, A.VanGinneken, Fermilab TM-977, 1980. Also in Proc. of the Workshop on High Intensity Targeting, Fermilab, April 1980.

[10]A.VanGinneken, private communication. See also H.Edwards, S.Mori and A.VanGinneken, Fermilab UPC-30, 1978.

[11]Y.S.Touloukian, Thermophysical Properties of Matter, Vol. 1, Plenum, New York-Washington, 1970.

[12]F.Turkot, T.Murphy, letter to H.Edwards, July 2, 1980, Fermilab.

Captions:

Figure 1 Energy deposition density as a function of depth Z in a graphite target (density = 1.71 g/cm^{-3}) for 100 GeV incident protons and for the radial regions indicated. The beam distribution is Gaussian in both vertical and horizontal profile with standard deviations of σ_v = 0.07 cm and σ_h = 0.14 cm, respectively. In Figs. 1-4: o - MARS-8, • - MAXIM, Δ - MARS-7, ▲ - CASIM results.

Figure 2 The same as in the previous figure but for E_0 = 400 GeV, BeO target (density = 2.85 g/cm^{-3}) and $\sigma_v = \sigma_h$ = 0.05 cm.

Figure 3 The same as in Fig. 1 but for E_0 = 1000 GeV.

Figure 4. The same as in Fig. 1 but for E_0 = 3000 GeV. Only MARS calculation results.

Figure 5 Energy deposition density spatial distribution in graphite for 3000 GeV incident protons. σ_v = 2 cm and σ_h = 4 cm. MARS-8 results are presented here and in the next figures.

Figure 6 Longitudinal distributions of maximum energy deposition in graphite for various incident energies. σ_v = 0.07 cm and σ_h = 0.14 cm.

Figure 7 Energy deposition density divided by various incident proton energies as function of radius at shower maximum in graphite. Beams have two sizes:
1) σ_v = 0.07 cm, σ_h = 0.14 cm; 2) σ_v = 0.7 cm, σ_h = 1.4 cm

Figure 8 Energy dependence of maximum energy deposition density in graphite for three incident proton beams:

● - σ_v = 0.07 cm, σ_h = 0.14 cm;

o - σ_v = 0.7 cm, σ_h = 1.4 cm;

▲ - σ_v = 2 cm, σ_h = 4 cm.

Figure 9 Maximum energy deposition density in graphite as a function of beam area for 0.1, 0.4, 1, 3 and 5 TeV incident protons. The beams are of the various shapes indicated only for 1 TeV case.

Figure 10. Enthalpy reserve for BeO and graphite as a function of temperature. Initial temperature T_0 = 20°C.

Figure 11 Square root of tolerable beam area for graphite (T_{max} = 2300°C) as a function of a number of protons per fast pulse for proton incident energies as indicated.

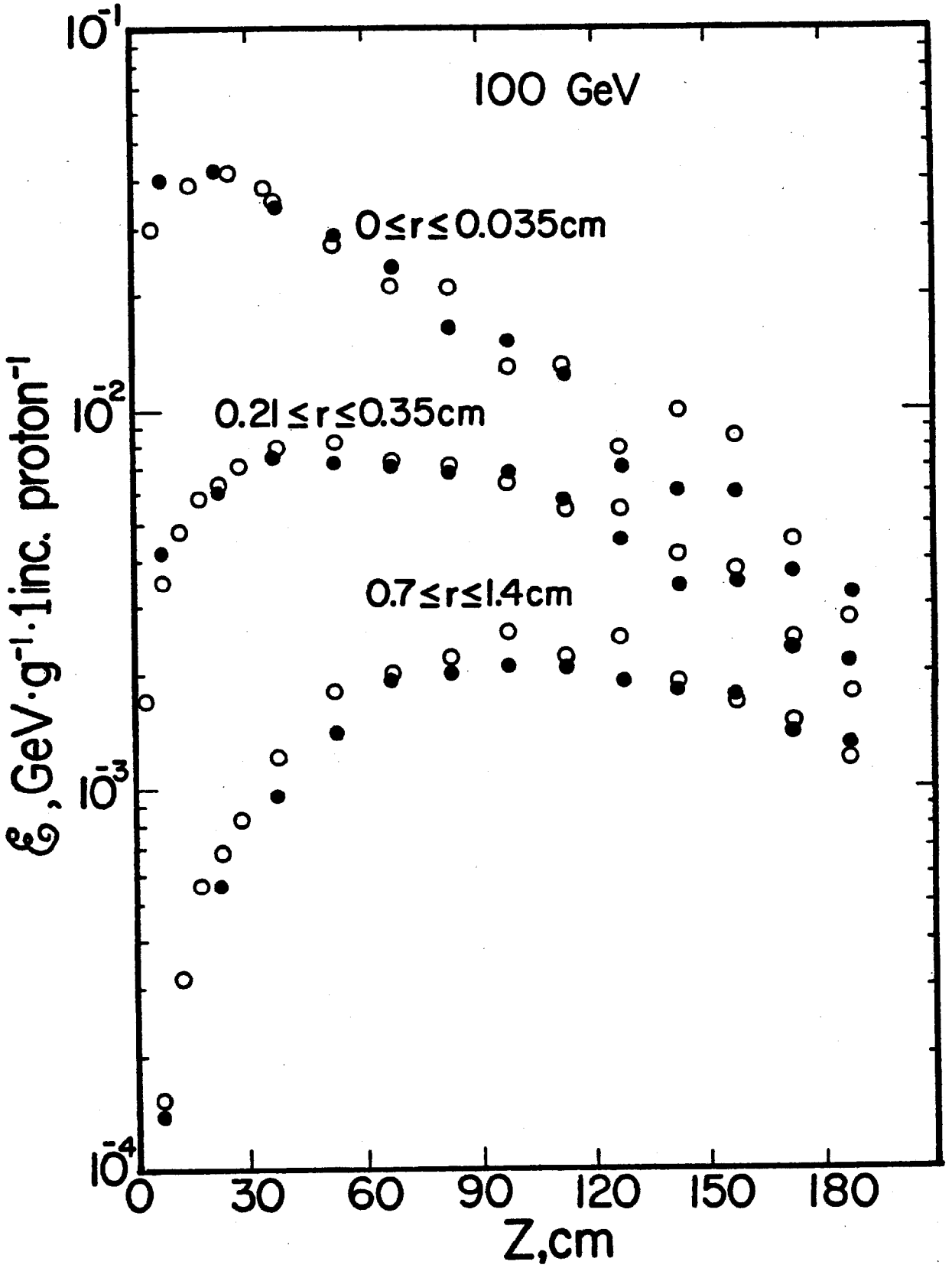
100 GeV
0≤r≤0.035cm
0.21≤r≤0.35cm
0.7≤r≤1.4cm
ℰ, GeV·g⁻¹·1inc. proton⁻¹
10⁻¹
10⁻²
10⁻³
10⁻⁴
0
30
60
90
120
150
180
Z,cm

Fig. 1

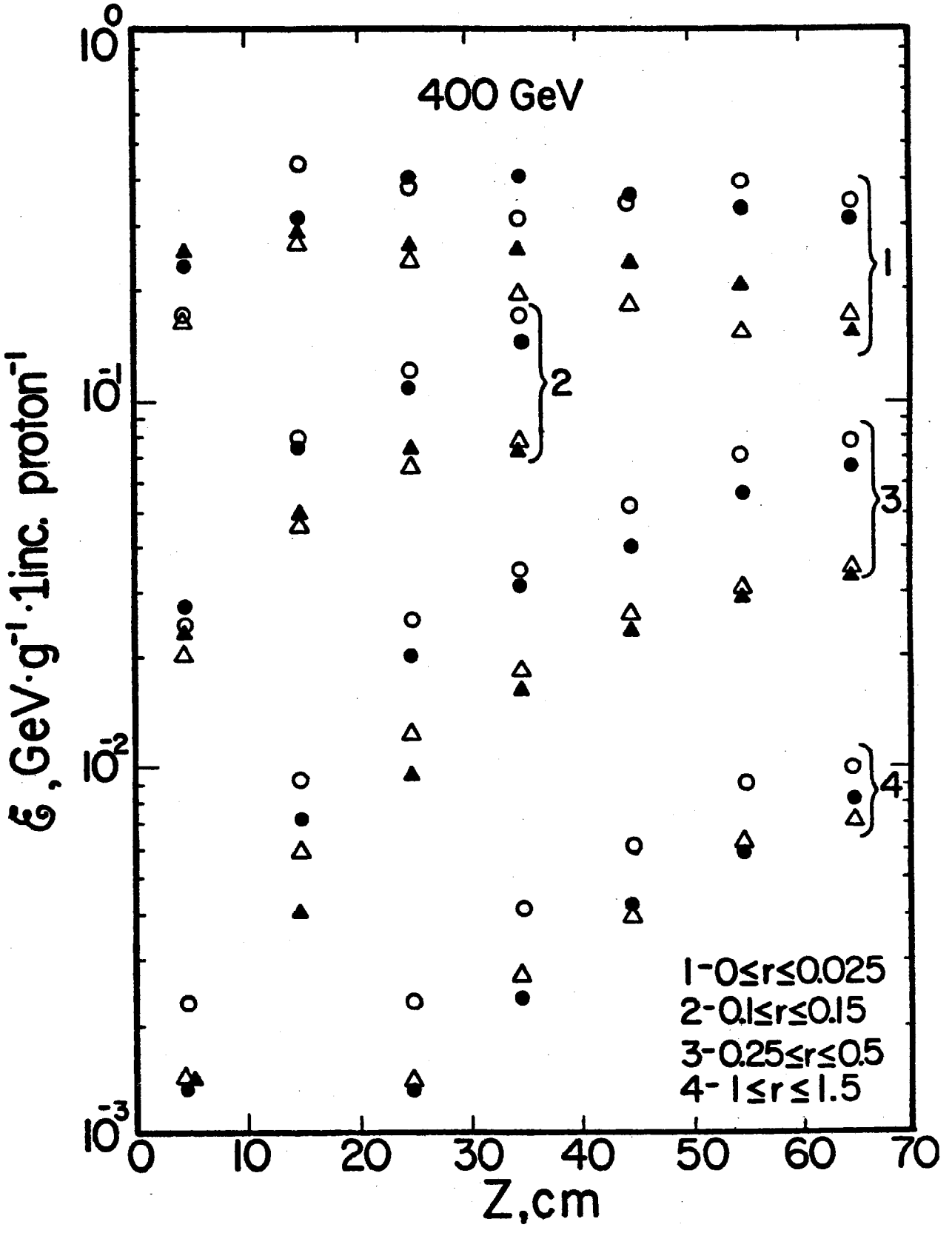
400 GeV
ε, GeV·g⁻¹·1inc. proton⁻¹
Z, cm
1-0≤r≤0.025
2-0.1≤r≤0.15
3-0.25≤r≤0.5
4-1≤r≤1.5

Fig. 2

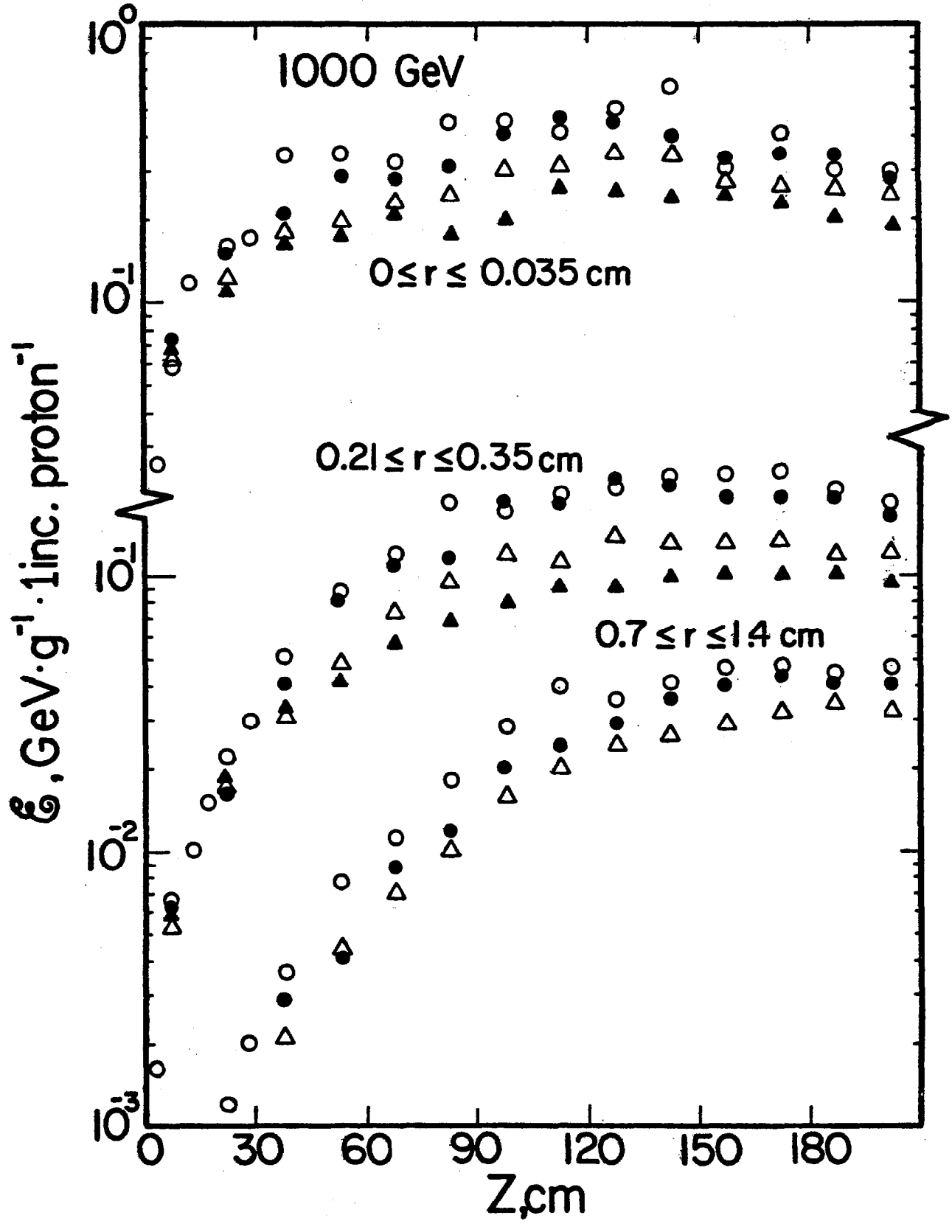
1000 GeV
0≤r≤0.035 cm
0.21≤r≤0.35 cm
0.7≤r≤1.4 cm
ℰ, GeV·g⁻¹·1inc. proton⁻¹
Z,cm
10⁰
10⁻¹
10⁻²
10⁻³
0
30
60
90
120
150
180

Fig. 3

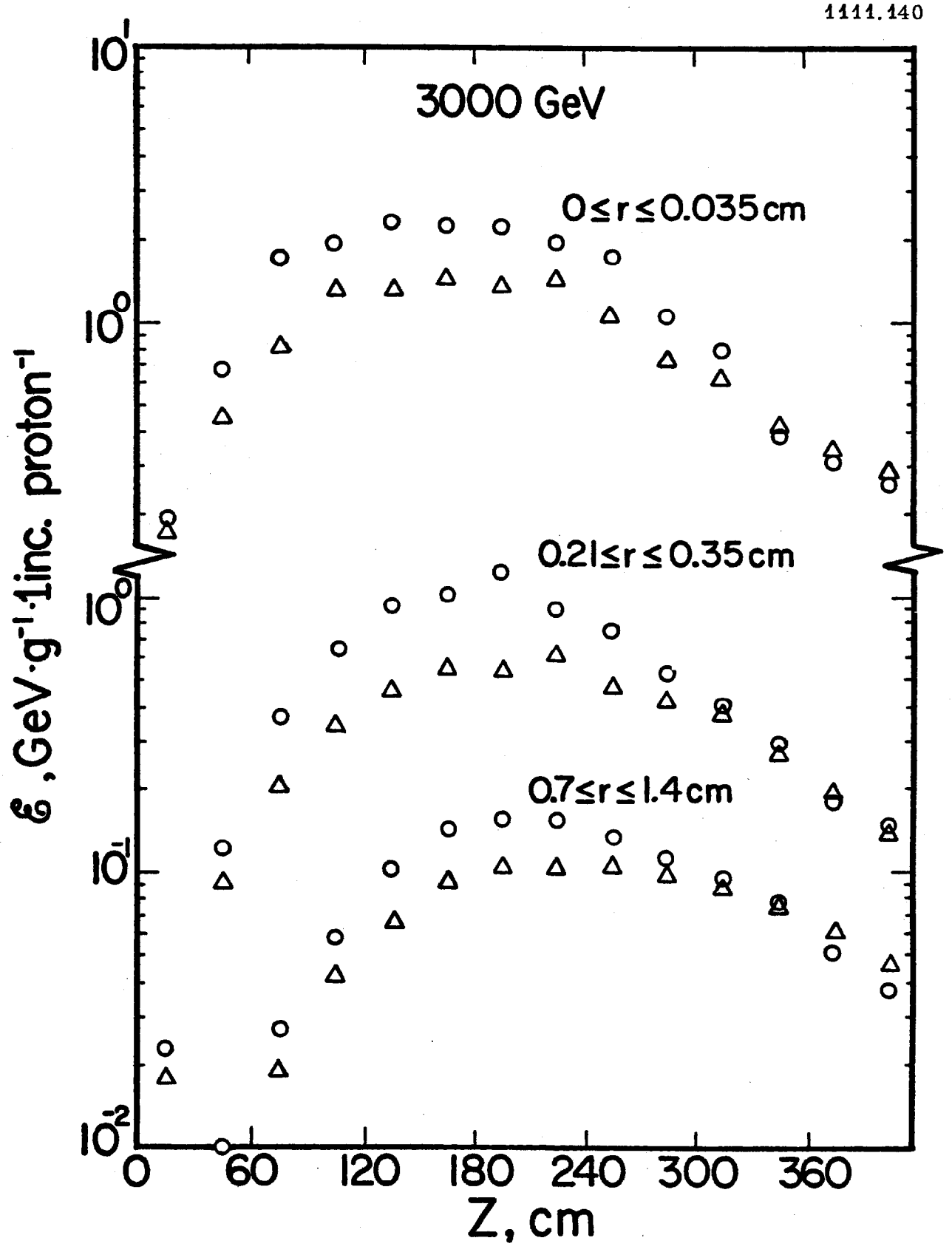
3000 GeV
0≤r≤0.035cm
0.21≤r≤0.35cm
0.7≤r≤1.4cm
ε, GeV·g⁻¹·1inc. proton⁻¹
Z, cm
10¹
10⁰
10⁻¹
10⁻²
0
60
120
180
240
300
360

Fig. 4

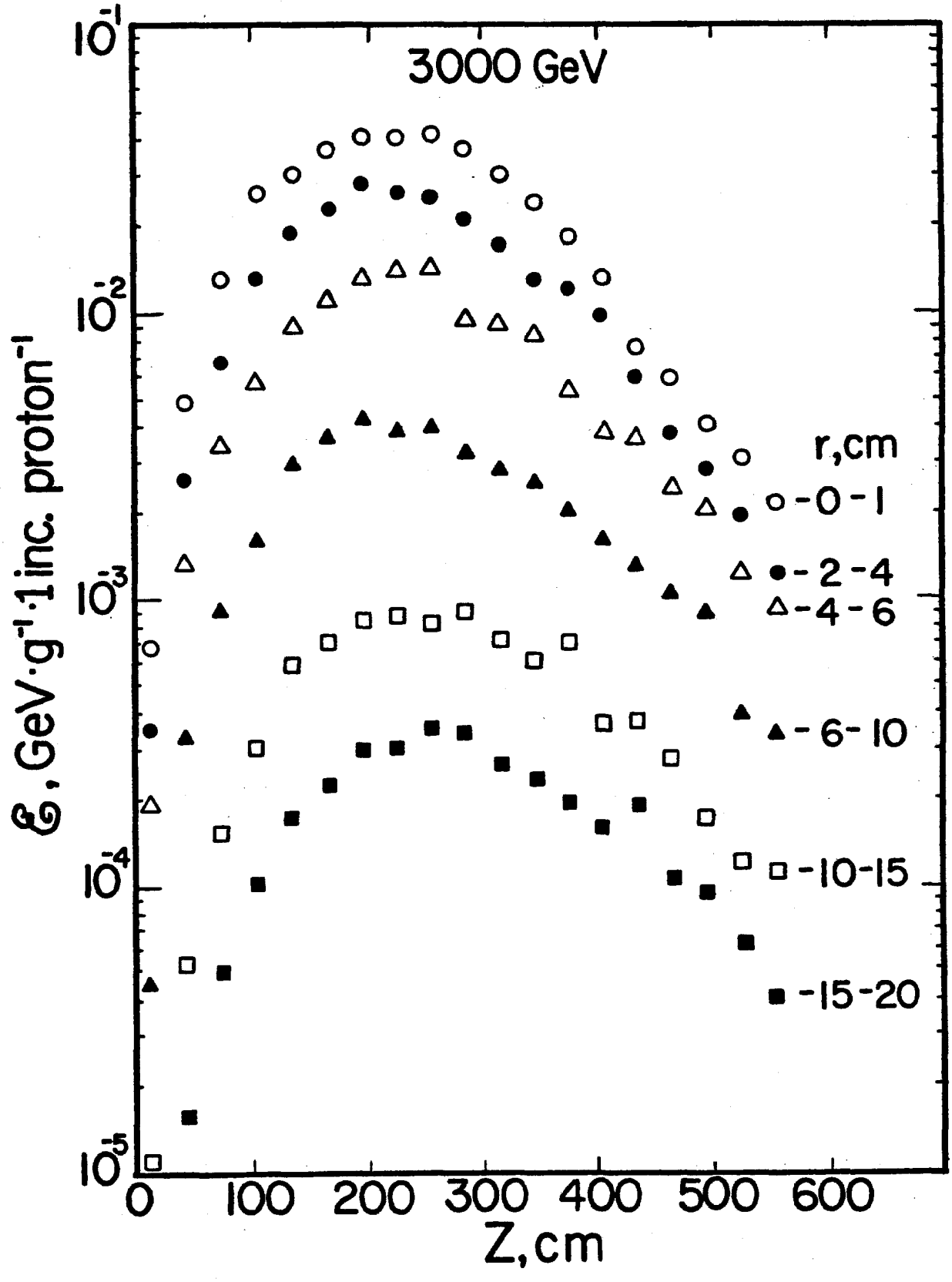
3000 GeV
10^{-1}
10^{-2}
10^{-3}
10^{-4}
10^{-5}
$\mathcal{G}$, GeV·g^{-1}·1 inc. proton^{-1}
0
100
200
300
400
500
600
Z, cm
r, cm
-0-1
-2-4
-4-6
-6-10
-10-15
-15-20

Fig. 5

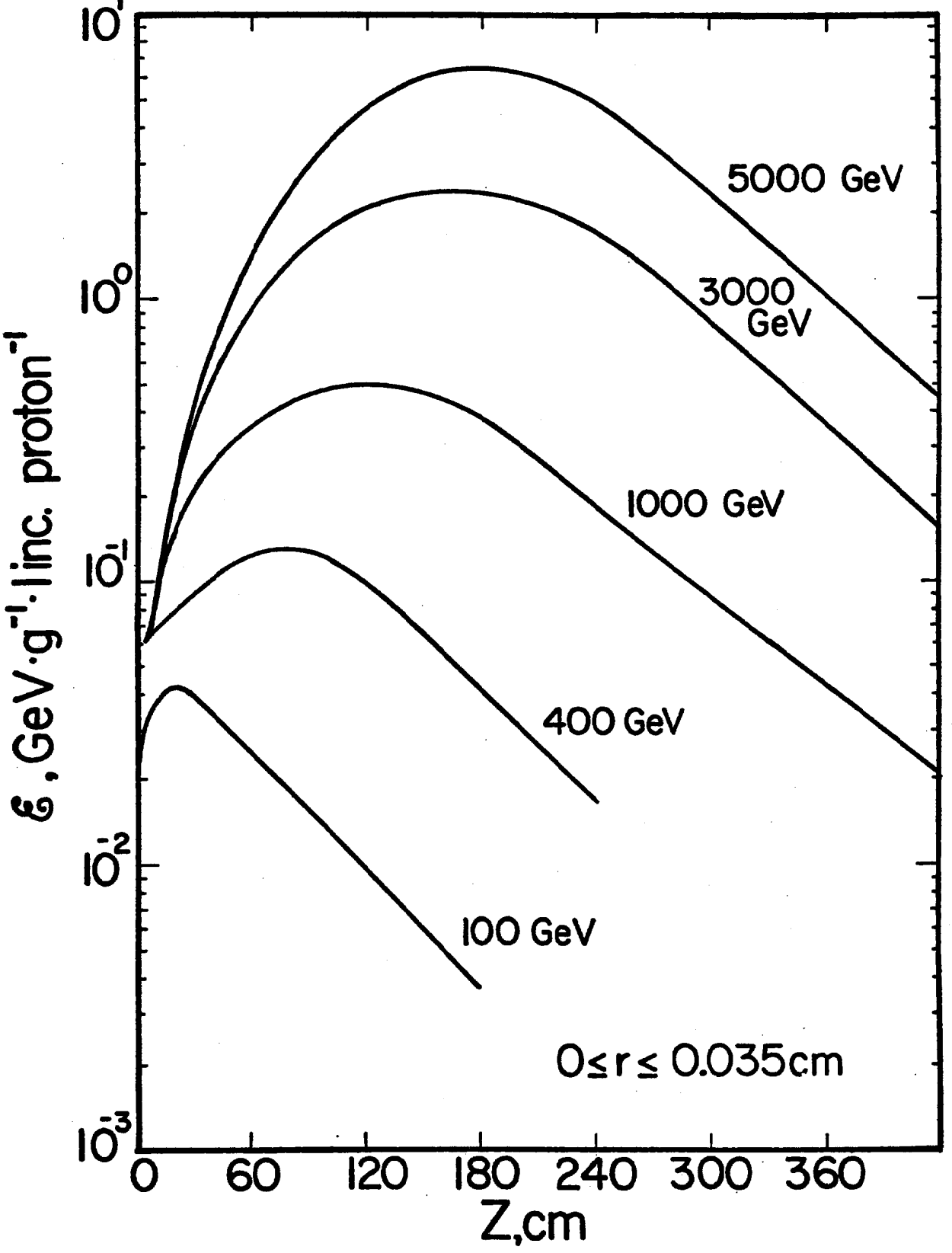
10^1
10^0
10^-1
10^-2
10^-3
ε, GeV·g^-1·1inc. proton^-1
5000 GeV
3000 GeV
1000 GeV
400 GeV
100 GeV
0≤r≤ 0.035cm
0
60
120
180
240
300
360
Z,cm

Fig. 6

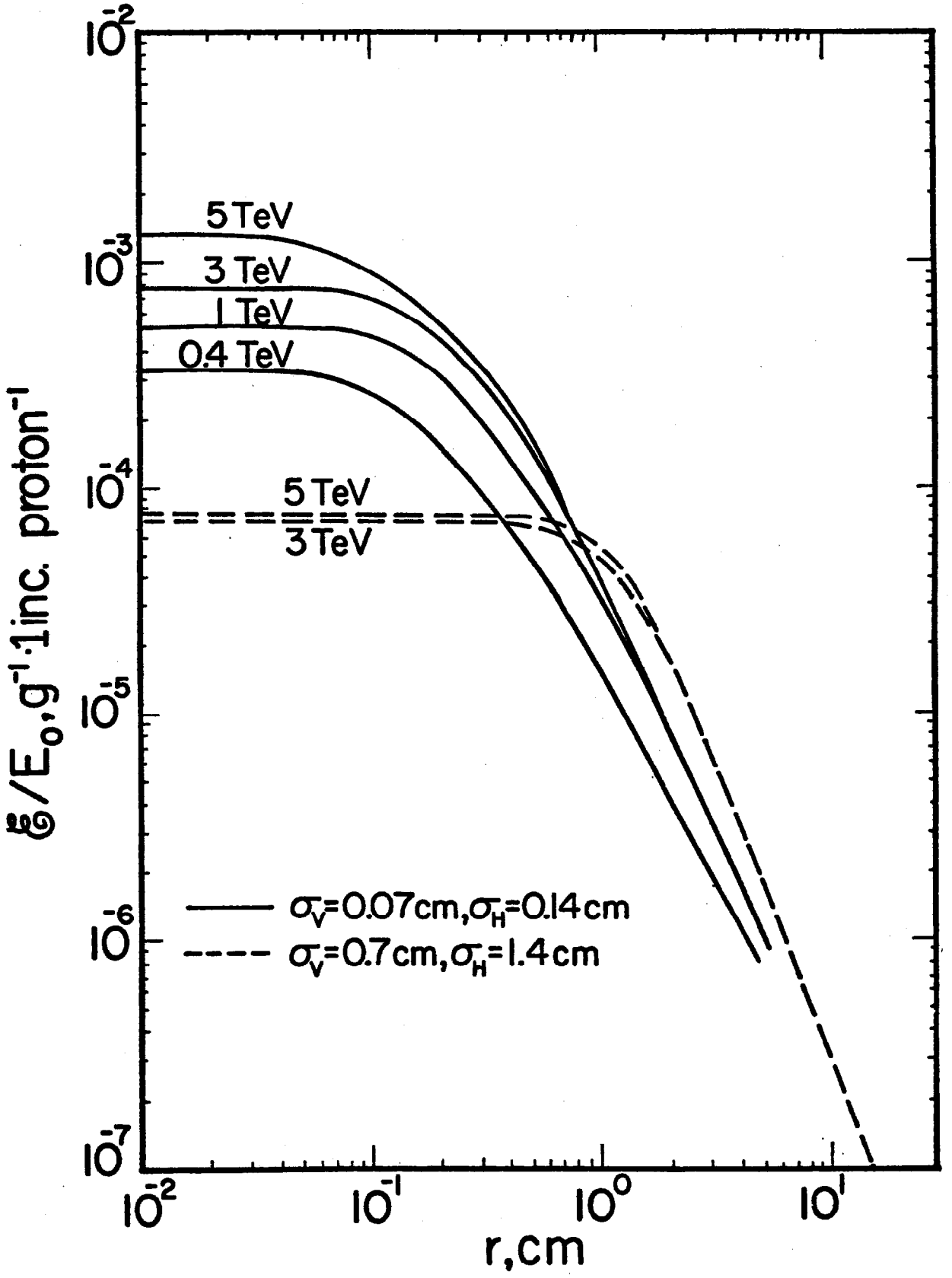
5 TeV
3 TeV
1 TeV
0.4 TeV
5 TeV
3 TeV
σ_V=0.07cm, σ_H=0.14cm
σ_V=0.7cm, σ_H=1.4cm
$\mathcal{E}/E_o$, g^{-1}·1 inc. proton^{-1}
r, cm
10^{-2}
10^{-3}
10^{-4}
10^{-5}
10^{-6}
10^{-7}
10^{-2}
10^{-1}
10^{0}
10^{1}

Fig. 7

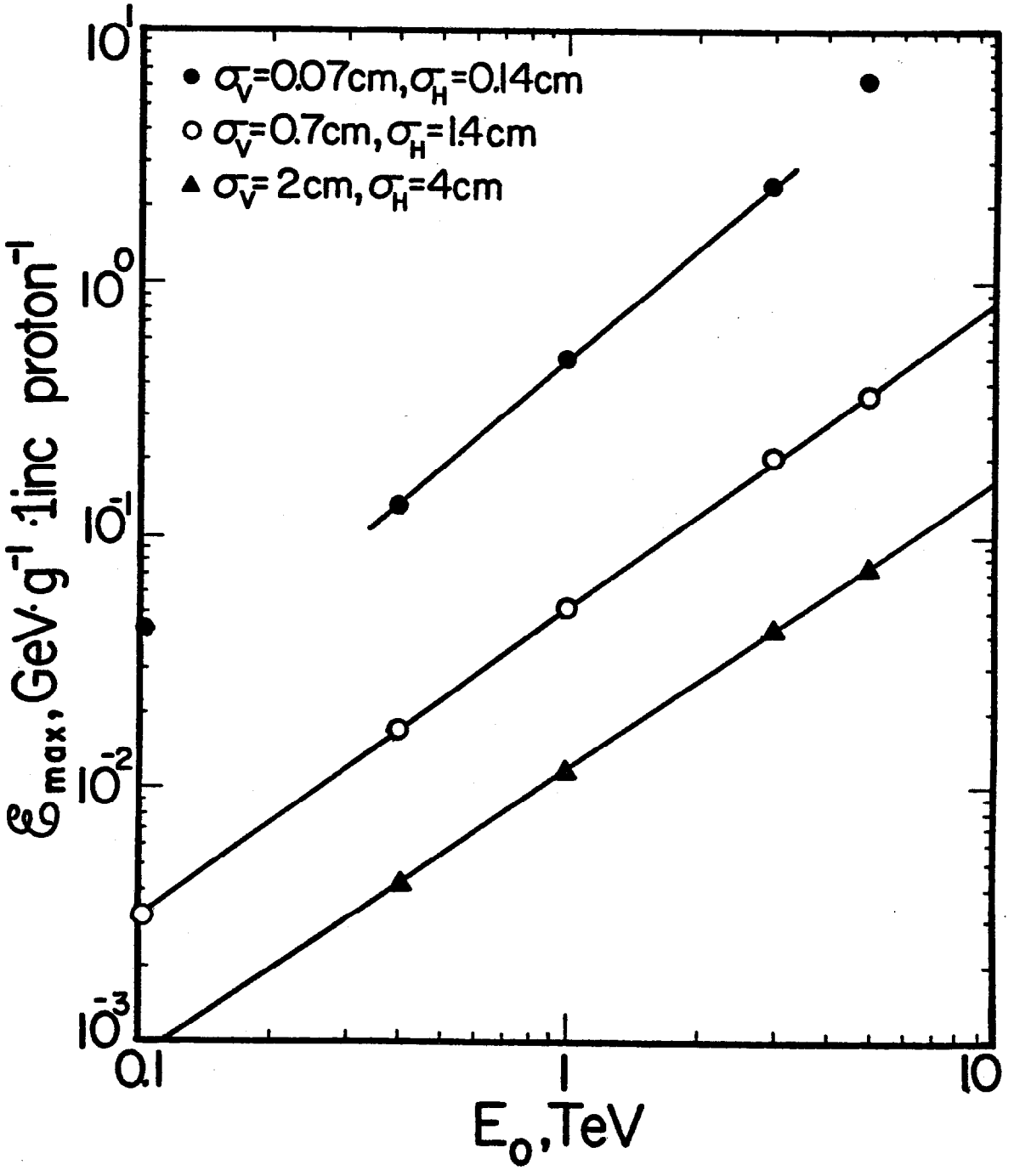
10^1
10^0
10^{-1}
10^{-2}
10^{-3}
$\mathcal{E}_{max}$, GeV·g^{-1}·1inc proton^{-1}
● σ_V=0.07cm, σ_H=0.14cm
○ σ_V=0.7cm, σ_H=1.4cm
▲ σ_V= 2cm, σ_H=4cm
0.1
1
10
E_0, TeV

Fig. 8

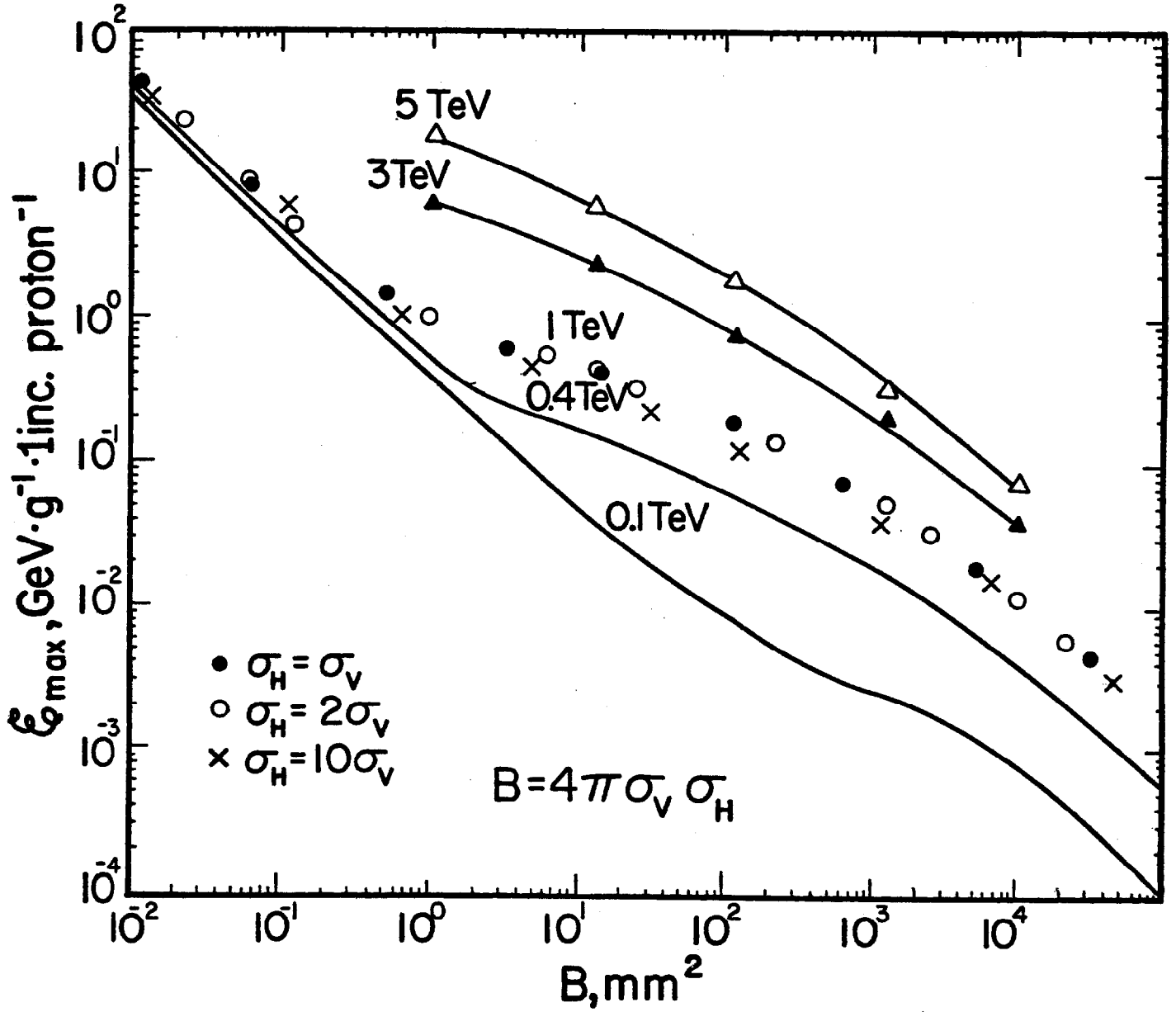
5 TeV
3TeV
1 TeV
0.4TeV
0.1TeV
$\sigma_H = \sigma_V$
$\sigma_H = 2\sigma_V$
$\sigma_H = 10\sigma_V$
$B = 4\pi\sigma_V\sigma_H$
ϵ_{max}, GeV·g^{-1}·1inc. proton^{-1}
B, mm^2

Fig. 9

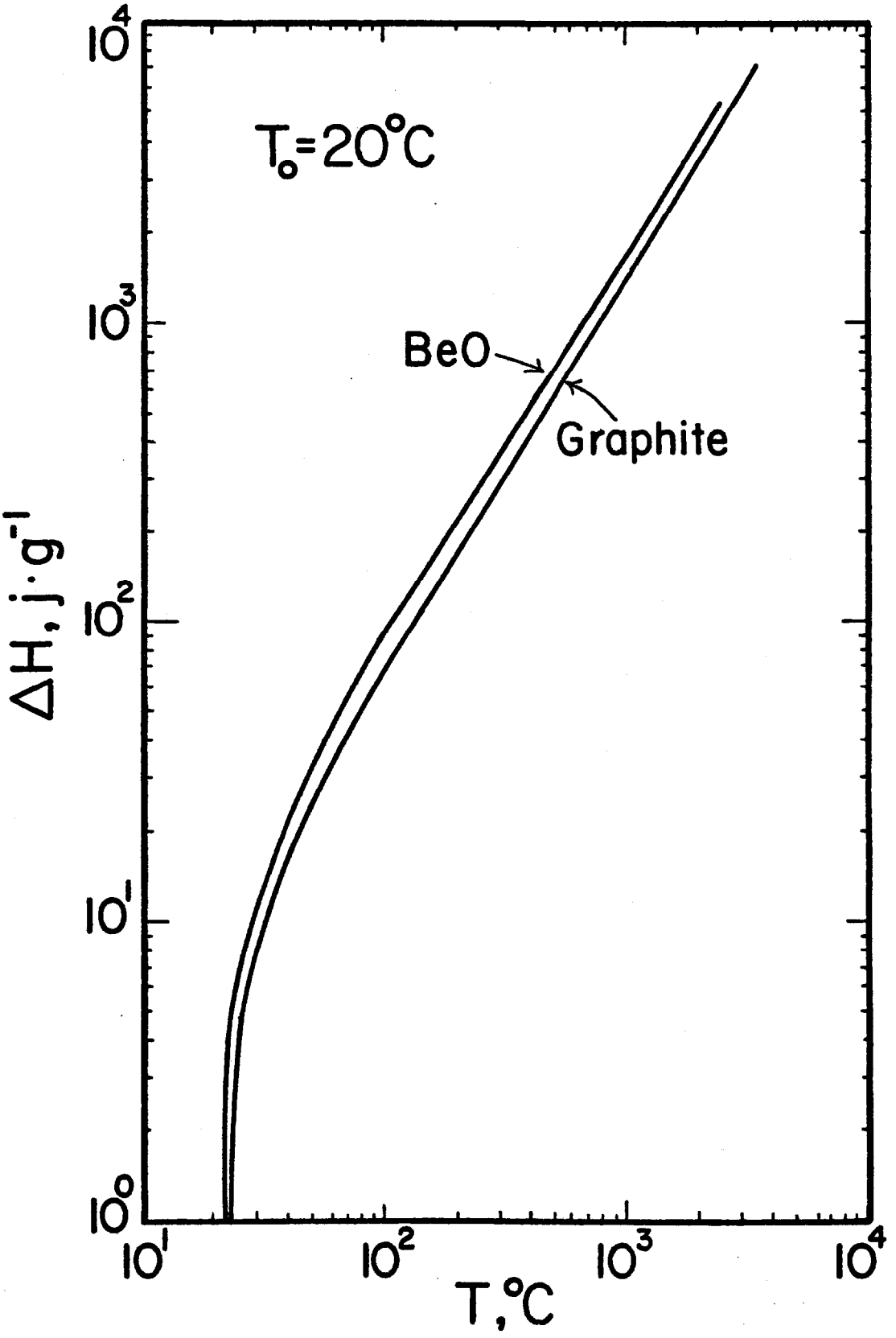
T_o=20°C
BeO
Graphite
ΔH, j·g^{-1}
10^4
10^3
10^2
10^1
10^0
10^1
10^2
10^3
10^4
T, °C

Fig. 10

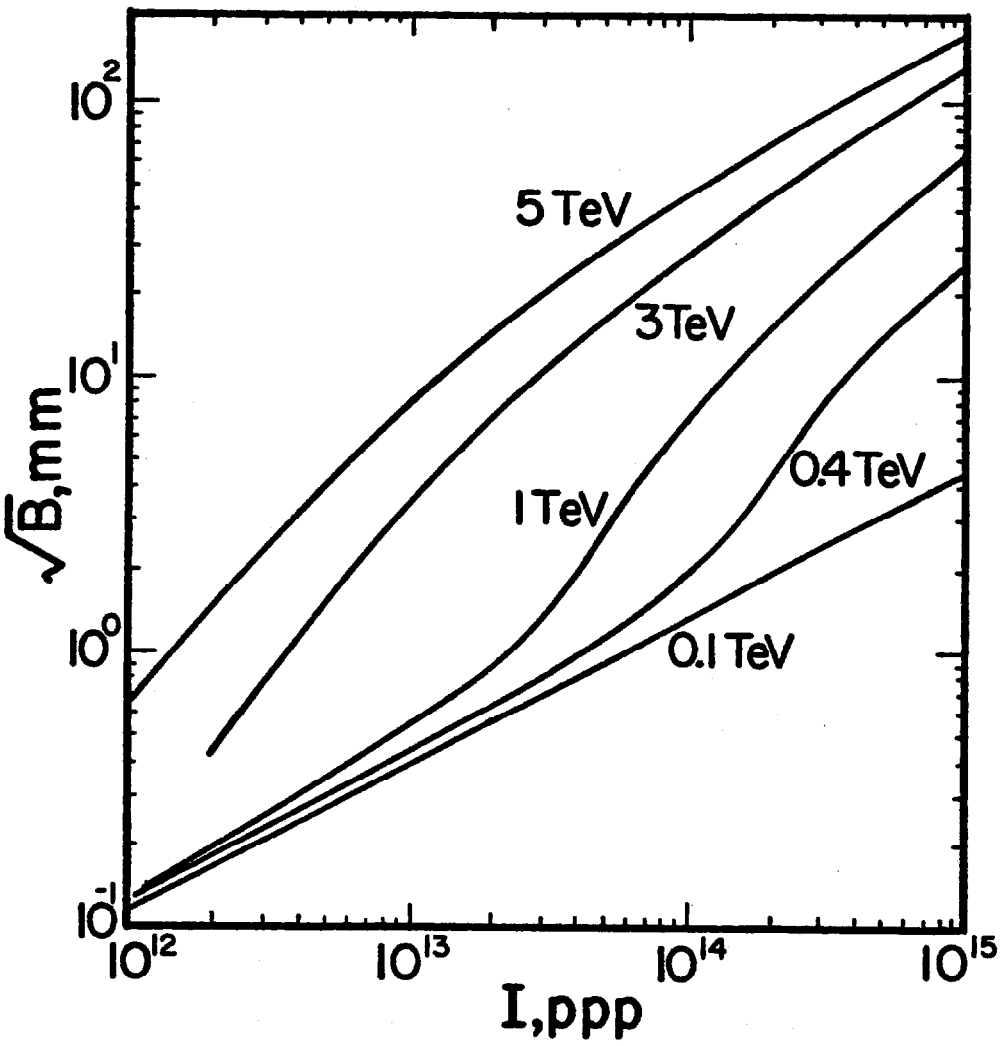
10^2
10^1
10^0
10^{-1}
$\sqrt{B}$,mm
5 TeV
3TeV
1TeV
0.4TeV
0.1 TeV
10^{12}
10^{13}
10^{14}
10^{15}
I,ppp

Fig. 11

APPENDIX V

ABORT DUMP MONITORING PROGRAM

A. Version I, June 7, 1983

B. Version II, August 18, 1983

Fermilab

TM-1196

June 7, 1983

TO: Howard Casebolt

FROM: Rich Orr/Thornton Murphy

SUBJECT: Implementation of an Abort Dump Monitoring Program

It is time to formalize our long held intention to monitor certain aspects of the abort dump usage in order to fulfill our obligation to environmental protection. I am charging you with the responsibility for producing a document which states clearly the required monitoring actions, required record keeping, limits which must not be exceeded, and what group is responsible for each item. The document should also state what further measurements need to be made once-only after the Energy Doubler reaches an appropriate intensity or energy.

The items which need monitoring have already been discussed in the Safety Analysis Review. We list them here without discussion, except to note the unanswered questions of frequency and methods which you must answer in your document.

1. The number of protons aborted per year must be limited to 7.6×10^{17} at an energy of 1 TeV, or twice that number at 500 GeV. According to Baker and VanGinneken, the relationship between primary proton energy and stars in uncontrolled soil is linear, so that lower energy aborts can be weighted by their energy divided by 1 TeV. Therefore, the number of protons aborted and the energy of each abort must be recorded in a permanent and reliable manner. There must be quarterly projections of the abort rate presented to the Head of the Accelerator Division to ascertain whether administrative restraints must be imposed to keep under the limit at the end of the calendar year.

   In implementing this requirement, you will need the cooperation of the Controls Group and the Operations Group. This recording task is an obvious job for our automatic data-logging system. You should determine whether a crude backup under your own control is necessary to cover for brief failures or erasures of the data-logging system. You should also determine the required record and hardcopy frequency required of the Operations Groups.

2. The tube leading from the tunnel to the inside of the concrete box surrounding the dump must be periodically pumped on to ascertain that there is no water inside the concrete box. How frequently should this be done? Who must do it? What record keeping should be established?

3. The tube leading from the tunnel to the underdrain under the abort must be periodically pumped out and the water analyzed for the concentration of radioactivity. If the tritium concentration exceeds some limit, action must be taken to pump this water out semicontinuously for proper handling above ground. What should this limit be? The Safety Analysis Report suggests 20pCi/mℓ, which may be far too conservative. How frequently should this be done? Who must do it? What record keeping should be established?

4. Two calorimeters, each with two temperature readouts, have been imbedded in the steel behind the graphite core for the purpose of verifying that the graphite is still intact and absorbing most of the deposited energy. One calorimeter is behind the Main Ring graphite, the other behind the Doubler graphite. They must be periodically examined in a controlled manner to verify that their response to a steady rate of energy deposition has not increased. We suggest that there should be scheduled periodic studies in which beam is aborted every pulse until thermal equilibrium is reached at an intensity, energy, and cycle time identical with the previous bench mark, for both the Main Ring and the Doubler. During operating periods between these studies, sensible alarm limits should be established for these calorimeters. At what level of increased temperature during these studies should an administrative alarm bell ring? What are sensible alarm limits between controlled studies?

5. There are a number of other temperature sensors in the dump not mentioned in the Safety Analysis Report. They serve as warnings that the LCW has been shut off, warning that the aluminum box is about to split open, or that the steel is about to crack the concrete box, as discussed in Ref. 1. What are sensible alarm limits on these sensors? What action is required if they alarm?

6. The LCW which cools the aluminum box is part of the Main Ring LCW system. It is conceivable that during continuous aborting, this water will become sufficiently radioactive to create a problem in the nearest above-ground service building to which it is circulated (either C1 or B4). What steps should be taken to monitor this potential problem?

7. A plan must be formulated to verify periodically that the LCW water is not leaking into the ground or into the abort shielding because of a cracked weld or failed fitting.

8. Alarm limits must be set on the position detectors in the Saver abort line and on the wire chamber common to both beams at the dump to assure that the beams are going cleanly to the dump and not scraping on the various underground flanges.

9. The above-ground muon dose rate has been calculated using the program CASIM, both at ground-level between the dump and the site boundary, and as a function of height above the ground at the site boundary. The predicted dose is quite tolerable, given the limit of Para. 2 (above) on the number of protons dumped per year. However, the program CASIM has not been compared with experiment at these new high energies. Therefore, muon dose measurements will be required. At what combination of energy and intensity will it be feasible to begin such measurements?

continued

10. The neutron rate above-ground near the dump has been predicted to be extremely small (between 0.3 and 3 mrem/hr for 10^{14} protons per minute dumped at 1 TeV). This inaccurate prediction should be replaced by measurements. At what combination of energy and intensity should these measurements begin?

11. The evacuated pipe leading from the tunnel to the dump must either remain evacuated or be filled with helium in order to limit ground water activation resulting from gas scattering. With what frequency should the Safety Group verify that the pipe is still holding vacuum?

In fleshing out the details of the above program, you should expect any help needed from Thornton Murphy, Frank Turkot, Andy VanGinneken and Sam Baker.

Implementation of Para. 1, even if the method is somewhat makeshift, is required by August 1, 1983. The remainder of the document, detailing both the periodic and once-only measurement program, is required by August 1, 1983. A final version of the program, appropriate for inclusion in the Accelerator Radiation Guide, will be due one month after all the once-only measurements have been made.

Ref. 1 E.Harms et al., "Instrumentation for the Tevatron Beam Dump," IEEE 1981 Particle Accel.Conf., Vol. II, p. 2771.

mhr
cc:Sam Baker
Larry Coulson
Bob Mau
Frank Turkot
Andy VanGinneken

Fermilab August 18, 1983 TM-1196

TO: J.R. Orr/C.T. Murphy

FROM: P. Yurista PMY

SUBJECT: Abort monitoring program

The preliminary monitoring program for the Main Ring abort at C0 is described in this memo. The final version will follow the initial measurements for muons and neutrons. Upgrading of the hardware and software involved will occur during this period and will be further described at that time. The items and monitoring are as follows:

1. The number of aborted protons per year-

   The limit for aborted protons is 7.7 E17 per year at 1 TeV as calculated by A. Van Ginneken (TM-1196). This is energy dependant and to preclude 8 GeV studies from exhausting the abort limit, energy discrimination and scaling will be used. The scaling is determined from MAXIM calculations by A. Van Ginneken and T. Murphy at various energies and is proportional to $E^{(3/4)}$. The Tevatron ring readily has energy available from existing ramp signals. The Main Ring does not presently have an energy available and hence initially aborts during Main Ring ramp will be assumed 150 GeV. Aborts prior to Main Ring ramp will be assumed 8 GeV. The previous MR abort monitor is being resurrected as best as possible and BPM monitoring signals in the Tevatron will be used to record intensities to the dump. Activation foils have been installed to back up these measures. Until the necessary hardware has been fabricated and the software written the foils will be used.

   Once the final system is operational the numbers aborted will be recorded shiftly in conjuction with the other intensities presently monitored by operating personnel for records. The monthly summary of

operations will include aborted protons for the operating period and year to date. A copy of this is forwarded to the Division Head.

2. Drain pipe from abort cavity-

The drain pipe from the abort cavity slopes to a lower elevation in the Main Ring tunnel and may be inspected by simply opening the valve and observing any discharge of water. This inspection will be performed on initial entry radiation surveys for the Main Ring tunnel. The results will be recorded on the survey map and later transfered to the abort log book.

3. Underdrain soil sampling-

The abort underdrain has a sample tube leading to it from within the Main Ring tunnel. This drain will be sampled initially on a quarterly basis to establish any pattern or rate of activation associated with aborting of protons. The frequency will be reviewed at a later date once operational energies and intensities have stabilized to some degree. The samples will be collected by the Accelerator Safety Group in cooperation with the Environmental Safety Group. The results will be maintained by the Environmental Group in their sump and ground water sampling logs. Collection of the sample should be noted in the abort log book. If the results are greater than 20 pCi/ml the drain should be pumped to Main Ring sumps for disposal as surface water. Once the concentration level has been reduced to less than 20 pCi/ml (as determined by sampling) the pumping may be secured.

4. Calorimeters-

There will be temperature alarm limits associated with the calorimeters. These will be set to alarm at 60°C. There are no associated inhibits. Appropriate procedures will be followed by operating personnel upon receipt of such an alarm. The cycle time is presently expected to be of such length that there is no build up to an equilibrium. Therefore recording various aborted pulses more or less on a spontaneous basis will provide a history for comparison purposes. A log sheet will be available in the control room to record energy, intensity and temperature rise for aborted pulses.

5. RTD's-

The RTD located in the steel following the calorimeters will have an alarm level of 50°C. Appropriate procedures will be followed by operating personnel. This is not expected to be a problem. Of more concern is that if the LCW system of the dump should become isolated, any of the temperature monitors including the calorimeters would not alarm before a pressure buildup could rupture the aluminumn box. The handles to the supply and return valves have been locked open to ensure an expansion path for temperature/pressure buildup. The key to the locks will be retained in the control room in the Crew Chiefs Key Cabinet. In addition, the RTD's located in the graphite will set an alarm at 60°C. The RTD temperature limits may be adjusted after some operating experience and data suggest this would be appropriate.

6. LCW Radiation levels-

The short lived radioactive products from spallation of water within the dump system will be greatly diluted by the volumn of the main ring LCW system. The resultant radiation levels in the nearest downstream service building (with regard to LCW flow) are expected to be very low. However, an area monitoring device with a GM detector will initially be installed to alert personnel in the vicinity of LCW piping within the service building of abnormal levels. Once the levels are confirmed to be low the detector may be removed.

7. LCW leakage to soil or abort cavity-

The abort LCW piping exterior to the Main Ring tunnel is buried and not available for inspection, hence any leakage to the soil may go unnoticed. The method to check for integrity is necessarily indirect. Quarterly this piping will be inspected by the following method:

1. A staff member of the accelerator safety group will obtain the key for the locks on the valves.

2. The main return isolation valve '1' (fig. 1) will be closed and pressure in the abort allowed to equalize with supply pressure.

3. The main supply isolation valve '2' will be closed and the pressure trapped between them observed for two (2) minutes. A cracked weld or fitting will show up very rapidly as a pressure drop. Should a leak be detected it may further be isolated as to which line it is in by repeating the procedure with

one of the two parallel flow paths isolated from the rest ('3' and '4', or '5' and '6' shut).

4. The valves will be returned to full open positions and properly locked prior to leaving the area. If the test is unsatisfactory the division head shall be informed and appropriate action taken.

The inspection and any necessary actions taken shall be recorded in the abort log book.

Figure 1

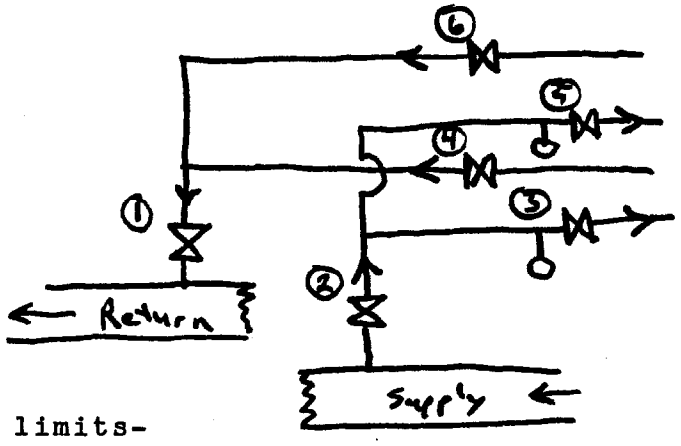

8. Beam position limits-

A microprocessor system is being developed by the operations group to monitor the aborted beam's position through the abort line. Coincidence circuitry will monitor whether or not an actual abort is in progress and whether it reaches the face of the dump. An appropriate alarm will be generated if the position is such that the beam may need tunning. Read back from position detectors upstream of the abort line and at the abort will be used upon occurance of abort commands.

9. Muon dose rates-

The abort line is being surveyed and marked with posts along the trajectory towards Butterfield Road. The MERL (Mobile Environmental Radiation Laboratory) and hand held portable instruments will be used to conduct muon measurements and will be operated by the Radiation Safety Group. Coordination of appropriate conditions with data collection will be made by the Accelerator Safety Group. The beam conditions necessary to produce measureable levels are expected to be 2E12 protons at 700 GeV.

10. Neutron dose rates-

The neutron dose rates above the dump will be measured at approximately the same time as the muon measurements although the conditions necessary may be greater. These measurements will be conducted cooperatively by the Radiation Safety Group and the Accelerator Safety Group. Followup measurements will be made as necessary. The results will be noted in the abort log book.

11. Underground transport pipe-

The evacuated pipe will be inspected for vacuum on initial entry radiation surveys for the Main Ring. A local indicating guage shall be read with the value recorded on the survey log and later transferred to the abort log book. A loss of vacuum shall be reported to the Division Head and appropriate procedures followed. This may be either to re-establish vacuum or use a helium atmosphere and adjust the yearly limits as necessary to account for scattering. Record any such action in the abort log book.

cc. S. Baker
H. Casebolt
J. Couch
C. Vanecek/Safety File

APPENDIX VI

REMOVING THE CORE BOX: DISCONNECTING THE INSTRUMENTATION LEADS

In Section VI.E of the main text, radiation hazards of removing the aluminum core box were discussed. The mechanical details of extracting the concrete and steel blocks directly above the core box were stated.

However, there is a further mechanical complication in the removal resulting from the fact that the instrumentation leads from the core box (RTD cables) feed into a pipe imbedded in the upstream vertical concrete wall. These cables must be cut before the box can be lifted straight up. Unfortunately, major surgery to the upstream wall must be performed to gain access to these cables. Fortunately this region is expected to give radiation doses of only 14 mrem/hr.

We describe here the optimum (i.e., minimal) surgery, based on conversations with Max Palmer who selected this cable routing. This description is probably understandable only if read while consulting photos in the abort dump photo album.

The concrete wall at the upstream face of the dump must be chipped out from the top of the dump down to the 18" pipe which feeds through the concrete wall to the face of the core box, for a width transverse to the beam of about 18". The top of the 18" pipe must then have a "window" cut out directly above the beam position monitor, sufficient to reach in with bolt cutters to cut the instrumentation leads as they emerge through the front face of the aluminum box. The instrumentation leads are not normal cables, but rather stainless steel tubes with radiation-hardened cable inside.

Having cut these tubes, the core box can probably be lifted straight up, with a little crow-barring at the upstream end to disengage this end from a plywood window in which it resides (see photos). The new aluminum box built to replace the failed box must have its instrumentation leads fed up through the LCW chimney. The original box should have been built this way.